

# Red meat and colon cancer

How dietary heme initiates  
hyperproliferation

Noortje IJssennagger

### **Thesis committee**

#### **Thesis supervisor**

Prof. Dr. Michael Müller  
Professor of Nutrition, Metabolism & Genomics  
Wageningen University

#### **Thesis co-supervisor**

Dr. Roelof van der Meer  
Senior Scientist, Nutrition and Health  
TI Food and Nutrition

#### **Other members**

Prof. Dr. Jaap Keijer, Wageningen University  
Prof. Dr. Bert Groen, Groningen University  
Prof. Dr. Ellen Kampman, Wageningen University  
Prof. Dr. Jan Knol, Wageningen University

This research was conducted under the auspices of the Graduate School VLAG (Advanced studies in Food Technology, Agrobiotechnology, Nutrition and Health Sciences).

# Red meat and colon cancer

## How dietary heme initiates hyperproliferation

Noortje IJssennagger

### **Thesis**

submitted in fulfillment of the requirements for the degree of doctor  
at Wageningen University  
by the authority of the Rector Magnificus  
Prof. dr. M.J. Kropff,  
in the presence of the  
Thesis Committee appointed by the Academic Board  
to be defended in public  
on Friday 2 November 2012  
at 1.30 p.m. in the Aula.

Noortje IJssennagger

Red meat and colon cancer: how dietary heme initiates hyperproliferation

Thesis Wageningen University, Wageningen, the Netherlands (2012)

With references, with summaries in English and Dutch

ISBN 978-94-6173-393-1

# Contents

<b>Chapter 1</b>	Introduction	7
<b>Chapter 2</b>	Dietary heme stimulates epithelial cell turnover by downregulating feedback inhibitors of proliferation in murine colon	15
<b>Chapter 3</b>	Dietary heme-mediated PPAR $\alpha$ activation does not affect the heme-induced epithelial hyperproliferation and hyperplasia in mouse colon	47
<b>Chapter 4</b>	Dietary heme induces acute oxidative stress but delayed cytotoxicity and compensatory hyperproliferation in mouse colon	65
<b>Chapter 5</b>	Dietary heme alters microbiota and mucosa of mouse colon without functional changes in host-microbe cross-talk	83
<b>Chapter 6</b>	Microbiota facilitates dietary heme-induced epithelial hyperproliferation and hyperplasia by breaking the mucus barrier	107
<b>Chapter 7</b>	General discussion and future perspectives	125
	<b>Summary</b>	139
	<b>Samenvatting</b>	143
	<b>Dankwoord</b>	149
	<b>About the author</b>	155



# Chapter 1

## General introduction

## Colorectal cancer

Colorectal cancer is a leading cause of cancer deaths in Western countries [1]. In the Netherlands, about 12,000 cases of colorectal cancer are diagnosed each year, and about 5,000 people die each year from colorectal cancer [2]. Incidence rates are higher in men than in women [3]. In the Netherlands, but also worldwide, colorectal cancer is the third most common cancer in men, after prostate and lung cancer [2,3]. In women, it is the second most common form, after breast cancer. Worldwide, there is at least a 10-fold variation between countries in the occurrence of colorectal cancer [3] and there are over one million new cases of colorectal cancer every year [4]. The highest incidence rates can be found in affluent societies.

## The colon

The colon is the last part of the digestive tract. Compounds that are undigested and unabsorbed in the small intestine reach the colon. The main function of the colon is to absorb water and minerals, thereby concentrating the fecal mass before excretion [5,6]. Furthermore, the colon contains an enormous population of microorganisms. This colonic microbiota plays a role in the digestion of unabsorbed components and produces fermentation products in the form of short chain fatty acids which can be used as energy source by the enterocytes [7].

The colonic wall consists of 4 layers [5]. The inner layer is the serosa, which is a layer of connective tissue. The next layer is the muscularis, a muscle layer which facilitates peristalsis. The third layer is the submucosa which is a highly vascular layer of connective tissue. The outer, luminal, layer of the colon is the mucosa (Figure 1). A thin layer of smooth muscle cells (the muscularis mucosa) separates the mucosa from the underlying submucosa. The mucosa contains a single layer of epithelial cells which forms the barrier between the outside luminal environment and the inside of the body. The epithelial cell layer contains both absorptive cells (enterocytes) and secretory cells. Hormone secreting cells are called enteroendocrine cells. Cells that secrete mucins, which are heavily glycosylated proteins, are called goblet cells [5]. Together, secreted mucins form a gel-like layer which covers the epithelium [8]. This mucus layer functions both as lubricant for the fecal mass transport, but also as protectant for the epithelial cells from toxic substances present in the colonic lumen [8,9]. These toxic substances can originate from the diet, or they can be formed by the bacteria present in the intestine. The mucus layer also protects the epithelial cells from direct exposure to bacteria, as the thick inner mucus layer present in the colon is devoid of bacteria [10].

The colonic mucosa is characterized by the presence of tightly packed crypts, which are finger-like invaginations of the epithelium into the underlying connective tissue (Figure 1). At the base of the crypts the stem cells reside. All cells present in the epithelial lining arise from these stem cells [11,12]. The proliferation of epithelial cells is



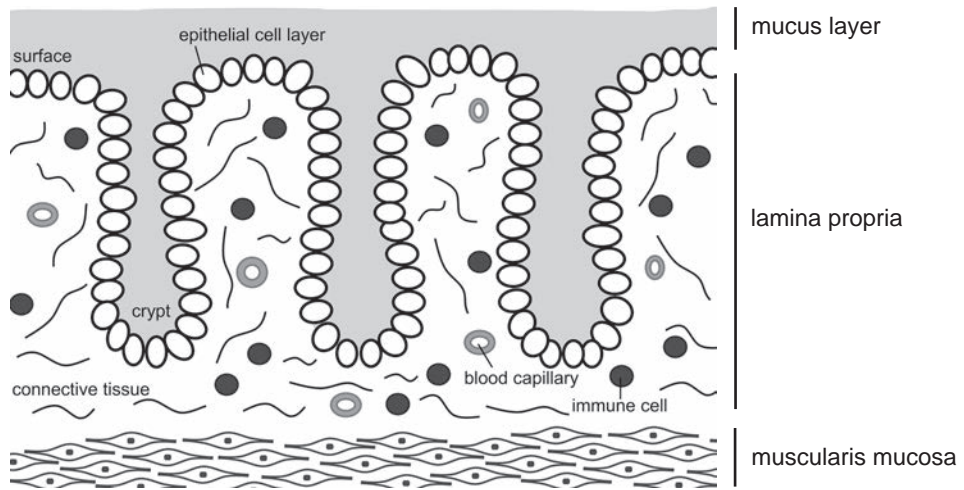


**Figure 1.** Schematic representation of the colonic mucosa. The single layer of epithelial cells is folded creating the crypts. At the bottom of the crypt the stem cells reside. Proliferation occurs from these stem cells and the newly formed cells migrate upwards to the surface epithelium, while differentiating into goblet cells, enteroendocrine cells or absorptive cells. The surface epithelium is protected by the mucus layer. Below the epithelial layer the lamina propria is located, which is a vascularized layer of loose connective tissue. The muscularis mucosa is a thin layer of smooth muscle separating the mucosa from the underlying submucosa.

controlled by the Wnt signaling pathway [13]. There is a constant migration of newly formed cells from the crypt compartment upwards to the surface epithelium. When cells are in the lower part of the crypt they undergo several rounds of replication. During the upwards migration the cells lose their ability to divide and they differentiate and get their final shape and function. The epithelial cells at the surface epithelium are exposed to the luminal contents. The average lifespan of an epithelial cell in the colon is about 3-5 days. After 3-5 days the cells can die by apoptosis (programmed cell death) or by necrosis (cell death caused by external factors).

The colonic epithelium is a highly proliferative tissue [14,15]. Normally, the loss of cells and the production of new cells is tightly regulated, in order to maintain the barrier function of the epithelial layer [16]. When a surface epithelial cell dies, a new cell should be formed to replace this dying cell. As the production of new cells occurs in the crypt, the dying surface cells should somehow signal to the stem cells in the crypt to initiate proliferation (Figure 2). When many surface cells die at the same time, for example if there is damage due to a toxic compound in the diet, many new cells have to be formed to replace the damaged cells. This increases the proliferative rate which leads to hyperproliferation and eventually hyperplasia. A consequence of this high self-renewing rate is a higher chance for endogenous mutations in tumor suppressor genes or oncogenes. Moreover, as the proliferation rate is higher, the growth of mutated cells is stimulated [17,18]. These mutations can eventually result in colon cancer. It is currently unknown how surface cells signal to crypt cells to regulate proliferation. In this thesis this surface to crypt signaling is studied.

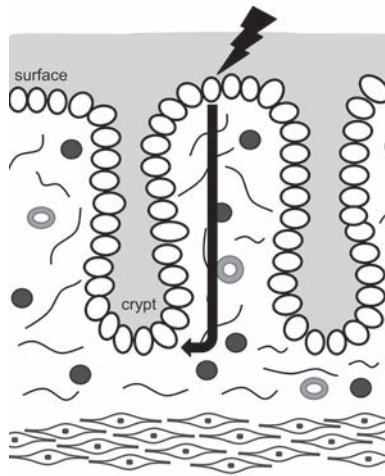


**Figure 2.** Model of the hypothesized surface to crypt signaling. Injured surface cells signal to the crypt to initiate compensatory hyperproliferation to replace the injured cells.

## Colorectal carcinogenesis

Between 5 and 10% of all colorectal cancers are hereditary [19,20], meaning that a germ line mutation plays a dominant role in these forms of colorectal cancer. The two main forms of hereditary colorectal cancer are Familial Adenomatous Polyposis (FAP) in which there is a mutation in the adenomatous polyposis (APC) gene, and Hereditary Nonpolyposis Colorectal Cancer (HNPCC) in which mutations in mismatch repair genes are present [4]. A further 20% of cases occur in people who have a family history of colorectal cancer [20]. However, the majority (approximately 75%) of colorectal cancers are sporadic, so without a family history of colorectal cancer, arising from somatic mutations and clonal evolution at the tumor site [4]. The incidence of sporadic colorectal cancer is strongly age-related (Figure 3). Moreover, lifestyle and dietary factors play an important role in colorectal cancer aetiology. This role of the environment is illustrated by the fact that there are large differences between countries in colorectal cancer incidence rates [3,4]. The highest rates are observed in New Zealand, Australia, North America, Europe and more recently also Japan [4]. Lower rates are reported in Asia and Africa. Furthermore, migrant studies show that when people migrate from a low risk area to a high risk area they quickly adapt to the increased risk [21,22].

An important environmental factor is diet. Of all common cancers, a dietary influence on colorectal cancer risk is most plausible as the colorectal mucosa is in contact with non-absorbed food components and is exposed to diet-induced metabolic and physiologic changes. However, studying the connection between diet and colorectal cancer risk is difficult because of complex dietary patterns, interactions between nutrients, interference of microbiota and the mucus layer, hormonal effects and gene-diet effects. Nevertheless, several dietary risk factors could be identified from epidemiological and experimental studies.

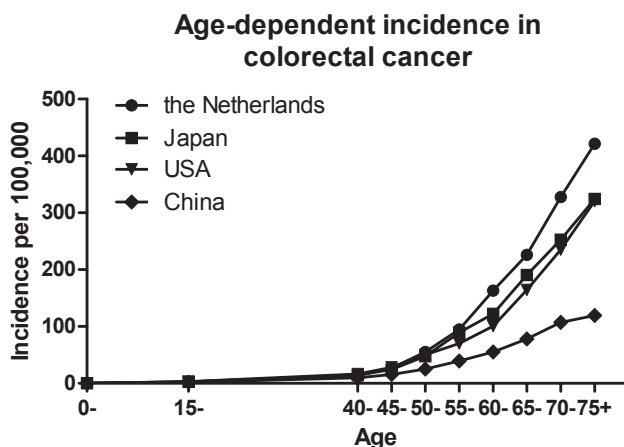


**Figure 3.** Age-dependent increase in colon cancer incidence in low and high risk countries in 2008. Data are age-standardized rates per 100,000 and originate from GLOBOCAN 2008 v1.2, Cancer Incidence and Mortality Worldwide: IARC CancerBase No. 10, Available from: <http://globocan.iarc.fr>, accessed on 6/6/2012.

### Red meat and the risk of colon cancer

There is evidence that diets high in red and processed meat are associated with a moderately increased risk of colon cancer [23,24]. In contrast, diets with a high content of white meat (poultry and fish) are not associated with an increased risk [25,26]. The mechanism behind the red meat-induced colon cancer risk is not precisely known. Heterocyclic amines, formed when heating meat, can play a role in the formation of colon cancer as they are potent mutagens and carcinogens in animal studies [27]. Whether they are relevant for colon cancer remains uncertain, as the human daily intake of heterocyclic amines is several times lower than doses required to induce tumors in animals [28]. Besides, cooked white meat also contains heterocyclic amines [29,30], which is not in line with the epidemiological data showing that red meat increases the colorectal cancer risk, while white meat does not. Another explanation for the association between red meat and colon cancer risk is the endogenous formation of N-nitrosocompounds in the intestine after red meat, but not after white meat consumption [31,32,33]. However, the exact chemical structures of these components and their effect on the colonic epithelium are unknown. Besides, also the mutational profile induced by N-nitrosocompounds is not a profile commonly observed in sporadic colon cancer. Both N-nitrosocompounds as well as heterocyclic amines form adducts with purine bases [34,35] leading to transversions such as G:C to T:A [36], while most common mutations in colon cancer are C-to-T transitions [17,37,38] probably caused by spontaneous deamination of methylcytosine to thymine. The fat content of meat may also influence the colorectal cancer risk by increasing the amount of cytotoxic bile acids and fatty acids in the colon [39,40]. However, epidemiological studies did generally not show a relation between the intake of fat and colon cancer risk [41].

## Dietary heme and the risk of colon cancer

Kinzler and Vogelstein [17] argued that dietary factors increasing the risk of colon cancer are probably not mutagens, but rather luminal irritants that damage colonic epithelial cells. Red meat contains heme, which is such a luminal irritant with a hydrophobic tetrapyrrole ring structure and two hydrophilic side chains (Figure 4). Heme is the iron-porphyrin pigment of red meat and is the prosthetic group in hemoglobin and myoglobin, which are proteins involved in oxygen transport. Red meat contains much higher heme levels than white meat. Several epidemiological studies show an association between heme intake and the risk of colon cancer [42,43,44].

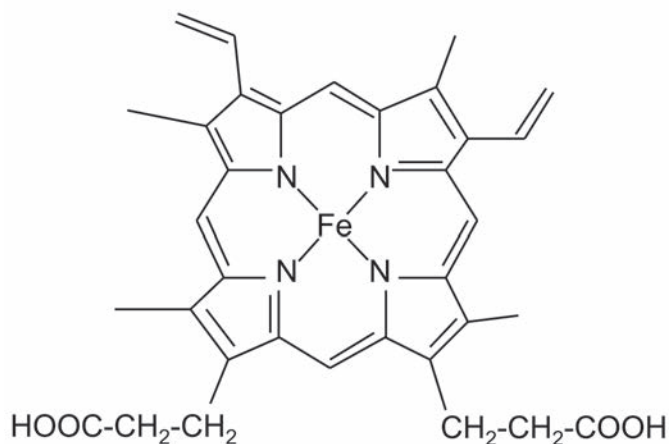


*Figure 4. The molecular structure of heme. Heme is an amphiphilic molecule with a hydrophobic tetrapyrrole ring and two hydrophilic side chains.*

Heme is poorly absorbed in the small intestine and therefore it ends up in the colon [45,46]. Adding dietary heme, but not its constituents, porphyrin or iron alone, to the diet of rodents induces cytotoxicity of gut contents, indicating an increased exposure of the colonic mucosa to luminal irritants [47]. Hyperproliferation was observed in rats receiving a heme diet. It is not heme in its native form which is inducing the observed hyperproliferation in the colon, but it is a toxic heme metabolite [47]. This heme metabolite is a covalently modified porphyrin [47] with a molecular weight higher than that of heme [48]. The toxic heme metabolite is formed in the intestinal tract during digestion. As there are no heme-induced effects seen on proliferation in the small intestine, it is speculated that the toxic metabolite is formed in the colon where the bacterial density is high [47], and there might be a role for the microbiota in its formation. The formation of the toxic metabolite might be radical-catalyzed [47], however its detailed structure is unknown as this modified porphyrin is refractory to ionization and could thus not be identified by mass spectrometry [48].

## **Aim and outline of the thesis**

The aim of this thesis was to elucidate the diet-modulated signaling from an injured colonic surface epithelium to the proliferative stem cells in the crypt to initiate compensatory hyperproliferation. The main questions addressed in this thesis are: 1) Are only surface cells injured by dietary heme, or does heme also have a direct effect on the proliferative crypt cells? If heme only injures surface cells, there must be an unknown, heme-modulated, surface to crypt signaling mechanism. 2) What are the signaling molecules from the injured surface epithelium to the proliferative part of the crypt to initiate hyperproliferation and hyperplasia? 3) What are the effects of heme on the colon in time? Is the heme-induced cytotoxic stress or the heme-induced oxidative stress causal to initiate hyperproliferation and hyperplasia? 4) Do heme-induced changes in microbiota play a role in the surface to crypt signaling, and thus in initiating hyperproliferation and hyperplasia? To answer these questions dietary heme was used to stress the surface epithelium and to induce hyperproliferation in the colon of mice. By inducing a higher proliferation rate the very early onset of carcinogenesis that can finally lead to colorectal cancer could be studied. If we get more insight in the signaling from surface epithelium to the crypt inducing an increased cell proliferation, we might use these signals as early biomarkers of colon cancer risk.

In chapter 2 of this thesis we described the effects of heme on colonic epithelial cell turnover in mice. Gene expression profiles of total colonic tissue, but also of surface and crypt cells specifically, were obtained and analyzed. As expected, many cell cycle and stress-related genes were differentially expressed on the heme diet. Several surface to crypt signaling molecules were defined. Unexpected was the observed induction of many lipid metabolism-related PPAR $\alpha$  target genes. Therefore, in chapter 3 we addressed the role of PPAR $\alpha$ , which is a nuclear receptor involved in fatty acid metabolism, in heme-induced hyperproliferation. In chapter 4 we investigated the effects of dietary heme on the luminal contents and on the mucosa in time to get more insight in the causality of heme-induced effects in the colon. In chapter 5 heme-induced changes in the composition of the gut microbiota were described, and the possible role for the microbiota in the heme-induced surface to crypt signaling and hyperproliferation was studied. Finally, in chapter 6 the effects of dietary heme on colonic epithelial cell proliferation in the absence of bacteria were investigated. In this study, broad-spectrum antibiotics were used to eliminate the majority of the colonic microbiota. Finally, the results described in this thesis were discussed in chapter 7 and recommendations for future research were provided.

## REFERENCES

- 1 Jemal A, Siegel R, et al. Cancer statistics, 2010. *CA: a cancer journal for clinicians* 2010;60:277-300.
- 2 Nederland IK. Cijfers over kanker. 2009.
- 3 Ferlay J, Shin HR, et al. Estimates of worldwide burden of cancer in 2008: GLOBOCAN 2008. *Int J Cancer* 2010;127:2893-917.
- 4 Boyle P, Levin B. *World Cancer Report*. IARCPress, Lyon, 2008.
- 5 Fox SI. *Human Physiology*. 2004;8th edition.
- 6 Cummings JH, Antoine JM, et al. PASSCLAIM--gut health and immunity. *Eur J Nutr* 2004;43 Suppl 2:II118-II73.
- 7 Cummings JH, Macfarlane GT. Colonic microflora: nutrition and health. *Nutrition* 1997;13:476-8.
- 8 McGuckin MA, Linden SK, et al. Mucin dynamics and enteric pathogens. *Nature reviews Microbiology* 2011;9:265-78.
- 9 Einerhand AW, Renes IB, et al. Role of mucins in inflammatory bowel disease: important lessons from experimental models. *Eur J Gastroenterol Hepatol* 2002;14:757-65.
- 10 Johansson ME, Phillipson M, et al. The inner of the two Muc2 mucin-dependent mucus layers in colon is devoid of bacteria. *Proc Natl Acad Sci U S A* 2008;105:15064-9.
- 11 Potten CS. Stem cells in gastrointestinal epithelium: numbers, characteristics and death. *Philos Trans R Soc Lond B Biol Sci* 1998;353:821-30.
- 12 Cheng H, Leblond CP. Origin, differentiation and renewal of the four main epithelial cell types in the mouse small intestine. V. Unitarian Theory of the origin of the four epithelial cell types. *Am J Anat* 1974;141:537-61.
- 13 van der Flier LG, Clevers H. Stem cells, self-renewal, and differentiation in the intestinal epithelium. *Annu Rev Physiol* 2009;71:241-60.
- 14 Crosnier C, Stamataki D, et al. Organizing cell renewal in the intestine: stem cells, signals and combinatorial control. *Nat Rev Genet* 2006;7:349-59.
- 15 Leedham SJ, Brittan M, et al. Intestinal stem cells. *J Cell Mol Med* 2005;9:11-24.
- 16 Hall PA, Coates PJ, et al. Regulation of cell number in the mammalian gastrointestinal tract: the importance of apoptosis. *J Cell Sci* 1994;107 ( Pt 12):3569-77.
- 17 Kinzler KW, Vogelstein B. Lessons from hereditary colorectal cancer. *Cell* 1996;87:159-70.
- 18 Thilly WG. Have environmental mutagens caused oncomutations in people? *Nat Genet* 2003;34:255-9.
- 19 World Cancer Research Fund. *Food, Nutrition, Physical Activity and the Prevention of Cancer: a Global Perspective*. Washington, DC: American Institute for Cancer Research, 2007.
- 20 Lynch HT, de la Chapelle A. Hereditary colorectal cancer. *N Engl J Med* 2003;348:919-32.
- 21 McMichael AJ, Giles GG. Cancer in migrants to Australia: extending the descriptive epidemiological data. *Cancer Res* 1988;48:751-6.
- 22 Armstrong B, Doll R. Environmental factors and cancer incidence and mortality in different countries, with special reference to dietary practices. *Int J Cancer* 1975;15:617-31.
- 23 Larsson SC, Wolk A. Meat consumption and risk of colorectal cancer: a meta-analysis of prospective studies. *Int J Cancer* 2006;119:2657-64.
- 24 Norat T, Bingham S, et al. Meat, fish, and colorectal cancer risk: the European Prospective Investigation into cancer and nutrition. *J Natl Cancer Inst* 2005;97:906-16.
- 25 Giovannucci E, Rimm EB, et al. Intake of fat, meat, and fiber in relation to risk of colon cancer in men. *Cancer Res* 1994;54:2390-7.
- 26 Larsson SC, Rafter J, et al. Red meat consumption and risk of cancers of the proximal colon, distal colon and rectum: the Swedish Mammography Cohort. *Int J Cancer* 2005;113:829-34.
- 27 Cross AJ, Sinha R. Meat-related mutagens/carcinogens in the etiology of colorectal cancer. *Environ Mol Mutagen* 2004;44:44-55.
- 28 Augustsson K, Skog K, et al. Dietary heterocyclic amines and cancer of the colon, rectum, bladder, and kidney: a population-based study. *Lancet* 1999;353:703-7.

- 29 Sinha R, Rothman N, et al. High concentrations of the carcinogen 2-amino-1-methyl-6-phenylimidazo- [4,5-b]pyridine (PhIP) occur in chicken but are dependent on the cooking method. *Cancer Res* 1995;55:4516-9.
- 30 Layton DW, Bogen KT, et al. Cancer risk of heterocyclic amines in cooked foods: an analysis and implications for research. *Carcinogenesis* 1995;16:39-52.
- 31 Bingham SA, Pignatelli B, et al. Does increased endogenous formation of N-nitroso compounds in the human colon explain the association between red meat and colon cancer? *Carcinogenesis* 1996;17:515-23.
- 32 Bingham SA, Hughes R, et al. Effect of white versus red meat on endogenous N-nitrosation in the human colon and further evidence of a dose response. *J Nutr* 2002;132:3522S-5S.
- 33 Cross AJ, Pollock JR, et al. Haem, not protein or inorganic iron, is responsible for endogenous intestinal N-nitrosation arising from red meat. *Cancer Res* 2003;63:2358-60.
- 34 Singer B, Kusmierek JT. Chemical mutagenesis. *Annu Rev Biochem* 1982;51:655-93.
- 35 Schut HA, Snyderwine EG. DNA adducts of heterocyclic amine food mutagens: implications for mutagenesis and carcinogenesis. *Carcinogenesis* 1999;20:353-68.
- 36 Jiao J, Douglas GR, et al. Analysis of tissue-specific lacZ mutations induced by N-nitrosodibenzylamine in transgenic mice. *Carcinogenesis* 1997;18:2239-45.
- 37 Harris CC, Hollstein M. Clinical implications of the p53 tumor-suppressor gene. *N Engl J Med* 1993;329:1318-27.
- 38 Nagase H, Nakamura Y. Mutations of the APC (adenomatous polyposis coli) gene. *Hum Mutat* 1993;2:425-34.
- 39 Newmark HL, Wargovich MJ, et al. Colon cancer and dietary fat, phosphate, and calcium: a hypothesis. *J Natl Cancer Inst* 1984;72:1323-5.
- 40 Reddy BS, Hanson D, et al. Effect of high-fat, high-beef diet and of mode of cooking of beef in the diet on fecal bacterial enzymes and fecal bile acids and neutral sterols. *J Nutr* 1980;110:1880-7.
- 41 Giovannucci E, Goldin B. The role of fat, fatty acids, and total energy intake in the etiology of human colon cancer. *Am J Clin Nutr* 1997;66:1564S-71S.
- 42 Larsson SC, Adami HO, et al. Re: Heme iron, zinc, alcohol consumption, and risk of colon cancer. *J Natl Cancer Inst* 2005;97:232-3; author reply 3-4.
- 43 Lee DH, Anderson KE, et al. Heme iron, zinc, alcohol consumption, and colon cancer: Iowa Women's Health Study. *J Natl Cancer Inst* 2004;96:403-7.
- 44 Balder HF, Vogel J, et al. Heme and chlorophyll intake and risk of colorectal cancer in the Netherlands cohort study. *Cancer Epidemiol Biomarkers Prev* 2006;15:717-25.
- 45 Sesink AL, Termont DS, et al. Red meat and colon cancer: dietary haem-induced colonic cytotoxicity and epithelial hyperproliferation are inhibited by calcium. *Carcinogenesis* 2001;22:1653-9.
- 46 Young G, Rose I, et al. Haem in the gut. I. Fate of haemoproteins and the absorption of haem. *J Gastroenterol Hepatol* 1989;4:537-45.
- 47 Sesink AL, Termont DS, et al. Red meat and colon cancer: the cytotoxic and hyperproliferative effects of dietary heme. *Cancer Res* 1999;59:5704-9.
- 48 de Vogel J, Jonker-Termont DS, et al. Green vegetables, red meat and colon cancer: chlorophyll prevents the cytotoxic and hyperproliferative effects of haem in rat colon. *Carcinogenesis* 2005;26:387-93.





## Chapter 2

### Dietary heme stimulates epithelial cell turnover by downregulating feedback inhibitors of proliferation in murine colon

Noortje IJssennagger, Anneke Rijnierse, Nicole de wit, Denise Jonker-Termont, Jan Dekker, Michael Müller and Roelof van der Meer

*Published in Gut. 2012; 61(7):1041-9.*

## ABSTRACT

Colon cancer is a leading cause of cancer deaths in Western countries and is associated with diets high in red meat. Heme, the iron-porphyrin pigment of red meat, induces cytotoxicity of gut contents and damages the colon surface epithelium. Compensatory hyperproliferation leads to epithelial hyperplasia which increases the risk of colon cancer. The aim of this study was to identify molecules signaling from the surface epithelium to the crypt to initiate hyperproliferation upon stress induced by heme.

C57Bl6/J mice (n=9/group) received a 'westernized' control diet (40 en% fat) with or without 0.5  $\mu\text{mol/g}$  heme for 14 days. Colon mucosa was used to quantify cell proliferation and for microarray transcriptome analysis. Gene expression profiles of surface and crypt cells were compared using laser capture microdissection. Protein levels of potential signaling molecules were quantified.

Heme-fed mice showed epithelial hyperproliferation and decreased apoptosis, resulting in hyperplasia. Microarray analysis of colon mucosa showed 3,710 differentially expressed genes (false discovery rate (q)<0.01), with many involved in the cell cycle. Expression levels of heme- and stress-related genes showed that heme affected surface cells, but did not directly affect crypt cells. Injured surface cells should therefore signal to crypt cells to induce compensatory hyperproliferation. Heme downregulated the inhibitors of proliferation, Wnt inhibitory factor 1, Indian Hedgehog and Bone morphogenetic protein 2. Interleukin-15 was also downregulated. Heme upregulated Amphiregulin, Epiregulin and Cyclooxygenase-2 mRNA in surface cells. Their protein/metabolite levels were, however, not increased as heme induced surface-specific inhibition of translation by increasing 4E-BP1.

Overall we conclude that heme induces colonic hyperproliferation and hyperplasia by inhibiting the surface to crypt signaling of feedback inhibitors of proliferation.

## INTRODUCTION

Colon cancer is a leading cause of cancer deaths in Western countries [1]. The risk of colon cancer is strongly associated with nutrition, especially with diets high in red meat [2]. Consumption of white meat (poultry and fish), however, is not associated with an increased colon cancer risk [3,4]. Kinzler and Vogelstein [5] argued that dietary factors increasing the risk of colon cancer are probably not mutagens, but rather luminal irritants that damage colonic epithelial cells. Red meat contains the iron-porphyrin pigment heme. Several epidemiological studies show an association between heme intake and the risk of colon cancer [6,7]. Intact heme, but not its constituents porphyrin and iron, induces the cytotoxicity of gut contents, indicating an increased exposure of the colonic mucosa to luminal irritants and inducing compensatory epithelial hyperproliferation [8]. Hyperproliferation increases the risk of endogenous mutations in tumor suppressor genes and oncogenes and thus the cancer risk [5].

Intestinal epithelial cell turnover is determined by the balance between cell proliferation and cell death. Colonic cell proliferation occurs from stem cells near the crypt bottom and is controlled by the Wnt signaling pathway [9]. The newly formed cells migrate up to the surface epithelium while they undergo mitosis and differentiation. Cells reach the surface epithelium and disappear after about 4 days by means of exfoliation and/or cell death (necrosis or apoptosis). It was recently shown that dietary heme increases cell death by damaging the surface cells, resulting in luminal necrosis and inhibition of active exfoliation [10]. This increased cell death at the surface was compensated by inhibition of apoptosis and by hyperproliferation of crypt cells causing hyperplasia. How these compensatory mechanisms are initiated in the crypt upon surface damage is not known. Most logically, signals from surface to crypt should increase proliferation. The aim of this study was therefore to identify heme-modulated molecules that signal from the surface epithelium to the crypt to increase cell proliferation and/or inhibit apoptosis.

## MATERIALS AND METHODS

### Animals and diets

Experiments were approved by the Ethical Committee on Animal Testing of Wageningen University and were in accordance with national law. Eight-week-old male C57Bl6/J mice (Harlan, Horst, the Netherlands) were housed individually in a room with controlled temperature (20-24°C), relative humidity (55%±15%) and a 12 h light dark cycle. Mice were fed diets and demineralized water ad libitum. To study effects of heme on colonic epithelium, mice (n=9/group) received either a 'westernized' control diet (40 en% fat (mainly palm-oil), low calcium (30 µmol/g)) or this diet supplemented with 0.5 µmol/g heme (Sigma-Aldrich, St. Louis, USA) for 14 days, as previously described [11]. Feces were quantitatively collected during days 11-14, frozen at -20°C and subsequently freeze-dried. After 14 days of intervention the colon was excised, mesenteric fat was removed

and the colon was opened longitudinally, washed in PBS and cut into three parts. The middle 1.5 cm colon tissue was snap-frozen in liquid nitrogen for cryostat sections for laser capture microdissection (LCM) or formalin-fixed and paraffin embedded for histology. The remaining proximal and distal parts were scraped. Scrapings were pooled per mouse, snap-frozen in liquid nitrogen and stored at -80°C until further analysis.

### **Cytotoxicity measurement**

Fecal water was prepared by reconstituting freeze-dried feces with double-distilled water to obtain a physiologic osmolarity of 300 mOsm/l, as described previously [8]. The cytotoxicity of fecal water was quantified by potassium release from human erythrocytes after incubation with fecal water, as previously described [8], and validated with human colon carcinoma derived Caco-2 cells [12]. Cytotoxicity was expressed as percentage of maximal lysis.

### **Immunohistochemistry**

Immunohistochemical and immunofluorescent stainings were performed on paraffin embedded colon sections. Details of antibodies and the procedure are shown in the Supplementary Methods. To quantify Ki67-positive colonocytes, 15 well-oriented crypts (longitudinal section, displaying the total crypt) per animal (n=9/group) were counted. These crypts were equally distributed over the middle 1.5 cm of the stained colon. Cells were scored Ki67-positive when their nucleus was distinctly brown. The number of Ki67-positive cells per crypt, the total number of cells per crypt and the labeling index (percentage of Ki67-positive cells per crypt) were determined.

### **RNA isolation and microarrays**

RNA was isolated from colon scrapings and individually hybridized (n=7 control; n=9 heme) to Affymetrix Mouse genome 430 2.0 arrays (Affymetrix, Santa Clara, CA, USA) (see Supplementary Methods). Genes that satisfied the criterion of false discovery rate <1% (q-value<0.01) were considered significantly differentially expressed between control and heme diets. Genes with signal intensities <20 in both treatments were considered absent and were excluded from further analysis. Array data have been submitted to the Gene Expression Omnibus, accession number GSE27849.

### **Laser capture microdissection**

Colon surface and crypt cells of 4 control mice and 3 heme-fed mice were separately isolated using LCM. RNA was isolated and analyzed with microarray to obtain surface and crypt-specific gene expression profiles (see Supplementary Methods).

## Protein/metabolite levels

Protein levels of Amphiregulin (Areg), Epiregulin (Ereg) (both n=8/group) and Interleukin-15 (IL-15) (n=9/group) were determined by ELISA in colon homogenates. 4E-BP1 levels of homogenate (pools of n=8/group) were determined by Western blot. Prostaglandin (PG) levels were measured by EIA in tissue culture supernatants (n=8 per group) (see Supplementary Methods).

## Statistical analysis

Data are presented as mean  $\pm$  SEM. Differences between mean values were tested for statistical significance by a two-tailed Student t-test. P-values  $<0.05$  were considered significant. Statistical considerations for microarray analysis were described above and in the Supplementary Methods.

## RESULTS

### Physiological changes induced by heme

After two weeks of diet intervention, heme-fed mice had a lower body weight than controls ( $25.4 \pm 0.2$  g vs  $29.1 \pm 0.8$ ,  $p < 0.05$ ). Fecal water of heme-fed mice was significantly more cytotoxic than control fecal water (Table 1). Histological examination of colon tissue showed that the surface epithelium of control mice is intact. However, heme-fed animals had a ruffled surface epithelium indicating disruption of surface epithelium architecture (Figure 1). There were no signs of inflammation, as infiltration of leukocytes was absent. This is in accordance with gene expression data, as Ingenuity pathway analysis shows no changes in inflammation-related pathways (Supplementary Figure 2B).

**Table 1.** Effect of dietary heme on fecal parameters and mucosal proliferation.

	Control	Heme
<b>Feces</b>		
Cytotoxicity of fecal water (% lysis)	$23.0 \pm 2.4$	$102.0 \pm 6.6$ *
Fecal output (g wet weight/d)	$0.25 \pm 0.03$	$0.58 \pm 0.04$ *
<b>Mucosa</b>		
Total number of cells per crypt	$45.5 \pm 2.1$	$61.1 \pm 2.5$ *
Number of Ki67-positive cells per crypt	$20.7 \pm 1.8$	$38.7 \pm 2.1$ *
Labeling index (%) <sup>#</sup>	$44.9 \pm 2.0$	$62.9 \pm 1.0$ *

<sup>#</sup> Calculated as percentage of Ki67-positive cells per crypt. Data are represented as mean  $\pm$  SEM. \*  $p < 0.05$

To measure colonocyte proliferation, colon tissue was stained with an antibody against Ki67. Stainings revealed a twofold increase in the number of Ki67-positive cells by heme and a 1.3-fold increase in the total number of cells per crypt (Table 1). Moreover, the labeling index increased significantly by 40%, indicating heme-induced increased cell

proliferation. This increased cell proliferation expanded the proliferative compartment of the crypts and increased crypt depth (Figure 1). Besides increased proliferation, decreased apoptosis also contributed to increased crypt depth and increased cell numbers. Immunostaining for active caspase-3 (Figure 1) showed that apoptotic cells were present in control mice, although numbers were low as apoptosis is a rapid process. However, there were no caspase-3-positive cells in surface epithelium of heme-fed mice. This is in line with our earlier study showing that heme abrogates apoptosis in colon mucosa [10]. All these physiological and histological changes are in line with the effects observed in heme-fed rats [10] and indicate that, also in mice, dietary heme injures the surface epithelium which is compensated by crypt cell hyperproliferation and by inhibition of apoptosis, resulting in hyperplasia.

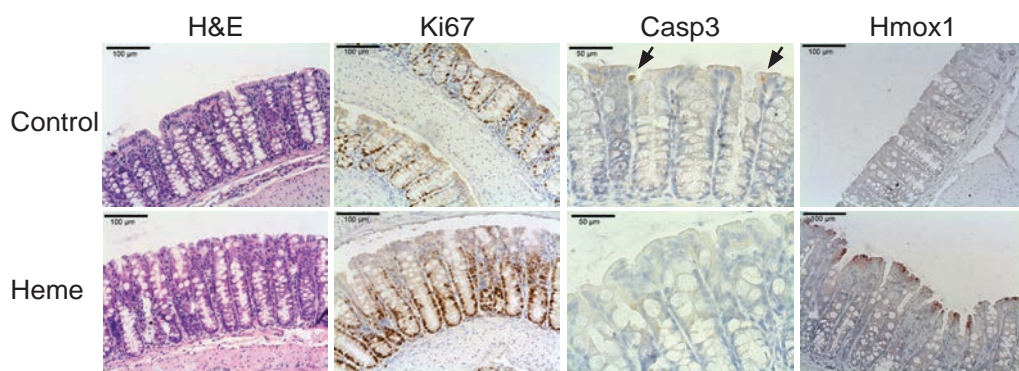


**Figure 1.** Stainings of mouse colonic mucosa after 14 days of control or heme diet. Following histological H&E staining, immunohistochemistry was performed using Ki67, heme oxygenase (Hmox1), and cleaved caspase-3 (Casp3) specific antibodies. Arrows in the latter staining indicate Casp3-positive cells.

## Heme-modulated transcriptomics

Transcriptome analysis was performed on colonic mucosal scrapings of individual mice to determine heme-induced differentially expressed genes. Applying the following selection criteria, false discovery rate ( $q$ ) $<0.01$  and signal intensity $>20$  in at least one of the arrays, we found 3,710 differentially expressed genes. The 50 most up- and downregulated genes are shown in Supplementary Table 2 and 3, respectively. Categorizing Gene Ontology Biological Process annotations of the differentially expressed genes showed that predominantly processes related to cell proliferation and differentiation were changed (Supplementary Figure 2A). Furthermore, stress- and immune response-related processes were influenced. Metabolism-related genes were mainly involved in lipid metabolism. Results were confirmed by Ingenuity canonical pathway analysis (Supplementary Figure 2B), showing that pathways related to cell cycle (control of chromosomal replication and G2/M DNA damage checkpoint regulation) and stress (NRF2-mediated oxidative stress response) were especially affected in colonic

mucosa. Supplementary Figure 2C shows that genes involved in progression of cell cycle were almost entirely upregulated by heme (e.g. cyclins, cyclin-dependent kinases, as well as ORC- and MCM-related genes involved in DNA replication), whereas genes controlling cell cycle arrest (Smad3/4) and DNA damage checkpoint (Prkdc and Atm) were downregulated. Together, the microarray data clearly indicate that proliferation was stimulated in colonic mucosa by heme, which is in accordance with the physiological findings described above.

**Table 2.** Identification and localization of heme-modulated cell turnover genes.

Gene name	Symbol	Total Scrapings Fold change <sup>a</sup>	LCM analysis		
			Ratio surface to crypt in controls <sup>b</sup>	Fold change on heme <sup>c</sup>	
				Surface	Crypt
Genes involved in cell cycle					
Antigen identified by monoclonal antibody Ki67	mKi67	1.7 *	0.2	1.2	2.0
Cyclin E1	Ccne1	1.8 *	0.6	1.0	2.4
Cyclin A2	Ccna2	2.6 *	0.1	1.8	3.2
Cyclin B2	Ccnb2	2.1 *	0.3	1.3	3.0
Frizzled homolog 5	Fzd5	-1.4 *	2.5	-1.9	-1.4
Inhibitors of Apoptosis					
Survivin	Birc5	2.6 *	0.5	1.0	3.1
X-linked inhibitor of apoptosis, Birc4	Xiap	-1.5 *#	1.7	1.7	1.0
Bcl2-like 1	Bcl2l1	-1.0 #	1.9	1.5	-1.1
Immediate early response 3	Ier3	6.5 *	1.5	4.0	1.1

<sup>a</sup> Gene expression in total mucosal scrapings shown as fold change of heme-treatment versus control. <sup>b</sup> Signal intensity of genes at surface divided by crypt signal intensity. <sup>c</sup> Heme-induced fold induction for surface and crypt separately. \* $q < 0.01$ ; # signal intensity  $< 20$  in total scrapings.

### Localization of heme-modulated cell turnover genes

To determine the localization of heme-modulated genes in the colon mucosa, LCM was applied to separately isolate surface cells and transit-amplifying (TA) cells of the lower part of the crypts (Supplementary Figure 1). Gene expression of these two compartments was analyzed by whole genome microarrays to obtain surface and crypt specific expression profiles. Using LCM, almost no lamina propria cells were isolated. This is in contrast to total scrapings, where the complete epithelial lining is present, as well as lamina propria cells.

As microarray analysis of mucosal scrapings showed that cell cycle is changed by heme, we first focused on the localization of cell turnover and apoptosis-related genes. In

both total scrapings and LCM samples, gene expression levels of Ki67 were analyzed to validate heme-induced hyperproliferation. Ki67 gene expression was 1.7-fold significantly upregulated in scrapings by heme (Table 2). Using LCM, Ki67 was shown to be predominantly expressed in crypt cells where proliferation is expected (Table 2). Heme doubled Ki67 expression only in the crypt compartment. This twofold upregulation of Ki67 mRNA is in line with its protein levels (Figure 1, Table 1).

The progression of cells through cell cycle is controlled by cyclins. In scrapings, cyclins E1, A2, and B2 (reflecting the G1/S, S and M-phase of cell cycle) were all approximately twofold increased by heme. LCM showed that this is a crypt specific upregulation (Table 2). Cyclins can be activated by growth-stimulating factors such as Wnt. However, no differences were observed in gene expression level of Wnts and their receptors, except for Frizzled 5 (Table 2). This Wnt receptor is mainly expressed and downregulated in surface cells, and therefore cannot mediate the hyperproliferative effect on crypt cells.

Array data showed that heme also modulated apoptosis-related genes. The apoptosis inhibitor survivin (Birc5) was 2.6-fold upregulated in scrapings. This increase was crypt-specific, as survivin was upregulated 3.1-fold at crypt level only (Table 2). Moreover, apoptosis inhibitors Xiap, Bcl2l1 and Ier3 were significantly upregulated by heme, but their upregulation was surface-specific. So, inhibition of apoptosis both in surface and crypt would contribute to the increased number of cells per crypt and therefore to the observed hyperplasia.

### **Heme modulated stress response genes in surface epithelium**

It is not known whether heme can reach the bottom of the crypt and directly modulate TA cells. To determine which cells were exposed to heme we studied expression of genes involved in heme metabolism and their localization. The enzyme heme-oxygenase 1 (Hmox1), known to be induced by its substrate heme and by various non-heme stressors [13], was 35-fold upregulated by heme in scrapings (Figure 2A). Hmox1 expression was specifically induced in surface epithelium (Figure 2A), which is in line with its protein expression (Figure 1). Apical heme uptake may occur through the putative heme transporter Slc46a1 [14]. This transporter was downregulated 10-fold by heme, probably to protect colonocytes from entry of large amounts of heme. This downregulation occurred only at the surface (Figure 2A). Abcg2 is proposed to transport the excess of heme and heme breakdown products out of enterocytes into the lumen [15]. In mucosal scrapings of heme-fed mice there was a 1.5-fold upregulation of Abcg2, and this upregulation occurred most profoundly at the surface (Figure 2A).

In addition to genes of the heme pathway being specifically changed in surface epithelium, stress-related genes such as the NF- $\kappa$ B essential modulator Nemo (Ikbkg) also showed a significant upregulation almost exclusively at the surface (Figure 2B). Upregulation of immediate early response genes c-Fos and Tis7 and the stress activated transcription



factor Creb3l3 [16] was also surface-specific (Figure 2B). Although Nrf2 was not itself changed on a heme diet, Nrf2-interacting proteins c-Fos, Creb3l3 and Atf4 (see below) were significantly increased in surface cells, indicating Nrf2-dependent transcription of stress-related genes, such as Hmox1. The changes in both heme- and stress-related genes show that dietary heme exerted its primary effect on the surface epithelium and that it has little or no direct effect on crypt cells. This raised the question of how heme-stressed surface cells signal to crypt TA cells to induce compensatory hyperproliferation.

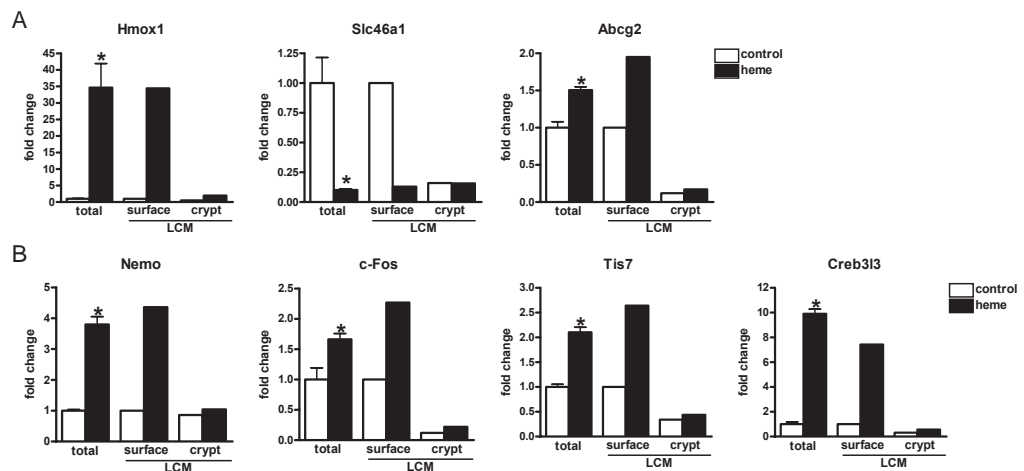


**Figure 2.** Differential expression of (A) heme metabolism- and (B) stress-related genes. Microarray analysis was performed on total scrapings of individual mice ( $n=7$  controls,  $n=9$  heme-fed mice). Relative gene expression changes (fold changes) on heme were calculated by setting RNA levels of control mice to 1 (mean  $\pm$  SEM,  $*q<0.01$ ). Surface- and crypt-specific microarray gene expression profiles are from pooled tissue samples obtained by LCM ( $n=4$  controls,  $n=3$  heme-fed mice). Relative gene expression changes were calculated by setting RNA levels in surface of controls to 1.

## Heme downregulated epithelial expression of feedback inhibitors of proliferation

To identify signaling molecules triggering the proliferative capacity in the crypt, differentially expressed genes were subjected to secretome analysis. Selection criteria and the secretome table can be found in Supplementary Table 4. We hypothesized that loss of feedback signals, and thus downregulation of gene expression, due to heme-induced stress at the surface, is a likely way to induce hyperproliferation of crypt cells. Indeed, we found in our secretome analysis more downregulated than upregulated signaling molecules (62 vs 25). We further selected downregulated genes coding for feedback inhibitors of proliferation or cytokines. In this way we identified Wnt Inhibitory factor 1 (Wif1), Indian Hedgehog (Ihh), Bone morphogenetic protein 2 (Bmp2) and Interleukin-15 (IL-15) as the most likely candidates to signal from surface to crypt to increase proliferation (Figure 3A).

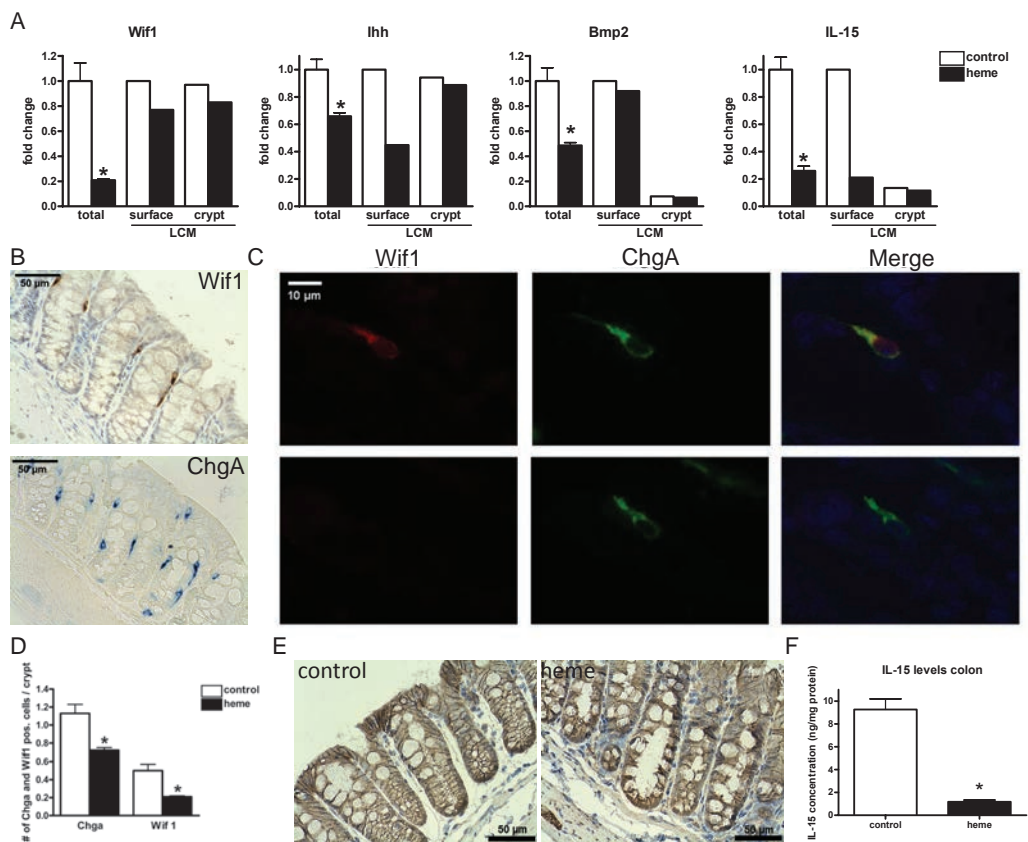


**Figure 3.** Gene and protein expression of downregulated signaling molecules Wif1, Ihh, Bmp2 and IL-15. (A) Gene expression levels in total scrapings (mean  $\pm$  SEM, \* $q < 0.01$ ) and in surface and crypt compartments. (B) Immunohistochemical staining for Wif1 and ChgA in mouse colon. (C) Immunofluorescent staining of mouse colon for Wif1 (Cy3.5-conjugated antibody: red) and ChgA (ALEXA488-conjugated antibodies: green). Stainings were merged, including nuclear DAPI staining (blue). Co-localization was indicated by yellow staining. (D) Number (mean  $\pm$  SEM) of ChgA- and Wif1-positive cells per crypt counted ( $n = 6$  mice per group). \* $p < 0.05$ . (E) Immunohistochemical staining for  $\beta$ -catenin in mouse colon. (F) IL-15 protein levels measured by ELISA in control and heme colon scraping homogenates ( $n = 9$  for both groups) represented as mean  $\pm$  SEM, \* $p < 0.001$

Wif1 antagonizes Wnt signaling by binding Wnts and thereby blocking binding of Wnts to their receptor. On the heme diet Wif1 was 5-fold downregulated. LCM analysis showed that the large overall downregulation of Wif1 could not be explained by the slight decrease in its expression in surface and TA cells (Figure 3A), indicating that Wif1 expression is concentrated in between these locations. Immunohistochemical staining for Wif1 confirmed LCM data by showing that Wif1 was located in the upper half of the crypt (Figure 3B), the part not included in LCM analysis (Supplementary Figure 1). The localization and morphology of Wif1-positive cells led us to hypothesize that Wif1 originates from enteroendocrine cells.

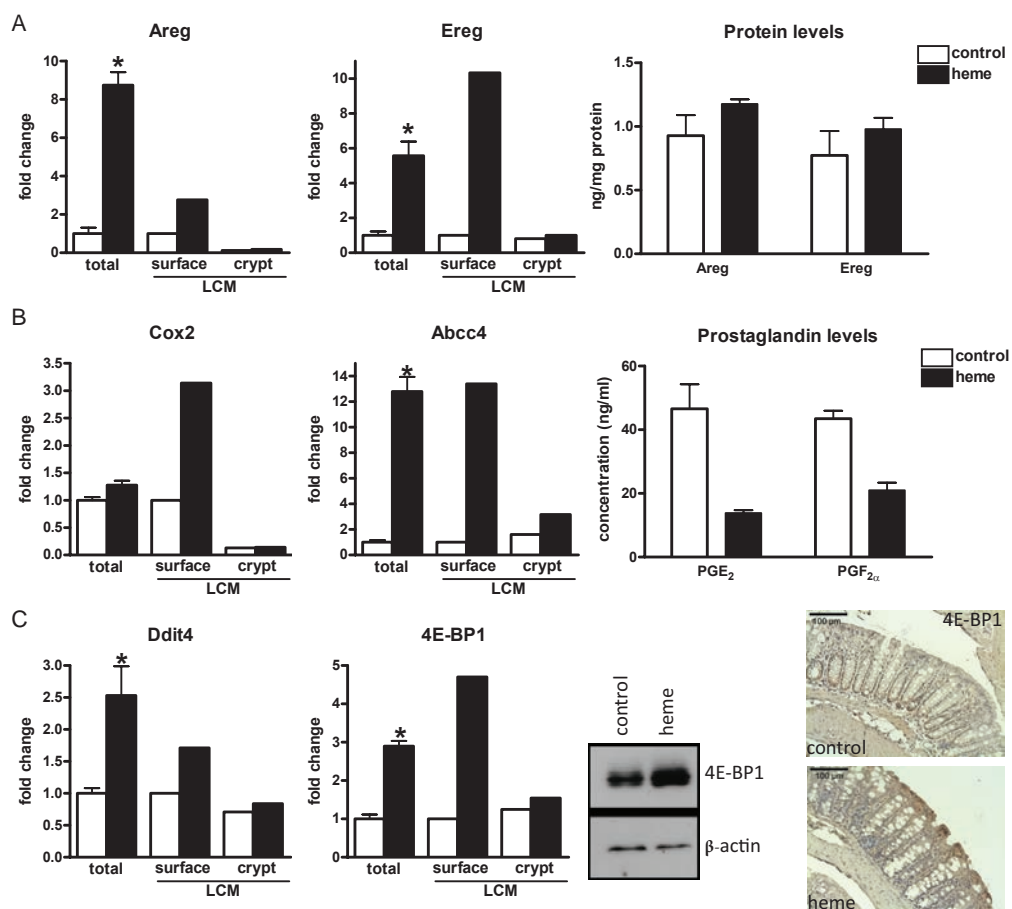


**Figure 4.** Gene expression and protein/metabolite levels of upregulated signaling molecules Areg, Ereg and prostaglandins and of translation-regulating proteins. (A) Gene expression levels in total scrapings (mean  $\pm$  SEM, \* $p$ <0.01) and in surface and crypt compartment. Protein levels measured in homogenates (mean  $\pm$  SEM,  $n$ =8 mice/group). (B) Expression levels of prostaglandin(PG)-related genes and PGE<sub>2</sub> and PGF<sub>2α</sub> levels in colon tissue culture supernatant measured by EIA (mean  $\pm$  SEM,  $n$ =8 mice/group, \* $p$ <0.01). (C) Expression levels of Ddit4 and 4E-BP1. Western blot analysis using 4E-BP1 and  $\beta$ -actin specific antibodies. Immunohistochemical staining for 4E-BP1.

Staining for chromogranin A (ChgA; enteroendocrine specific) showed the same staining pattern as Wif1 (Figure 3B). Moreover, immunofluorescent double-staining for Wif1 and ChgA visualized co-localization (Figure 3C), and demonstrated that all Wif1-positive cells were of enteroendocrine origin (Figure 3C upper panels), but not all enteroendocrine cells express Wif1 (Figure 3C lower panels). Quantification of Wif1-positive cells showed that Wif1-positive cells were less abundant in heme-fed mice (Figure 3C), which is in line with the heme-induced downregulation of Wif1 gene expression in scrapings. Quantification of ChgA positive cells showed that there were less enteroendocrine cells present per crypt in heme-fed mice (Figure 3D).

To investigate whether there was a downstream effect on Wnt signaling,  $\beta$ -catenin staining was performed (Figure 3E). Staining showed that, in controls  $\beta$ -catenin is mainly located on the cell membrane while, in heme-fed mice, it was concentrated more in the cytosol and nucleus indicating activation of Wnt signaling.

Another downregulated secreted inhibitor of proliferation is Ihh. Ihh was 1.5-fold downregulated in total scrapings, and this was a surface-specific effect (Figure 3A). Ihh antagonizes proliferation by stimulating the secretion of Bmps by lamina propria cells [17]. These Bmps are Wnt antagonists. In line with this, heme also decreased the expression of Bmp2. This downregulation was not reflected in surface or crypt cells illustrating that LCM samples hardly contain lamina propria cells. Unfortunately, decreased Ihh protein expression could not be verified due to lack of an appropriate antibody. It should be noted that Bmp8a and b were upregulated, instead of downregulated, by heme (Supplementary Table 4). The function of these Bmps in colon is unknown and there are no indications that they play a role in epithelial cell proliferation.

Additionally, IL-15 mRNA was downregulated 4-fold by heme, exclusively in surface epithelium (Figure 3A). IL-15 is a pleiotropic cytokine that inhibits proliferation of tumor cells independent of natural killer cells [18]. IL-15 protein was 8 times lower in heme-exposed colons compared to control animals (Figure 3F). So, protein levels were decreased even to a higher extent than IL-15 mRNA levels.

### **Heme increased transcription of growth factor genes, but this was not translated into mitogenic signals**

Growth factors are obvious candidates to trigger hyperproliferation in the crypt. As mentioned above, Wnts were not changed, but the growth factors Amphiregulin (Areg) and Epiregulin (Ereg) were dramatically upregulated at mRNA level (Figure 4A). However, these increased mRNA levels were not translated into increased Areg and Ereg protein levels (Figure 4A). Furthermore, mitogenic metabolites, such as prostaglandins (PGs), might influence cell proliferation. Heme increased Cox-2 expression and the expression of the PGE<sub>2</sub> efflux transporter, Abcc4, in surface epithelium (Figure 4B). Genes involved in PGE<sub>2</sub> catabolism, such as the organic anion transporter Slco2a1 and the hydroxyprostaglandin dehydrogenase-15 (Hpgd), were significantly downregulated in total scrapings (data not shown). Since production and secretion of PGE<sub>2</sub> was increased and catabolism decreased, this should lead to higher extracellular PGE<sub>2</sub> concentrations. However, PGE<sub>2</sub> levels of tissue culture supernatant were significantly decreased by heme (Figure 4B). PGE<sub>2</sub> can easily be converted to PGF<sub>2 $\alpha$</sub> , however, PGF<sub>2 $\alpha$</sub>  levels were also reduced by heme (Figure 4B).

Taken together, these results show that upregulation of mRNAs for mitogenic signals was not translated into effective products. Furthermore, as mentioned above, protein levels of the downregulated IL-15 were also twofold lower than expected from mRNA levels.

This suggests that translation of mRNAs coding for secretory proteins is compromised by heme. In line with this, we found that the ER protein synthesis inhibitor Redd1 (Ddit4) was upregulated 2.5-fold, mainly in surface cells (Figure 4C). Moreover, the cap-dependent translation inhibitor Eif4ebp1 (4E-BP1) was upregulated threefold, also mainly in surface epithelium. Western blot analysis of colon homogenates showed that 4E-BP1 was increased at protein level (Figure 4C). Immunohistochemical staining showed that 4E-BP1 protein expression is increased by heme in surface epithelium (Figure 4C). Together these results indicate that the heme-stressed surface cells repress the ER translation of messengers for secretory proteins. Therefore, we conclude that heme increased proliferation by downregulating feedback inhibitors of proliferation and not by upregulating mitogenic signals.

## DISCUSSION

To our knowledge, this is the first study showing that a non-absorbed nutrient, heme, induces colonic hyperproliferation and hyperplasia by repressing surface secretion of feedback inhibitors of proliferation. Microarray analysis of colonic mucosa showed that cellular stress-response and cell cycle control were the processes most prominently changed by heme. LCM analysis revealed that stress responses occurred in surface cells only, whereas cell cycle control was changed near the bottom of the crypt. Furthermore, our results show that heme did not reach the TA crypt cells, as gene expression levels of heme-sensing genes (such as *Hmox1*, *Slc46a1* and *Abcg2*) and stress-related genes (such as *Nemo*, *Cox-2*, *Tis7*) are surface-specific differentially expressed. Heme probably cannot reach TA cells because fluid efflux from the crypt counteracts the diffusion-driven influx of heme. Consequently, heme only enters the crypt lumen over a limited length. This implies that modulated signals from the stressed surface epithelium have to trigger compensatory cell proliferation in the crypt compartment.

Our data show that heme activates the oxidative stress-sensing transcription factor Nrf2 (Nfe2l2) and upregulates the expression of other stress-sensing transcription factors, as summarized in Figure 5A. This is corroborated by our earlier studies showing that heme induces stress by generating reactive oxygen species (ROS) in the colonic lumen, reflected by a heme-dependent increase in fecal thiobarbituric acid reactive substances (TBARS) [8]. Moreover, dietary antioxidants inhibit the effects of heme on TBARS, luminal cytotoxicity and on colonic mucosa [19]. This is because antioxidants block the radical-mediated synthesis of the cytotoxic heme factor, which is a covalently modified porphyrin molecule derived from heme [11]. Unfortunately, the detailed structure of this heme metabolite remains uncertain as this modified porphyrin is refractory to ionization and thus cannot be identified by mass spectrometry. We think that this cytotoxic factor, together with heme-induced ROS, triggers the activation of the stress-dependent transcription factors and their targets in surface cells (summarized in Figure 5A).

For instance, the significant upregulation of glutathione transferases (Gsta2, 3 and 4), synthases (Gclc and Gclm) and reductase (Gsr) indicates protection against noxious compounds that oxidize cellular SH groups. It has been shown that toxic and oxidative stress inhibits ER protein synthesis [20]. In line with this, upregulated Ddit4 levels lead to inactivation of mTOR and thereby inhibit protein synthesis [21]. Furthermore, increased mRNA and protein levels of 4E-BP1 can contribute to the inhibition of cap-dependent translation specifically in surface epithelium. In our study the increase in mRNA transcripts of secreted proteins such as Areg and Ereg was not translated into protein. The increased synthesis of heme metabolism- and stress-related proteins (e.g. Hmox1, 4E-BP1, respectively) is not in conflict with this mechanism, because stress-response genes can be translated cap-independently by using internal ribosome entry sites [22].

The observed upregulation of the anti-apoptotic NF- $\kappa$ B target genes Xiap and Bcl2l1 in surface cells can be either a response to oxidative or cytotoxic stress. It has recently been shown that upregulation of these NF- $\kappa$ B targets is a protective response in the surface epithelium to compensate for injured cells [23]. In concert with Ier3, this may explain the inhibition of apoptosis observed in surface cells. Combined with the crypt-specific upregulation of survivin, this also explains the heme-reduced amount and activity of cleaved caspase-3 in mucosal homogenate as reported previously [10].

The mucosal signaling of surface cells might not only be compromised by inhibition of ER protein translation, but also by Tis7-mediated repression of transcription which reduces histone-deacetylase activation [24]. Recently, it has been shown that the Tis7-null mutant is not able to initiate compensatory hyperproliferation after mucosal injury, indicating that Tis7 is crucial in the signaling from injured cells to TA crypt cells [25]. Our search for injury-signaling molecules was focused on downregulated feedback inhibitors of proliferation. This is because homeostasis of epithelial cell turnover is theoretically only possible if differentiated surface cells feedback negatively on the TA cells. Furthermore, it is not so likely that damaged surface cells will invest much energy in producing a signaling molecule. Our secretome analysis showed that injured cells indeed regulate more signals down than up. The most relevant surface-specific downregulated candidate signaling molecules were Wif1, Ihh, and IL-15. Our hypothesis about how these proteins can signal to the TA cells is presented in Figure 5B.

Wif1 is a secreted Wnt antagonist that inhibits the Wnt signaling pathway [26]. Heme-induced downregulation of Wif1 gene expression would lead to a more active Wnt-pathway and to increased proliferation. Immunohistochemistry demonstrated that Wif1 protein resides in the upper-half of the crypt in enteroendocrine cells. This is supported by previously reported Wif1 expression by Colo320 cells, a cell line of enteroendocrine origin [26]. The fact that not all enteroendocrine cells express Wif1 reflects the different types of enteroendocrine cells in the gastrointestinal tract [27]. Our novel finding of



basic Wif1 expression in mouse colon contrast with an earlier study indicating Wif1 expression only in colonic and small intestinal tumor tissue, but not in normal wild-type tissue [28]. However, our results are supported by two separate studies showing Wif1 expression in normal human colon tissue and its downregulation in primary colon cancer [26,29]. The question remains whether Wif1 is a primary signaling molecule influencing proliferation rate or whether its downregulation is a secondary effect. For Wif1 to be an initiating factor, enteroendocrine cells should be able to sense the heme-induced cytotoxicity in the lumen. Wif1 downregulation can be a secondary effect if there is a molecule signaling from the surface to cells in the upper-half of the crypt (for instance Ihh, see below). Another possibility is that the downregulation of Wif1 can be attributed to cell fate decisions and/or cell maturation under the influence of dietary heme, as the number of ChgA positive enteroendocrine cells per crypt also decreases. These different, but not mutually exclusive, possibilities require further studies focusing on epithelial cells in the upper half of the crypt.

Crypt cell proliferation can also be controlled by epithelium-to-mesenchyme interactions. For instance, Ihh can influence Bmp secretion from the lamina propria cells [9]. Bmps are members of the TGF $\beta$  family of growth factors that act as Wnt antagonists. Bmp4 has previously been identified as an Ihh-modulated mediator of mesenchymal-epithelial interactions [30] but Bmp2 and 7 might also play a role [17]. Our data indicate that heme downregulated Bmp2 mainly in lamina propria (i.e. mesenchymal) cells. We propose that this lowering of Bmp2 is caused by the lowered expression and secretion of Ihh from surface cells. Ihh also plays a role in epithelial cell differentiation [30]. Whether this is a direct effect of Ihh on nascent epithelial cells or occurs via mesenchymal interactions is not known. Our LCM dataset shows that the Ihh receptor Patched-1 (Ptch1) was expressed both in surface and crypt cells and downregulated by heme (data not shown). This suggests that Ihh may also directly affect epithelial cells. We therefore speculate that Ihh supports the differentiation into Wif1-positive enteroendocrine cells, which might explain their reduced cell number on the heme diet. Mucosal signaling of Ihh requires further investigation, but pertinent to our study is the consistent finding that activation of Ihh signaling inhibits proliferation [17] whereas blocking of Ihh signaling induces hyperproliferation [30].

Our third, surface-specific, downregulated signal is IL-15. IL-15 is a pleiotropic cytokine that can inhibit tumor growth in murine models of cancer by stimulating natural killer cells and CD8<sup>+</sup> cells [31]. However, IL-15 also has direct anti-proliferative effects as it inhibits tumor cell proliferation in mice lacking these cells [18]. IL-15 knockout mice are protected against colitis induced by dextran sulfate sodium that injures the surface epithelium [32]. This suggests that IL-15 must be downregulated for proper compensatory hyperproliferation of colonic epithelium. Alternatively, IL-15 stimulates cell differentiation [33] and thus may affect the number of Wif1-positive enteroendocrine cells. Note that

epithelial cells can sense IL-15 as its receptor (IL-15Ra) is expressed in surface and crypt epithelium (data not shown). These proposed effects of IL-15 require further nutritional studies in IL-15 knockout mice using control and heme-supplemented diets.

In conclusion, this study shows that heme induces hyperproliferation and hyperplasia by repressing the feedback inhibition of proliferation. The heme-induced aberrant turnover of crypt cells observed in this study is identical to that in rats [10], indicating that this heme effect is species-independent. This is further supported by the finding that the protective effect of chlorophyll against heme found in rats is also observed in epidemiological studies in humans [7]. These species-independent effects suggest that the mechanism proposed in this study can be extrapolated to humans. Studies on repression of mucosal signaling by heme in humans would provide further insight into the molecular mechanisms of the relationship between red meat consumption and the risk of colon cancer observed in epidemiological studies.

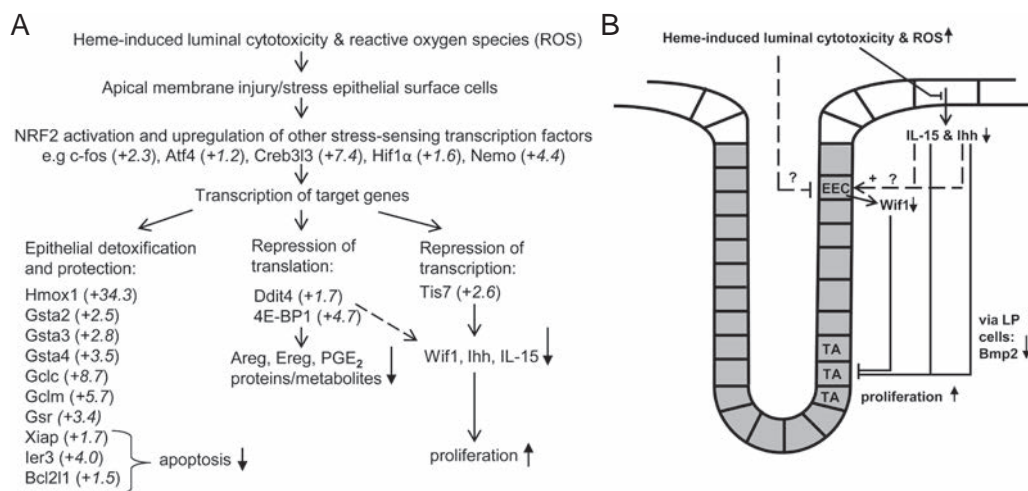


**Figure 5.** Model of proposed mechanism by which heme stresses surface cells and increases crypt cell proliferation. (A) Overview of main pathways changed by heme in surface cells. Fold changes in surface cells are shown in *italics*. (B) Model of heme-modulated signaling from surface to crypt cells. TA; transit-amplifying cell, EEC; enteroendocrine cell. Bold arrowheads indicate direction of heme-induced changes.

## ACKNOWLEDGEMENTS

The authors thank Mechteld Grootte Bromhaar, Jenny Jansen, Philip de Groot and Mark Boekschoten for microarray analysis and Bert Weijers for technical assistance.



## REFERENCES

- 1 Jemal A, Siegel R, et al. Cancer statistics, 2008. *CA Cancer J Clin* 2008;58:71-96.
- 2 World Cancer Research Fund. Food, Nutrition, Physical Activity and the Prevention of Cancer: a Global Perspective. Washington, DC: American Institute for Cancer Research, 2007.
- 3 Giovannucci E, Rimm EB, et al. Intake of fat, meat, and fiber in relation to risk of colon cancer in men. *Cancer Res* 1994;54:2390-7.
- 4 Larsson SC, Rafter J, et al. Red meat consumption and risk of cancers of the proximal colon, distal colon and rectum: the Swedish Mammography Cohort. *Int J Cancer* 2005;113:829-34.
- 5 Kinzler KW, Vogelstein B. Lessons from hereditary colorectal cancer. *Cell* 1996;87:159-70.
- 6 Lee DH, Anderson KE, et al. Heme iron, zinc, alcohol consumption, and colon cancer: Iowa Women's Health Study. *J Natl Cancer Inst* 2004;96:403-7.
- 7 Balder HF, Vogel J, et al. Heme and chlorophyll intake and risk of colorectal cancer in the Netherlands cohort study. *Cancer Epidemiol Biomarkers Prev* 2006;15:717-25.
- 8 Sesink AL, Termont DS, et al. Red meat and colon cancer: the cytotoxic and hyperproliferative effects of dietary heme. *Cancer Res* 1999;59:5704-9.
- 9 van der Flier LG, Clevers H. Stem cells, self-renewal, and differentiation in the intestinal epithelium. *Annu Rev Physiol* 2009;71:241-60.
- 10 de Vogel J, van-Eck WB, et al. Dietary heme injures surface epithelium resulting in hyperproliferation, inhibition of apoptosis and crypt hyperplasia in rat colon. *Carcinogenesis* 2008;29:398-403.
- 11 de Vogel J, Jonker-Termont DS, et al. Green vegetables, red meat and colon cancer: chlorophyll prevents the cytotoxic and hyperproliferative effects of haem in rat colon. *Carcinogenesis* 2005;26:387-93.
- 12 Lapre JA, Termont DS, et al. Lytic effects of mixed micelles of fatty acids and bile acids. *Am J Physiol* 1992;263:G333-7.
- 13 Loboda A, Jazwa A, et al. Heme oxygenase-1 and the vascular bed: from molecular mechanisms to therapeutic opportunities. *Antioxid Redox Signal* 2008;10:1767-812.
- 14 West AR, Oates PS. Mechanisms of heme iron absorption: current questions and controversies. *World J Gastroenterol* 2008;14:4101-10.
- 15 Latunde-Dada GO, Simpson RJ, et al. Recent advances in mammalian haem transport. *Trends Biochem Sci* 2006;31:182-8.
- 16 Zhang K, Shen X, et al. Endoplasmic reticulum stress activates cleavage of CREBH to induce a systemic inflammatory response. *Cell* 2006;124:587-99.
- 17 van Dop WA, Uhmman A, et al. Depletion of the colonic epithelial precursor cell compartment upon conditional activation of the hedgehog pathway. *Gastroenterology* 2009;136:2195-203 e1-7.
- 18 Davies E, Reid S, et al. IL-15 has innate anti-tumor activity independent of NK and CD8 T cells. *J Leukoc Biol*;88:529-36.
- 19 Pierre F, Tache S, et al. Meat and cancer: haemoglobin and haemin in a low-calcium diet promote colorectal carcinogenesis at the aberrant crypt stage in rats. *Carcinogenesis* 2003;24:1683-90.
- 20 Messner DJ, Kowdley KV. Biting the iron bullet: endoplasmic reticulum stress adds the pain of hepcidin to chronic liver disease. *Hepatology* 2010;51:705-7.
- 21 Jacinto E. What controls TOR? *IUBMB Life* 2008;60:483-96.
- 22 Sonenberg N, Hinnebusch AG. Regulation of translation initiation in eukaryotes: mechanisms and biological targets. *Cell* 2009;136:731-45.
- 23 Pasparakis M. Regulation of tissue homeostasis by NF-kappaB signalling: implications for inflammatory diseases. *Nat Rev Immunol* 2009;9:778-88.
- 24 Viator I, Huber LA. Role of TIS7 family of transcriptional regulators in differentiation and regeneration. *Differentiation* 2007;75:891-7.
- 25 Yu C, Jiang S, et al. Deletion of Tis7 protects mice from high-fat diet-induced weight gain and blunts the intestinal adaptive response postresection. *J Nutr*;140:1907-14.
- 26 Taniguchi H, Yamamoto H, et al. Frequent epigenetic inactivation of Wnt inhibitory factor-1 in human gastrointestinal cancers. *Oncogene* 2005;24:7946-52.

- 27 Rindi G, Leiter AB, et al. The "normal" endocrine cell of the gut: changing concepts and new evidences. *Ann N Y Acad Sci* 2004;1014:1-12.
- 28 Cebrat M, Strzadala L, et al. Wnt inhibitory factor-1: a candidate for a new player in tumorigenesis of intestinal epithelial cells. *Cancer Lett* 2004;206:107-13.
- 29 He B, Reguart N, et al. Blockade of Wnt-1 signaling induces apoptosis in human colorectal cancer cells containing downstream mutations. *Oncogene* 2005;24:3054-8.
- 30 van den Brink GR, Bleuming SA, et al. Indian Hedgehog is an antagonist of Wnt signaling in colonic epithelial cell differentiation. *Nat Genet* 2004;36:277-82.
- 31 Carson WE, Giri JG, et al. Interleukin (IL) 15 is a novel cytokine that activates human natural killer cells via components of the IL-2 receptor. *J Exp Med* 1994;180:1395-403.
- 32 Yoshihara K, Yajima T, et al. Role of interleukin 15 in colitis induced by dextran sulphate sodium in mice. *Gut* 2006;55:334-41.
- 33 Barao I, Hudig D, et al. IL-15-mediated induction of LFA-1 is a late step required for cytotoxic differentiation of human NK cells from CD34+Lin- bone marrow cells. *J Immunol* 2003;171:683-90.

## SUPPLEMENTARY METHODS

### Immunohistochemistry

Paraffin embedded colon sections of 5  $\mu\text{m}$  were deparaffinized and rehydrated in a series of graded alcohols. Sections were incubated for 25 min in 3%  $\text{H}_2\text{O}_2$  in PBS to block endogenous peroxidase activity. Sections were placed in antigen retrieval solution (sodium citrate buffer, pH=6) and heated in a microwave oven for 5 min 700W followed by 20 min 500W, after which they were cooled to room temperature. Subsequently, the single immunostainings were performed according to standard procedures with components mentioned in Supplementary Table 1. Unless states otherwise, incubations were performed at room temperature and were followed by three 5 min washing steps with PBS. Dilutions were made with 1% BSA in PBS. Incubation without first antibodies served as negative control.

To visualize co-localization of Wnt Inhibitory Factor 1 (Wif1) and chromogranin A (ChgA), immunofluorescence was performed. Paraffin sections were blocked for endogenous peroxide and treated for optimal antigen retrieval as described above. Sections were incubated with 10% normal donkey serum (Sigma-Aldrich Chemie) in 0.05 M - 0.05% v/v TBS-Tween 20 for 30 min. Sections were then incubated with 1:100 goat anti-mouse Wif1 antibody (R&D Systems, Minneapolis, USA) overnight at 4°C. Subsequently sections were incubated with 1:100 rabbit anti-mouse ChgA (Abcam, Cambridge, UK) for 1h. To visualize Wif1, sections were then incubated with donkey anti-goat Cy3.5-conjugated (Abcam) in a 1:1500 dilution for 1h. Non-specific binding of the second antibody of ChgA was blocked by 20% normal goat serum for 30 min followed by incubation of 1:100 goat anti-rabbit Alexa488-conjugated (Active Motif, Rixensart, Belgium) for 1h. Nuclei were visualized with DAPI staining. Unless stated otherwise, incubations were done at room temperature and were followed by three 5-min washing steps with 0.05 M - 0.05% v/v TBS-Tween 20. Incubation without the first antibody served as negative control.

### RNA isolation

Total RNA was isolated by using TRIzol reagent (Invitrogen, Breda, the Netherlands) according to the manufacturer's protocol. For microarray hybridization isolated RNA was further column purified (SV total RNA isolation system Promega, Leiden, the Netherlands). RNA concentration was measured on a Nanodrop ND-1000 UV-Vis spectrophotometer (Isogen, Maarssen, the Netherlands) and analyzed on an Agilent 2100 bioanalyzer (Agilent Technologies, Amsterdam, the Netherlands) with 6000 Nano Chips, according to the supplier's protocol. RNA was judged as suitable for array hybridization only if samples exhibited intact bands corresponding to the 18S and 28S ribosomal RNA subunits, and displayed no chromosomal peaks or RNA degradation products (RNA Integrity Number > 8.0). Two control mice did not meet the criteria and were excluded from array analysis.

**Supplementary Table 1.** *Antibodies and staining protocol.*

Antibody	Block	1st Ab	Dilution, incubation time	2nd Ab	Dilution, incubation time	Enhancing component	Visuali- zation	Counter stain
Ki67	normal goat serum	DakoCytomation, Heverlee, Belgium	1:200, 90 min	biotinylated goat- anti-rat Ig	1:200, 30 min	AB complex (Vector laboratories) (1:100), 45 min	DAB	haema toxylin
Cleaved Casp3	TENG-T	Cell Signaling Technology, Danvers, USA	1:100 Overnight at 4°C	biotinylated goat- anti-rabbit Ig	1:2000, 1h	AB complex (1:100) 60 min	DAB	haema toxylin
Hmox1	normal goat serum	Abcam, Cambridge, UK	1:100, 2 h	biotinylated goat- anti-rabbit Ig	1:200, 30 min	AB complex (1:100) 45 min	AEC	haema toxylin
Wif1	normal goat serum	R&D Systems, Minneapolis, USA	1:100, 1h	biotinylated goat- anti-rat Ig	1:100, 1h	AB complex (1:100) 45 min	AEC	none
Chromo- granin A	normal donkey serum	Abcam, Cambridge, UK	1:100, 1h	donkey anti- rabbit alkaline phosphatase- conjugated	1:100, 1h		Fast Blue	none
β-catenin	normal goat serum	BD Transduction Laboratories, Lexington, USA	1:100 Overnight at 4°C	biotinylated goat- anti-mouse Ig	1:200, 30 min	AB complex (1:100) 45 min	DAB	haema toxylin
4E-BP1	normal goat serum	Cell Signaling Technology Danvers, USA	1:5000 Overnight at 4°C	biotinylated goat- anti-rabbit Ig	1:200, 1h	AB complex (1:100) 45 min	DAB	haema toxylin

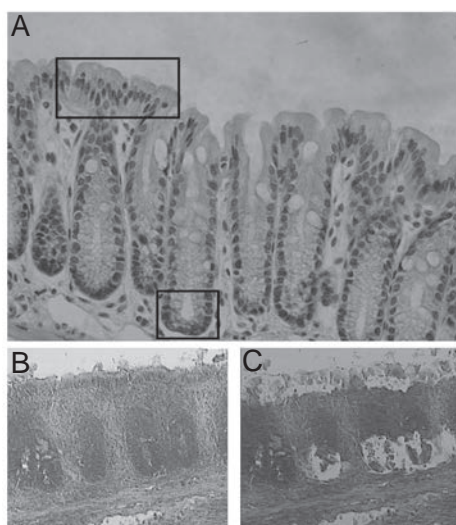
## **Array hybridization and microarray data analysis**

For each individual mouse (n=7 control; n=9 heme) colon RNA was hybridized to Affymetrix Mouse genome 430 2.0 arrays (Affymetrix, Santa Clara, CA, USA). Detailed methods for labeling and hybridizations to the arrays are described in the eukaryotic section in the GeneChip Expression Analysis Technical Manual Rev. 3 from Affymetrix, which is available upon request. Arrays were scanned on a GeneChip Scanner 3000-7G (Affymetrix). Expression levels of probe sets were calculated using GCRMA[1] and probesets were redefined according to Dai et al. [2]. Differential gene expression was determined using Limma [3] and p-values were corrected for multiple testing using a false discovery rate method [4]. Genes that satisfied the criterion of false discovery rate < 1% (q-value < 0.01) were considered to be significantly differentially expressed between control and heme diet. Genes with signal intensities below 20 in both treatments were considered absent and were excluded from further analysis. To identify biological processes influenced by dietary heme, differentially expressed genes were categorized based on their Gene Ontology Biological Process annotation. Furthermore, pathway analysis was performed using Ingenuity Canonical Pathway Analysis (Ingenuity® Systems, [www.ingenuity.com](http://www.ingenuity.com)). This analysis identifies the pathways from the Ingenuity Pathways Analysis library of canonical pathways that are most significant to a microarray data set. Fisher's exact test was used to calculate a p-value determining the probability that the association between the genes in the dataset and the canonical pathway is explained by chance alone. To determine the direction of dietary heme-induced changes in cell cycle-related processes, microarray data were overlaid on the KEGG Cell Cycle Reference pathway ([www.genome.jp/kegg/pathway.html](http://www.genome.jp/kegg/pathway.html)).

## **Laser Capture Microdissection**

Seven-  $\mu\text{m}$  cryo-sections of colon tissue of 4 control- and 3 heme-fed mice were cut at  $-20^{\circ}\text{C}$ . Four serial sections were transferred onto one glass-slide (Superfrost plus, VWR international, Leuven, Belgium) and stored at  $-80^{\circ}\text{C}$ . Immediately before performing LCM, slides were thawed for 1 min at room temperature. Sections were dehydrated in resp. 70% EtOH, 90 % EtOH and 100% EtOH, all steps for 30 seconds. Sections were then incubated in xylene for 2 min and air-dried for 2 min at room temperature. A  $7.5\ \mu\text{m}$  laser beam was used for LCM using the Pix-cell II apparatus (Arcturus, MountainView, CA, USA). HS caps (Arcturus) were used to capture cells. For each animal surface epithelium and lower crypt transit amplifying (TA) cells, from well oriented crypts (longitudinal section), were isolated from 24 sections. Using this technique, samples were almost free of lamina propria cells. Pictures of colon tissue before and after applying LCM can be found in Supplementary Figure 1. RNA was isolated from caps by using the PicoPure RNA isolation kit (Arcturus), according to manufacturer's protocol. Total RNA was pooled for the 4 groups: Control Surface, Control Crypt, Heme Surface and Heme Crypt.

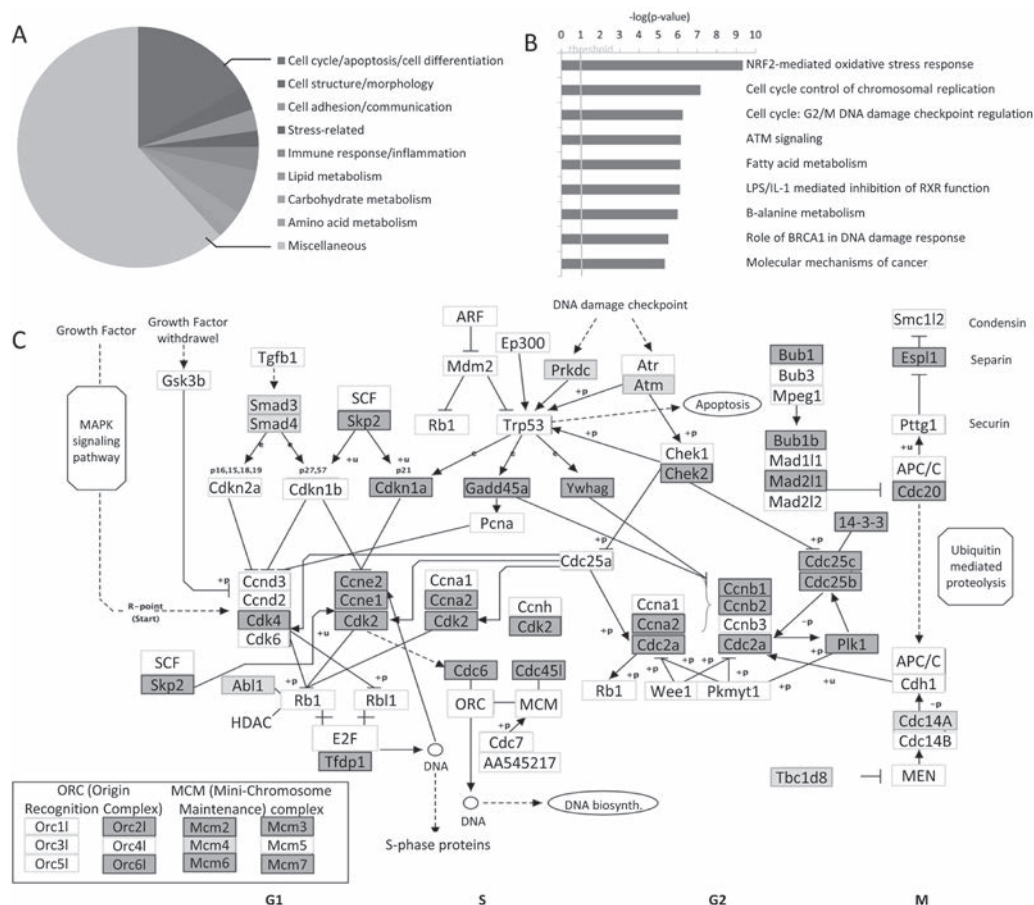
Array analysis was performed with Affymetrix Mouse Gene 1.0 ST arrays with 100 ng of RNA. Labeling was performed with 'Affymetrix Whole Transcript Sense Labeling without rRNA reduction step' according to the WT Sense Target Labeling Assay Manual (Affymetrix Santa Clara, CA). Arrays were normalized using the Robust Multi-array Average (RMA) method [5,6]. Further microarray analysis was performed as described above. LCM microarray results were validated with the crypt marker cystic fibrosis transmembrane conductance regulator (CFTR) known to be high expressed in the crypt and the surface marker carbonic anhydrase 1 (CAR1) which is mainly present at the surface epithelium. In control mice CFTR was higher expressed at the crypt (signal intensity 1449 vs 225) and Car1 had a higher expression at the surface (signal intensity 7295 vs 1656).



**Supplementary Figure 1.** Isolated parts of colon tissue by LCM. Colon tissue with indicated the surface and crypt cells that were isolated with LCM (A). Representative pictures of colon tissue before LCM procedure (B) and after using LCM (C) to remove the lower crypt cells and the surface cells. Cells residing halfway the crypt are not isolated in this study. Tissue is defrosted and dehydrated by a gradient of alcohols and xylene. In LCM the tissue is not stained.

### **Determination of amphiregulin, epiregulin, IL-15, PGE<sub>2</sub> and PGF<sub>2α</sub>**

Quantitative determination of Amphiregulin (Areg), Epiregulin (Ereg) and Interleukin-15 (IL-15) was done by specific ELISA (Areg and Ereg: Douset Elisa Development System, R&D Systems, IL-15: Mouse IL-15 ELISA Ready-SET-Go, eBioscience, San Diego, CA, USA). Briefly, homogenates of colon tissue were made by adding 1 ml of PBS containing protease inhibitors (CompleteMini, Roche Diagnostics, Mannheim, Germany) to a mucosal scraping of one animal. Tissue was homogenized using a turrax. Homogenates were centrifuged for 10 min at 4°C at 20,000xg and supernatant was collected. For Areg and Ereg ELISAs, samples were used undiluted. For the IL-15 ELISA samples were diluted to a concentration of 150 µg/ml total protein. All ELISA samples were added in duplicate to a 96-well plate coated with Areg, Ereg or IL-15 capture antibody, respectively. Samples and standards (processed according to the manufacturer's protocol) were incubated for 2 h at room temperature. Reactions were measured using an ELISA photometer



**Supplementary Figure 2.** Pathway analysis of heme-induced differentially expressed genes in colonic mucosal scrapings. For all analyses, only differentially expressed genes meeting the selection criteria ( $q < 0.01$  and signal intensity  $> 20$  in at least of the treatments) were included. (A) Categorization of differentially expressed genes according to their GO Biological Process annotation. The miscellaneous category contains processes with broad and thus unspecific biological process terms. (B) Top 10 of canonical pathways that are influenced by dietary heme using Ingenuity Canonical pathway analysis.  $P$ -value  $< 0.05$  was set as a threshold for significant associations between differentially expressed genes in a canonical pathway. (C) Microarray data were overlaid on the KEGG Cell Cycle Reference pathway. Dark and light gray indicate up and downregulation, respectively.

plate reader at a wavelength of 450 nm with a wavelength correction of 540 nm. Prostaglandin (PG) levels were measured in tissue culture supernatants, as EIA was not suitable for measuring PGs in homogenates. Thereto, colon tissue was taken into culture immediately after sacrificing the mice. The colon was cut open and washed in cold PBS with 1% penicillin/streptomycin. From the colon 6 pieces of 1 cm were cut. Two pieces (1 cm from proximal and 1 cm from distal part) were incubated in 500  $\mu$ l serum-free RPMI 1640 medium with 1% penicillin/streptomycin at 37°C/5% CO<sub>2</sub>. Incubations were performed in triplicate. After 24h incubation the medium was harvested, pooled per



animal and centrifuged for 10 min at 10,000xg to get rid of sediments. Supernatant was used 150-fold diluted for PGE<sub>2</sub> and the PGF<sub>2α</sub> EIA assay (Cayman Chemical Company, Ann Arbor, Michigan, USA) and performed according to the manufacturer's protocol.

## Western blotting

Colon tissue homogenates were prepared as described above. Samples were applied to SDS-PAGE (12% gel) and transferred to polyvinylidene fluoride membranes. Ten µg total protein was loaded for detection of 4E-BP1 and β-actin. Membranes were blocked with Tris-buffered saline with 0.1% Tween20 and 5% dry milk (ELK) and probed overnight at 4°C with antibodies against 4E-BP1 (Cell Signaling Technology, Danvers, USA) and β-actin (Sigma-Aldrich) both diluted 1:1000. Blots were incubated with 5000x diluted HRP-linked goat anti-rabbit antibody (Sigma-Aldrich) at room temperature for 1 h. The signals were detected with the enhanced chemiluminescence detection system (Amersham ECL, GE Healthcare, Little Chalfont, UK).

**Supplementary Table 2.** *The 50 highest significantly upregulated genes in mouse colon scrapings upon heme-feeding, as determined by microarray analysis. Mean signal intensities ± SEM for control (n=7) and for heme (n=9) are given.*

	Description	Gene name	Control	Heme	FC <sup>a</sup>
1	fatty acid binding protein 1, liver	Fabp1	27±8	3458±315	127.8
2	cytochrome P450, family 4, subfamily a, polypeptide 10	Cyp4a10	6±1	544±77	97.9
3	secretory leukocyte peptidase inhibitor	Slpi	36±3	2961±498	82.8
4	heme oxygenase (decycling) 1	Hmox1	12±1	425±89	34.6
5	RIKEN cDNA 2010109I03 gene	2010109I03Rik	16±2	294±53	18.6
6	malic enzyme 1, NADP(+)-dependent, cytosolic	Me1	83±21	1103±61	13.3
7	ATP-binding cassette, sub-family C (CFTR/MRP), member 4	Abcc4	51±9	646±58	12.8
8	apolipoprotein C-II	Apoc2	35±7	445±46	12.8
9	carbonyl reductase 3	Cbr3	510±31	6402±226	12.5
10	small proline-rich protein 1A	Sprr1a	139±47	1664±144	11.9
11	glutathione S-transferase, alpha 2 (Yc2)	Gsta2	8±1	89±12	11.2
12	aldo-keto reductase family 1, member B8	Akr1b8	679±20	6909±168	10.2
13	cAMP responsive element binding protein 3-like 3	Creb3l3	63±12	626±23	9.9
14	creatine kinase, mitochondrial 2	Ckmt2	38±5	362±19	9.5
15	acyl-Coenzyme A oxidase 2, branched chain	Acox2	9±1	81±10	9.0
16	amphiregulin	Areg	85±26	743±58	8.7
17	metallothionein 4	Mt4	6±0	54±15	8.5
18	glutathione S-transferase, alpha 3	Gsta3	38±5	321±19	8.4
19	tripartite motif protein 29	Trim29	7±1	51±4	7.7
20	acyl-CoA thioesterase 1	Acot1	116±19	827±66	7.1
21	RIKEN cDNA E130012A19 gene	E130012A19Rik	16±4	113±26	7.1



22	pyruvate dehydrogenase kinase, isoenzyme 4	Pdk4	335±130	2348±195	7.0
23	angiopoietin-like 4	Angptl4	56±19	380±37	6.8
24	pleckstrin homology-like domain, family A, member 2	Phlda2	7±1	48±8	6.7
25	immediate early response 3	Ier3	68±9	436±39	6.5
26	capping protein (actin filament), gelsolin-like	Capg	360±42	2321±122	6.4
27	solute carrier family 27 (fatty acid transporter), member 2	Slc27a2	48±7	304±34	6.3
28	cell death-inducing DFFA-like effector c	Cidec	36±8	226±12	6.2
29	pirin	Pir	58±7	354±13	6.1
30	histocompatibility 2, Q region locus 10	H2-Q10	26±2	154±9	5.9
31	acyl-CoA thioesterase 2	Acot2	30±3	178±14	5.8
32	expressed sequence AI747448	AI747448	61±17	345±73	5.7
33	epiregulin	Ereg	16±4	91±13	5.6
34	RIKEN cDNA 2310016C08 gene	2310016C08Rik	26±2	143±10	5.5
35	retinol binding protein 2, cellular	Rbp2	128±21	666±71	5.2
36	aldehyde dehydrogenase family 1, subfamily A7	Aldh1a7	274±27	1377±57	5.0
37	proprotein convertase subtilisin/kexin type 9	Pcsk9	35±3	174±12	4.9
38	glutamate-cysteine ligase, catalytic subunit	Gclc	1267±103	5789±425	4.6
39	aldo-keto reductase family 1, member C18	Akr1c18	104±23	470±43	4.5
40	transmembrane 6 superfamily member 2	Tm6sf2	118±11	513±56	4.4
41	acetyl-Coenzyme A acyltransferase 1B	Acaa1b	1754±271	7541±361	4.3
42	scavenger receptor class B, member 1	Scarb1	75±5	314±20	4.2
43	phosphoserine aminotransferase 1	Psat1	38±2	161±13	4.2
44	transferrin	Trf	49±12	203±22	4.2
45	solute carrier family 1 member 4	Slc1a4	101±8	420±48	4.1
46	adenosine deaminase	Ada	85±17	352±21	4.1
47	plasminogen activator, urokinase receptor	Plaur	47±5	188±16	4.0
48	acyl-CoA thioesterase 4	Acot4	23±3	88±4	3.9
49	fatty acid desaturase 1	Fads1	27±2	105±11	3.9
50	polo-like kinase 1 (Drosophila)	Plk1	108±22	419±22	3.9

<sup>a</sup> FC (fold change) calculated by dividing average heme signal by average control signal. Table includes significant different genes ( $q < 0.01$ ) and only genes with a signal intensity  $> 20$  in at least one condition.

**Supplementary Table 3.** The 50 highest significantly downregulated genes in mouse colon scrapings upon heme-feeding, as determined by microarray analysis. Mean signal intensities  $\pm$  SEM for control ( $n=7$ ) and for heme ( $n=9$ ) are given.

	Description	Gene name	Control	Heme	FC <sup>a</sup>
1	solute carrier family 13 (sodium/sulphate symporters), member 1	Slc13a1	956±147	37±4	-26.1
2	cubilin (intrinsic factor-cobalamin receptor)	Cubn	313±61	17±2	-18.7
3	fatty acid binding protein 6, ileal (gastrotrypin)	Fabp6	2324±467	193±25	-12.1
4	regulated endocrine-specific protein 18	Resp18	85±10	7±0	-11.5
5	solute carrier family 46, member 1	Slc46a1	140±30	14±1	-9.8

6	D site albumin promoter binding protein	Dbp	434±116	44±10	-9.8
7	granzyme A	Gzma	111±13	12±1	-9.7
8	chromogranin A	Chga	902±86	103±11	-8.8
9	cytochrome P450, family 27, subfamily a, polypeptide 1	Cyp27a1	254±20	32±2	-8.0
10	serum amyloid A 3	Saa3	415±100	52±5	-8.0
11	X transporter protein 3 similar 1 gene	Xtrp3s1	87±11	12±1	-7.4
12	endothelin 1	Edn1	266±44	37±3	-7.2
13	cytochrome P450, family 4, subfamily v, polypeptide 3	Cyp4v3	73±7	10±1	-7.2
14	angiogenin, ribonuclease A family, member 4	Ang4	2737±1259	391±61	-7.0
15	glutamyl aminopeptidase	Enpep	878±154	126±27	-6.9
16	ATP-binding cassette, sub-family G (WHITE), member 5	Abcg5	59±19	9±0	-6.7
17	tryptophan hydroxylase 1	Tph1	506±63	80±7	-6.4
18	solute carrier family 10, member 2	Slc10a2	280±37	44±5	-6.3
19	calponin 1	Cnn1	52±33	9±1	-6.0
20	transmembrane protein 86A	Tmem86a	113±33	19±1	-5.9
21	myelin and lymphocyte protein, T-cell differentiation protein	Mal	180±33	31±3	-5.8
22	butyrylcholinesterase	Bche	211±32	37±1	-5.7
23	transgelin	Tagln	191±107	34±5	-5.6
24	cytochrome P450, family 2, subfamily d, polypeptide 12	Cyp2d12	437±83	84±14	-5.2
25	actin, gamma 2, smooth muscle, enteric	Actg2	303±157	59±8	-5.1
26	interferon-induced protein with tetratricopeptide repeats 1	Ifit1	129±26	25±7	-5.1
27	carboxypeptidase B2 (plasma)	Cpb2	41±10	8±1	-4.9
28	transforming growth factor, beta induced	Tgfb1	886±61	183±21	-4.8
29	myosin, heavy polypeptide 11, smooth muscle	Myh11	104±34	22±3	-4.8
30	Wnt inhibitory factor 1	Wif1	79±11	16±1	-4.8
31	peroxisome proliferative activated receptor, gamma, coactivator 1 alpha	Ppargc1a	460±46	96±8	-4.8
32	cytochrome P450, family 2, subfamily f, polypeptide 2	Cyp2f2	54±15	11±1	-4.7
33	tyrosine aminotransferase	Tat	106±10	23±3	-4.7
34	chemokine (C-C motif) ligand 5	Ccl5	58±7	13±1	-4.6
35	RIKEN cDNA 5430427M07 gene	5430427M07Rik	41±12	9±1	-4.5
36	amionless	Amn	139±27	32±3	-4.3
37	deiodinase, iodothyronine, type I	Dio1	3889±110	917±88	-4.2
38	myosin, light polypeptide 9, regulatory	Myl9	75±29	18±3	-4.2
39	histocompatibility 2, T region locus 3	H2-T3	141±40	33±2	-4.2
40	RIKEN cDNA 2210407C18 gene	2210407C18Rik	852±141	209±26	-4.1
41	deoxyribonuclease 1-like 2	Dnase1l2	68±12	17±1	-4.0
42	zinc finger protein 677	Zfp677	76±9	19±2	-4.0
43	RIKEN cDNA 1810030J14 gene	1810030J14Rik	11385±2408	2892±423	-3.9
44	CD83 antigen	Cd83	49±6	13±1	-3.9
45	interleukin 15	Il15	345±31	89±12	-3.9

46	homeo box B5	Hoxb5	108±12	29±2	-3.8
47	syncollin	Sycn	2876±522	786±118	-3.7
48	RIKEN cDNA 2010002M12 gene	2010002M12Rik	94±8	26±4	-3.6
49	zonadhesin	Zan	36±4	10±0	-3.6
50	sulfotransferase family, cytosolic, 1C, member 2	Sult1c2	930±54	260±28	-3.6

<sup>a</sup>FC (fold change) calculated by dividing average heme signal by average control signal. Table includes significant different genes ( $q < 0.01$ ) and only genes with a signal intensity > 20 in at least one condition.

**Supplementary Table 4.** Secretome Table. Mean signal intensities ± SEM for control (n=7) and for heme (n=9) are given. From the microarray dataset of total scrapings genes with a GO Cellular Localization of extracellular space or extracellular region were selected. Of those genes, genes with plasma membrane, integral to membrane, mitochondrion, nucleus, peroxisome and intracellular in their GO localization were excluded, except if they have cytokine or growth factor activity. Genes were further selected on outer membrane or extracellular secretion in GeneRif and Pubmed.

Description	Gene name	Control	Heme	FC <sup>a</sup>
secretory leukocyte peptidase inhibitor	Slpi	36±3	2961±498	82.8
apolipoprotein C-II	Apoc2	35±7	445±46	12.8
amphiregulin	Areg	85±26	743±58	8.7
angiopoietin-like 4	Angptl4	56±19	380±37	6.8
epiregulin	Ereg	16±4	91±13	5.6
proprotein convertase subtilisin/kexin type 9	Pcsk9	35±3	174±12	4.9
transferrin	Trf	49±12	203±22	4.2
cystatin E/M	Cst6	35±5	130±9	3.7
mast cell protease 1	Mcpt1	7±1	24±5	3.5
phospholipase A2, group V	Pla2g5	48±10	149±29	3.1
sulfatase 2	Sulf2	71±7	182±11	2.6
bone morphogenetic protein 8b	Bmp8b	8±0	20±1	2.5
ependymin related protein 1 (zebrafish)	Epdr1	11±1	24±1	2.2
lipase, endothelial	Lipg	39±3	86±7	2.2
vanin 1	Vnn1	818±93	1740±99	2.1
growth differentiation factor 15	Gdf15	10±1	22±1	2.1
lipoprotein lipase	Lpl	322±43	662±61	2.1
tissue factor pathway inhibitor 2	Tfpi2	231±34	470±23	2.0
CEA-related cell adhesion molecule 12	Ceacam12	27±4	54±6	2.0
bone morphogenetic protein 8a	Bmp8a	38±2	65±4	1.7
betacellulin, epidermal growth factor family member	Btc	16±1	23±1	1.4
DNA segment, Chr 17, Wayne State University 104, expressed	D17Wsu104e	370±16	532±22	1.4
chemokine-like factor	Cklf	52±3	68±2	1.3
arginine-rich, mutated in early stage tumors	Armet	2485±174	3157±117	1.3
hepatoma-derived growth factor	Hdgf	396±12	472±20	1.2
acid phosphatase 5, tartrate resistant	Acp5	3030±52	2665±60	-1.1
testis expressed gene 264	Tex264	449±12	387±9	-1.2
transmembrane protease, serine 8 (intestinal)	Tmprss8	4041±169	3415±99	-1.2

trefoil factor 3, intestinal	Tff3	10224±161	8536±290	-1.2
stromal cell derived factor 4	Sdf4	83±2	69±2	-1.2
protease, serine, 32	Prss32	5262±159	4304±116	-1.2
cystatin C	Cst3	2786±87	2179±37	-1.3
Niemann Pick type C2	Npc2	1899±129	1467±34	-1.3
cathepsin L	Ctsl	3084±86	2371±67	-1.3
kallikrein 1	Klk1	20514±540	15756±567	-1.3
left right determination factor 1	Lefty1	23±2	17±1	-1.4
tubulointerstitial nephritis antigen	Tinag	869±47	632±28	-1.4
CEA-related cell adhesion molecule 10	Ceacam10	580±51	415±27	-1.4
KTEL (Lys-Tyr-Glu-Leu) containing 1	Ktelc1	29±3	20±1	-1.4
tachykinin 1	Tac1	316±10	218±7	-1.4
somatostatin	Sst	21±1	14±1	-1.5
Indian hedgehog	Ihh	571±43	376±15	-1.5
platelet derived growth factor, alpha	Pdgfa	277±32	179±10	-1.5
colony stimulating factor 2 receptor, alpha, low-affinity	Csf2ra	124±6	79±7	-1.6
kallikrein 1-related peptidase b4	Klk1b4	68±8	43±2	-1.6
hepatocyte growth factor activator	Hgfac	2413±61	1518±57	-1.6
ficolin A	Fcna	28±3	17±0	-1.7
fibrinogen-like protein 2	Fgl2	914±85	540±29	-1.7
selenoprotein P, plasma, 1	Sepp1	14434±182	8138±440	-1.8
serum amyloid A 1	Saa1	12634±520	7122±481	-1.8
serum amyloid A 2	Saa2	269±19	149±9	-1.8
growth arrest specific 6	Gas6	2797±96	1493±41	-1.9
platelet-derived growth factor, C polypeptide	Pdgfc	48±6	25±1	-1.9
thrombospondin 1	Thbs1	43±2	22±1	-2.0
neurotensin	Nts	1455±202	720±55	-2.0
bone morphogenetic protein 2	Bmp2	543±57	263±12	-2.1
complement factor B	Cfb	524±16	242±11	-2.2
carboxylesterase 6	Ces6	4367±303	1961±253	-2.2
neuroblastoma, suppression of tumorigenicity 1	Nbl1	37±5	16±1	-2.2
transcobalamin 2	Tcn2	1126±41	501±28	-2.2
angiogenin, ribonuclease, RNase A family, 5	Ang	813±34	361±19	-2.3
tumor necrosis factor (ligand) superfamily, member 13b	Tnfsf13b	32±6	14±1	-2.3
dipeptidylpeptidase 7	Dpp7	137±12	57±4	-2.4
colipase, pancreatic	Clps	363±25	146±25	-2.5
secretin	Sct	213±44	85±4	-2.5
chemokine (C-C motif) ligand 6	Ccl6	3341±147	1336±97	-2.5
carboxypeptidase E	Cpe	727±50	289±17	-2.5
secretogranin V	Scg5	27±3	11±1	-2.5
amiloride binding protein 1 (amine oxidase, copper-containing)	Abp1	4398±111	1654±93	-2.7

protease, serine, 23	Prss23	835±84	297±22	-2.8
chemokine (C-C motif) ligand 25	Ccl25	84±22	30±2	-2.8
procollagen, type VIII, alpha 1	Col8a1	20±5	6±0	-3.2
endothelin 2	Edn2	245±30	74±9	-3.3
chromogranin B	Chgb	5025±397	1497±54	-3.4
proprotein convertase subtilisin/kexin type 1 inhibitor	Pcsk1n	23±1	7±0	-3.4
proprotein convertase subtilisin/kexin type 1	Pcsk1	75±13	21±1	-3.5
interleukin 15	Il15	345±31	89±12	-3.9
chemokine (C-C motif) ligand 5	Ccl5	58±7	13±1	-4.6
Wnt inhibitory factor 1	Wif1	79±11	16±1	-4.8
transforming growth factor, beta induced	Tgfb1	886±61	183±21	-4.8
carboxypeptidase B2 (plasma)	Cpb2	41±10	8±1	-4.9
angiogenin, ribonuclease A family, member 4	Ang4	2737±1259	391±61	-7.0
endothelin 1	Edn1	266±44	37±3	-7.2
serum amyloid A 3	Saa3	415±100	52±5	-8.0
chromogranin A	Chga	902±86	103±11	-8.8
granzyme A	Gzma	111±13	12±1	-9.7
regulated endocrine-specific protein 18	Resp18	85±10	7±0	-11.5

<sup>a</sup> fold change calculated by dividing average heme signal by average control signal. Table includes significant different genes ( $q < 0.01$ ) and only genes with a signal intensity > 20 in at least one condition.

## SUPPLEMENTARY REFERENCES

- 1 Wu Z, Irizarry RA, et al. A Model-Based Background Adjustment for Oligonucleotide Expression Arrays. Journal of the American Statistical Association 2004;99 909-17.
- 2 Dai M, Wang P, et al. Evolving gene/transcript definitions significantly alter the interpretation of GeneChip data. Nucleic Acids Res 2005;33:e175.
- 3 Smyth GK. Linear models and empirical bayes methods for assessing differential expression in microarray experiments. Stat Appl Genet Mol Biol 2004;3:Article3.
- 4 Storey JD, Tibshirani R. Statistical significance for genomewide studies. Proc Natl Acad Sci U S A 2003;100:9440-5.
- 5 Bolstad BM, Irizarry RA, et al. A comparison of normalization methods for high density oligonucleotide array data based on variance and bias. Bioinformatics 2003;19:185-93.
- 6 Irizarry RA, Bolstad BM, et al. Summaries of Affymetrix GeneChip probe level data. Nucleic Acids Res 2003;31:e15.



## Chapter 3

### Dietary heme-mediated PPAR $\alpha$ activation does not affect the heme-induced epithelial hyperproliferation and hyperplasia in mouse colon

Noortje IJssennagger\*, Nicole de Wit\*, Michael Müller and Roelof van der Meer  
*\*both authors contributed equally*

*Published in PLoS One. 2012; 7(8):e43260.*

## ABSTRACT

Red meat consumption is associated with an increased colon cancer risk. Heme, present in red meat, injures the colon surface epithelium by luminal cytotoxicity and reactive oxygen species. This surface injury is overcompensated by hyperproliferation and hyperplasia of crypt cells. Transcriptome analysis of mucosa of heme-fed mice showed, besides stress- and proliferation-related genes, many upregulated lipid metabolism-related PPAR $\alpha$  target genes. The aim of this study was to investigate the role of PPAR $\alpha$  in heme-induced hyperproliferation and hyperplasia.

Male PPAR $\alpha$  KO and WT mice received a purified diet with or without heme. As PPAR $\alpha$  is proposed to protect against oxidative stress and lipid peroxidation, we hypothesized that the absence of PPAR $\alpha$  leads to more surface injury and crypt hyperproliferation in the colon upon heme-feeding. Heme induced luminal cytotoxicity and lipid peroxidation and colonic hyperproliferation and hyperplasia to the same extent in WT and KO mice. Transcriptome analysis of colonic mucosa confirmed similar heme-induced hyperproliferation in WT and KO mice. Stainings for alkaline phosphatase activity and expression levels of Vanin-1 and Nrf2-targets indicated a compromised antioxidant defense in heme-fed KO mice. Our results suggest that the protective role of PPAR $\alpha$  in antioxidant defense involves the Nrf2-inhibitor Fosl1, which is upregulated by heme in PPAR $\alpha$  KO mice. We conclude that PPAR $\alpha$  plays a protective role in colon against oxidative stress, but PPAR $\alpha$  does not mediate heme-induced hyperproliferation. This implies that oxidative stress of surface cells is not the main determinant of heme-induced hyperproliferation and hyperplasia.



## INTRODUCTION

Colon cancer is a leading cause of cancer deaths in Western countries [1]. Epidemiological studies show that consumption of diets high in red and processed meat is associated with the risk to develop colon cancer [2,3]. Red meat is high in heme levels and it is shown that the addition of heme to diets of rats and mice induces hyperproliferation of colon epithelial cells [4,5]. Hyperproliferation is a risk marker of colon cancer [6]. In contrast to the consumption of red meat, the consumption of white meat, which is low in heme, is not associated with an increased risk of colon cancer [7,8]. In our recent studies we fed rodents a heme diet or a control diet for 14 days [4,5]. The heme diet increased the reactive oxygen species (ROS) levels, as well as cytotoxicity, of the colonic contents and induced damage to the surface epithelium. To compensate for the heme-induced damaged surface cells, hyperproliferation was initiated in the proliferative crypts and this eventually led to hyperplasia.

Microarray analysis of samples from whole colonic mucosa and from surface and crypt cells shows that heme regulates many stress- and signaling-related genes in surface cells, and cell cycle genes specifically in crypt cells [5]. It is not known whether this heme-related surface to crypt signaling is caused by either oxidative stress or cytotoxic stress of surface cells. With regard to this, it may be of relevance that we found many PPAR $\alpha$  target genes among the highest upregulated genes [5]. PPAR $\alpha$  belongs to the superfamily of nuclear hormone receptors and known endogenous PPAR $\alpha$  ligands are fatty acids and their derivatives such as oxidized fatty acids. Little is known, however, about the function of PPAR $\alpha$  in colon. In the small intestine PPAR $\alpha$  is mainly involved in lipid metabolism and absorption, but these processes are not likely to occur in the colon upon heme feeding. Based on literature, we hypothesize that PPAR $\alpha$  is activated on a heme-rich diet to induce a protective mechanism against heme-induced oxidative stress and/or lipid peroxidation [9], facilitating the Nrf2-dependent antioxidant response. This potential PPAR $\alpha$ -mediated protection against oxidative stress and/or lipid peroxidation could limit cell damage at the colonic surface epithelium and its compensatory hyperproliferation. This implies that knocking out PPAR $\alpha$  would increase ROS-induced injury of surface cells and trigger the compensatory hyperproliferation of crypt cells.

The aim of this study was to investigate the role of PPAR $\alpha$  in heme-induced hyperproliferation and hyperplasia in colon. Therefore, in our study wild-type (WT) mice were compared to PPAR $\alpha$  knockout (PPAR $\alpha$  KO) mice on a control or heme diet. Colonic cell damage and hyperproliferation were investigated and gene expression profiles were analyzed using microarrays.

## **MATERIALS AND METHODS**

### **Ethics statement**

The institutional and national guidelines for the care and use of animals were followed and the experiment was approved by the Local Committee for Care and Use of Laboratory Animals at Wageningen University.

### **Animals and diets**

A breeding colony of pure-bred SV129 PPAR $\alpha$  knockout (KO) mice (129S4/SvJae) and corresponding wild-type (WT) mice (129S1/SvImJ) was purchased from Jackson Laboratory (Bar Harbor, ME) and bred at the animal facility of Wageningen University. Genotyping by performing quantitative PCR analysis for the ligand binding domain in exon 8 of the PPAR $\alpha$  gene (primers: F: 5'-agaagttgcaggaggggatt-3' and R: 5'-ttgaaggagcttgggaaga-3'), which was disrupted in the KO mice to disturb its function [10], verified that the mice were genuine PPAR $\alpha$  KO mice. The WT and KO mice were housed individually in a room with controlled temperature (20-24°C), relative humidity (55%±15%) and a 12 h light dark cycle. To study whether PPAR $\alpha$  plays a role in heme-induced hyperproliferation, 7-9 week old PPAR $\alpha$  KO mice and wild-type mice received either a Westernized, purified, control diet (40 en% fat (mainly palm oil) low calcium (30  $\mu$ mol/g)) or this diet supplemented with 0.5  $\mu$ mol heme/g diet (Sigma-Aldrich Chemie, St. Louis) for 14 days (n=6 per group, 4 groups) as previously described [11]. Body weight was recorded and feces were quantitatively collected during days 11-14, frozen at -20°C and subsequently freeze dried. After 14 days of intervention, the colon was excised, mesenteric fat was removed and the colon was opened longitudinally, washed in PBS, and cut into three parts. The middle 1.5 cm of the colon was formalin-fixed and paraffin embedded for histology. The remaining proximal and distal parts were scraped. Scrapings were pooled per mouse, snap-frozen in liquid nitrogen and stored at -80°C until further analysis.

### **Fecal analyses**

Fecal water was prepared and cytotoxicity was measured for each mouse as previously described [5]. To determine lipid peroxidation products in the gut lumen Thiobarbituric Acid Reactive Substances (TBARS) in fecal water were quantified. The assay determines lipid peroxidation by quantifying the concentration of malondialdehyde (MDA) in fecal water [12]. Briefly, fecal water was diluted 4-fold with double-distilled water. To 100  $\mu$ l of this dilution, 100  $\mu$ l of 8.1% SDS and 1 ml of 0.11 mol/L 2,6-di-tert-butyl-p-cresol, 0.5% TBA in 10% acetic acid (pH 3.5) was added. To correct for background, TBA was omitted from the assay. TBARS were extracted, after heating for 75 minutes at 82°C, with 1.2 ml n-butanol. The absorbance of the extracts was measured at 540 nm. The amount of TBARS was calculated as MDA equivalents using 1,1,3,3,-tetramethoxypropane as standard.

## **Immunohistochemistry**

Hematoxylin and Eosin staining was performed to assess the morphology of the tissue. To stain proliferating cells, paraffin embedded colon sections of 5  $\mu$ m were deparaffinized and stained with an anti-mouse Ki67 antibody as described previously [5]. Colonocytes from 15 well-oriented crypts (longitudinal section, displaying the total crypt) were counted per animal. These crypts were equally distributed over the middle 1.5 cm of the colon. A cell was scored Ki67-positive when the nucleus of the cell was distinctly brown. The number of Ki67-positive cells per crypt, the total number of cells per crypt and the labeling index (percentage of Ki67-positive cells per crypt) were determined. To determine alkaline phosphatase activity, colon tissue slides were deparaffinized and incubated with the alkaline-dye mixture (Alkaline phosphatase kit 85L2-1KT Sigma-Aldrich) for 90 min at 37°C. Slides were rinsed with water and mounted.

## **RNA isolation**

Total RNA was isolated by using TRIzol reagent (Invitrogen, Breda, the Netherlands) according to the manufacturer's protocol. For microarray hybridization the isolated RNA was further column purified (SV total RNA isolation system Promega, Leiden, the Netherlands). RNA concentration was measured on a nanodrop ND-1000 UV-Vis spectrophotometer (Isogen, Maarsse, the Netherlands) and analyzed on an Agilent 2100 bioanalyzer (Agilent Technologies, Amsterdam, the Netherlands) with 6000 Nano Chips, according to the supplier's protocol. RNA was judged suitable for array hybridization only if samples exhibited intact bands corresponding to the 18S and 28S ribosomal RNA subunits, and displayed no chromosomal peaks or RNA degradation products (RNA Integrity Number > 8.0).

## **Array hybridization and microarray data analysis**

One-hundred nanograms of RNA from each mouse (n=6 per group) were used for whole-transcript cDNA synthesis with the Ambion WT expression kit (Applied Biosystems). Hybridization, washing and scanning of an Affymetrix GeneChip Mouse Gene 1.1 ST 24-array plate was carried out according to standard Affymetrix protocols on a GeneTitan instrument (Affymetrix). Quality control of the datasets was performed using Bioconductor packages [13] integrated in an on-line pipeline [14]. Due to insufficient quality, array results of 1 WT control mouse had to be excluded. Arrays were normalized using the Robust Multi-array Average method [15,16]. Probe sets were defined according to Dai et al. [17]. Probe sets that satisfied the criterion of a False Discovery Rate (FDR) < 1% (q-value < 0.01) were considered to be significantly regulated. Genes with a signal intensity below 20 in both treatments were considered absent and excluded from further analyses. Array data were submitted to the Gene Expression Omnibus, accession number GSE37006.

Pathway analysis was performed using Ingenuity IPA Canonical Pathway Analysis (Ingenuity® Systems, May 2011, [www.ingenuity.com](http://www.ingenuity.com)). This analysis identifies the pathways from the Ingenuity Pathways Analysis library of canonical pathways that are most significant to a microarray data set. Fisher's exact test was used to calculate a p-value determining the probability that the association between the genes in the dataset and the canonical pathway is explained by chance alone.

### Statistical analysis

Data are presented as mean  $\pm$  SEM. Differences between the mean values of the 4 groups were tested for main effects by a two-way ANOVA. A Bonferroni's Multiple Comparison Test determined differences between groups. P-values  $<0.05$  were considered significant.

## RESULTS

### Heme induced the expression of PPAR $\alpha$ target genes

Our recent studies show that the addition of heme to the diet of rats and C57Bl6/J mice led to increased luminal reactive oxygen species (ROS) production and to increased cytotoxicity of the colonic luminal contents [4,5]. This increase in heme-induced cytotoxicity damaged the surface cells in the colon and led to compensatory epithelial hyperproliferation [4,5]. Microarray analysis of the colonic mucosa showed that most of the genes changed on the heme diet were involved in cell cycle/apoptosis/cell differentiation (Figure 1A, adapted from [5]). Furthermore, the study indicated that heme-induced hyperproliferation and hyperplasia was triggered by downregulating feedback inhibitors of proliferation, such as Wnt inhibitory factor 1 (Wif1), Interleukin-15 (IL-15), Indian Hedgehog (Ihh) and Bone morphogenetic protein 2 (Bmp2) in the surface epithelium [5].

Besides cell- and apoptosis-related genes, also lipid metabolism-related genes were highly regulated by the heme diet (Figure 1A). Of these lipid metabolism-related genes 30% were PPAR $\alpha$  target genes as defined by Bunger et al. [18]. Amongst these PPAR $\alpha$  targets Fabp1 and Cyp4a10 were the two highest upregulated genes with fold changes of 128 and 98 respectively [5]. PPAR $\alpha$  target genes and their change in expression in heme-fed C57Bl6/J mice are summarized in Figure 1B (first fold change listed between brackets). Next to gene expression of total colonic mucosa, gene expression levels of colon surface cells and colon crypt cells were separately determined by performing laser capture microdissection (LCM) [5]. The LCM study showed that most of the differentially expressed PPAR $\alpha$  targets were present in the colonic surface cells (Gene Expression Omnibus, accession number GSE27849). No changes in PPAR $\alpha$  targets were found in the lower crypt cells. This indicates that PPAR $\alpha$  plays a role in the surface cells, where it possibly functions as a protective mechanism against e.g. oxidative stress and lipid peroxidation induced by the heme diet.

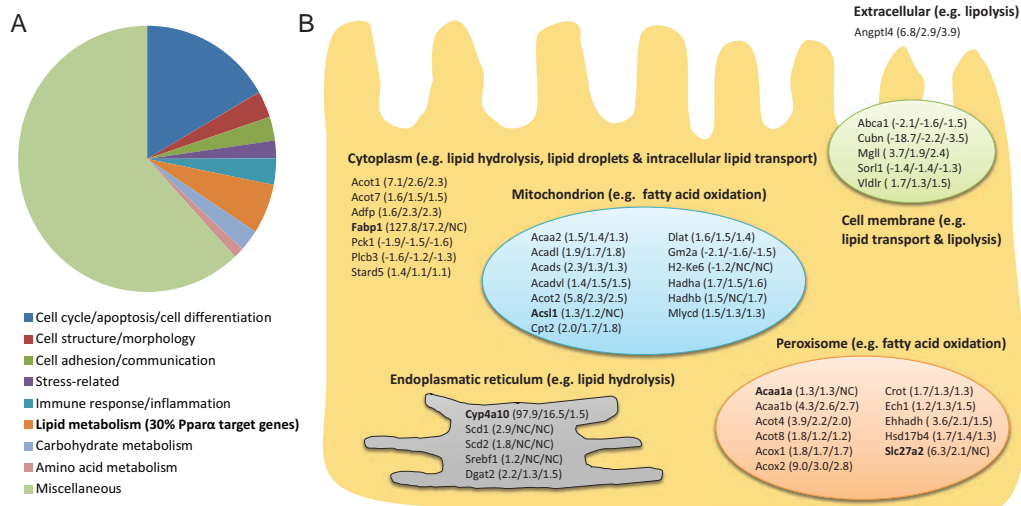


**Figure 1.** Effect of heme on PPARα target genes. **A.** Categorization of heme-induced differentially expressed genes ( $q < 0.01$  and signal intensity  $> 20$  in at least treatment) according to GO Biological Process annotation. Figure is based on results from Ijssennagter et al. [5] showing that lipid metabolism-related gene expression is substantially influenced by heme. Thirty percent of these heme-induced lipid metabolism-related genes are PPARα target genes [18]. Miscellaneous contains processes with broad and thus unspecific biological process terms. **B.** Expression of PPARα target genes in enterocytes is mainly upregulated. Behind the gene the fold-changes are indicated from colonic scrapings from heme-fed vs. control mice from resp. the previous experiment with C57Bl6/J mice, current experiment WT SV129 mice and current experiment KO SV129 mice. In bold are PPARα targets of which no significant induction is seen in the KO mice.

## Heme induces similar lipid peroxidation, cytotoxicity, and hyperproliferation in colon of WT and KO mice

As our previous studies show that heme injures the surface epithelium resulting in hyperproliferation, and we found that PPARα targets are highly induced in the surface epithelium, we now explored the potential role of PPARα in heme-induced hyperproliferation. We hypothesize that when there is no PPARα present in the colon, there is less protection against oxidative stress and/or lipid peroxidation. This attenuated protection would lead to an increase in heme-induced mucosal injury. As a damaged surface epithelium must trigger the compensatory hyperproliferation in the colonic crypt, the absence of PPARα would thus lead to an increased proliferation. To test this hypothesis, an experiment was performed in which PPARα knockout (KO) mice and wild-type (WT) mice (both on a SV129 background) received either a control or a heme diet for 2 weeks. After 2 weeks of diet intervention, both the WT and the PPARα KO heme-fed mice had an increased cytotoxicity of the colonic contents (Table 1). Luminal levels of lipid peroxidation products were determined by measuring TBARS in fecal water. TBARS were increased on the heme diet in both the WT and the PPARα KO compared to their control groups (Table 1). No significant differences between the heme-fed PPARα KO and the heme-fed WT mice were observed for body weight ( $23.0 \pm 0.8$  and

21.8±1.0 g, respectively), cytotoxicity and TBARS. To measure colonocyte proliferation colon tissue was stained with an antibody against Ki67, a marker for proliferating cells. Cell counts revealed heme-induced increases in Ki67-positive cells per crypt as well as total number of cells per crypt in both the PPAR $\alpha$  KO mice and WT mice, resulting in similar increases in the crypt labeling index (Table 1). Overall, there were no significant differences between the KO and the WT mice on the heme diet.

**Table 1.** Physiological changes induced by heme in colon of WT and PPAR $\alpha$  KO mice.

	WT control	WT heme	KO control	KO heme
<b>Luminal contents</b>				
Cytotoxicity (% lysis)	0±0.8 <sup>a</sup>	88.3±5.8 <sup>b</sup>	1.8±2.7 <sup>a</sup>	93.6±6.3 <sup>b</sup>
TBARS (MDA equivalents, $\mu$ mol/L)	28.3±6.8 <sup>a</sup>	51.1±10.5 <sup>b</sup>	28.3±6.4 <sup>a</sup>	42.6±8.3 <sup>b</sup>
<b>Mucosa</b>				
Total number of cells/crypt	41.1±2.0 <sup>a</sup>	61.2±3.0 <sup>b</sup>	45.4±2.2 <sup>a</sup>	56.6±3.1 <sup>b</sup>
Ki67-positive cells/crypt	15.8±1.2 <sup>a</sup>	37.5±2.7 <sup>b</sup>	17.7±1.9 <sup>a</sup>	30.7±2.0 <sup>b</sup>
Labeling index (%) <sup>#</sup>	38.5±2.1 <sup>a</sup>	60.9±2.6 <sup>b</sup>	38.2±2.4 <sup>a</sup>	54.1±1.6 <sup>b</sup>

<sup>#</sup> Calculated as percentage Ki67-positive cells per crypt. Data are represented as mean  $\pm$  SEM. Groups indicated with 'a' are significantly ( $p < 0.05$ ) different from 'b' by ANOVA with Bonferroni post-hoc testing. N=6 per group, except for mucosa measurements where proliferation of one KO heme animal could not be determined due to poor tissue quality.

### Most PPAR $\alpha$ targets were also induced in the KO mice on the heme diet

Although proliferation was not higher in the KO mice compared to the WT on the heme diet, microarrays were performed to determine whether the heme-induced expression of lipid metabolism-related genes and stress-related genes were changed in KO mice compared to WT mice. Hierarchical clustering of the microarray data revealed that the diet-induced effect on gene expression is stronger than the effect of genotype (Figure 2A). Figure 2B shows that there is a pronounced overlap in heme-induced differentially expressed genes between the WT mice and the KO mice. Pathway analysis using the Ingenuity Canonical Pathways program revealed that among the overlapping genes, genes involved in pathways related to cell cycle (open arrows), Nrf2-mediated oxidative stress response (light gray arrow) and lipid metabolism (black arrow) were present. The induction of cell cycle genes in both the WT and the KO is in line with the Ki67 results showing similar hyperproliferation in both heme-fed groups. We verified the expression of our previously identified downregulated feedback inhibitors of proliferation Wif1, IL-15, Ihh and Bmp2 [5]. In the current study, these signaling molecules were similarly downregulated on the heme-diet in both WT and KO mice (Figure 3A). Remarkably, Wnt/ $\beta$ -catenin signaling was the most significant pathway that was changed in the KO mice (Figure 2B, open arrow). Looking at this pathway in more detail revealed that changes in genes in this pathway were not related to changes in cell cycle, but to a 4-fold

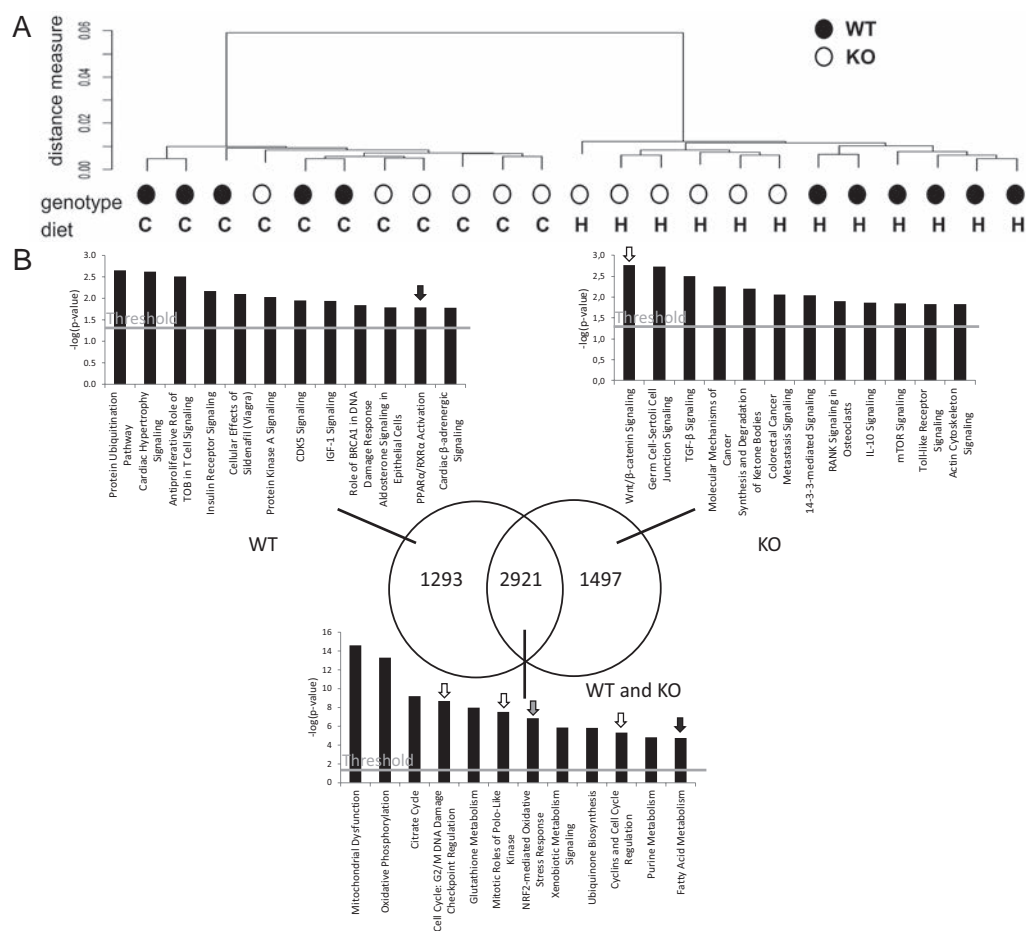


**Figure 2.** Microarray clustering and pathway analysis of heme-induced differentially expressed genes. (A) Hierarchical clustering of the microarray data showing that the diet-effect (C=control and H=heme) is more pronounced than the genotype-effect. (B) Venn-diagram showing that 69% of the heme-induced changes ( $q < 0.01$  and signal intensity  $> 20$  in at least one of the treatments) in WT mice could also be found in KO mice. Ingenuity canonical pathway analysis shows that overlapping genes in Venn-diagram are involved in cell cycle-related processes (open arrows) and Nrf2-mediated oxidative stress response (gray arrow). There is hardly any effect of genotype on fatty acid metabolism-related processes (black arrow). WT mice show PPAR $\alpha$  activation (black arrow in WT panel) and KO mice Wnt signaling (white arrow in KO panel). Note that pathways in overlap are much more significant than the WT or KO specific pathways.

upregulation of Fosl1 (also called Fra1), which is known to repress the Nrf2-dependent antioxidant response [19,20].

As expected, pathway analysis showed that changes in PPAR $\alpha$ /RXR $\alpha$  activation are restricted to the WT mice (Figure 2B, black arrow). However, a more detailed analysis showed that also in the KO mice still numerous PPAR $\alpha$  target genes are regulated by heme, most of them to a similar extent as in WT mice (Figure 1B, the 2nd (WT) and 3rd (PPAR $\alpha$  KO) fold change listed between brackets). Only for Cyp4a10, Fabp1, Acs11, Slc27a2 and Acaa1a the heme-induced regulation is absent in the PPAR $\alpha$  KO mice.



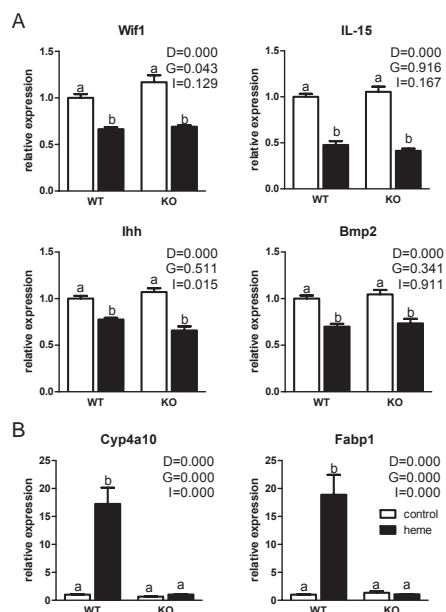


**Figure 3.** Gene expression of signaling molecules involved in hyperproliferation (A) and of PPAR $\alpha$  targets Cyp4a10 and Fabp1 (B). Expression of the WT control group is set to one. Expression of all other groups is relative to WT control. P-values for main effects (D for diet, G for genotype and I for interaction) by a two-way ANOVA are indicated. A and b indicate significant different groups ( $p < 0.05$ ) determined by a Bonferroni post-hoc test.

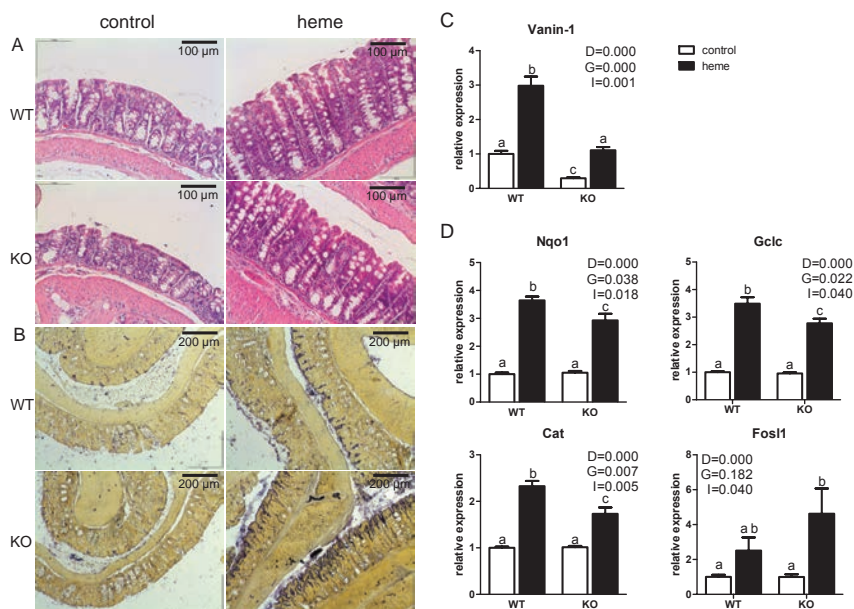


**Figure 4.** Heme-induced stress response. (A) Representative pictures of H&E staining of mouse colonic mucosa after 14 days of control- versus heme diet. (B) Representative pictures of colon tissue stained for Alkaline phosphatase activity, a marker for ROS stress. (C) Expression of Vanin-1. (D) Expression of genes involved in antioxidant response Nqo1, Cat, Gclc and Fosl1. Expression of the WT control group is set to one. Expression of all other groups is relative to WT control. P-values for main effects (D for diet, G for genotype and I for interaction) by a two-way ANOVA are indicated. A, b and c indicate significant different groups ( $p < 0.05$ ) determined by a Bonferroni post-hoc test.



For Cyp4a10 and Fabp1, the highest upregulated genes in our previous experiment, expression levels in WT and KO mice are depicted in Figure 3B, showing the lack of a heme-induced upregulation in the KO mice. This indicates that differences in  $\omega$ -oxidation of fatty acids by Cyp4a10 and in binding hydrophobic lipids by Fabp1 do not affect the heme-induced hyperproliferation. The heme-induced upregulation was thus blocked for five PPAR $\alpha$  target genes only, implying that lipid metabolism can still play a role in the heme-induced hyperproliferation, but that this is not dependent on PPAR $\alpha$  per se.

### **Antioxidant defense was compromised in KO mice on a heme diet**

As describes above, Figure 2B shows that, both in WT and KO mice, heme changes the NRF2-mediated oxidative stress response. To investigate whether this occurs to a different extent we determined the levels of oxidative stress and damage to the colon tissue in the 4 groups. The overall morphology of the tissue was visualized by an H&E staining (Figure 4A), showing a similar ruffled surface epithelium and deep crypts in the heme-fed WT and KO mice. This indicates similar heme-induced surface injury and luminal necrosis which have been investigated in detail earlier [5,21]. Alkaline phosphatase activity is a marker of ROS stress [22], and colon sections were stained for alkaline phosphatase activity (Figure 4B). A higher staining intensity was found in the heme-fed groups, which indicated that the ROS stress was higher in these mice compared to the controls. Furthermore, KO mice on a heme diet displayed an even more pronounced staining than WT mice on a heme diet.

Vanin-1 is induced by oxidative stress [23], and was upregulated by dietary heme both in the WT (3-fold) and in the KO mice (4-fold) (Figure 4C), indicating that there is oxidative stress in both WT as well as KO mice on the heme diet. The stress-related induction of Vanin-1 is thus PPAR $\alpha$  independent. However, the basal expression level of Vanin-1 was about 3-fold lower in the KO mice compared to the WT, which indicates that the basal vanin-1 levels are controlled by PPAR $\alpha$  (also shown in [24]). Other oxidative stress markers, such as expression levels of Metallothionein-1 (Mt1) [25], mast cell hyperplasia [26] (shown by expression levels of e.g. Mcpt1 and 2, Cpa3), Hif1 $\alpha$  expression [27] and Mmp9 expression [28] were also explored. These markers showed subtle higher inductions by heme in KO mice compared to WT mice, but these differences did not reach significance (data not shown). Together these data indicated that there is slightly more oxidative stress in the KO compared to the WT mice.

Next we determined whether the increased heme-induced oxidative stress in KO animals is due to a compromised antioxidant defense. This implies that a heme-genotype interaction should determine the expression of antioxidant genes. Indeed, antioxidant defense genes show a significant interaction and were induced to a lower extent in the KO mice compared to the WT mice by heme (shown for NAD(P)H quinone oxidoreductase 1 (Nqo1), glutamate-cysteine ligase (Gclc), and catalase (Cat) in Figure 4D. Superoxide

Dismutase 1 (Sod1) expression shows a similar pattern although not significant). This shows that the protective response of the mucosa to the heme-induced ROS production was attenuated in the KO mice compared to the WT mice. The significant upregulation of *Fos1* in the KO mice (Figure 4C) could have contributed to the attenuation of these Nrf2-induced antioxidant responses. Together our data indicate that this attenuated defense against oxidative stress in the epithelial surface of the colon does not affect heme-induced hyperproliferation.

## DISCUSSION

This study shows that the transcription factor PPAR $\alpha$  does not play a causal role in the heme-induced hyperproliferation and hyperplasia, despite the very high upregulation of PPAR $\alpha$  target genes in the colonic mucosa of mice on a heme diet. Lipid metabolism per se can however still play a role in the heme-induced hyperproliferation as most of the lipid metabolism-related genes, including numerous PPAR $\alpha$  target genes are still induced in PPAR $\alpha$  KO mice on the heme diet. Dietary heme catalyzed the production of ROS which results in the production of oxidized lipids. These oxidized lipids are ligands for PPAR $\alpha$ , and this could explain the induction of PPAR $\alpha$  target genes in WT mice on the heme diet. It is unlikely that heme itself activates PPAR $\alpha$  as planar molecules, such as heme, do not fit in the Y-shaped ligand-binding cavity of PPAR $\alpha$  isotypes [29]. Although the differentially expressed genes are well-known PPAR $\alpha$  target genes, our results indicate that other transcription factors, e.g. PPAR $\gamma$  or PPAR $\beta/\delta$ , can take over the role of PPAR $\alpha$  in the PPAR $\alpha$  KO mice [30,31]. The general expression of PPAR $\gamma$  in colon makes it a reasonable candidate to compensate for the lack of PPAR $\alpha$ . PPAR $\gamma$  is previously described to be able to compensate for PPAR $\alpha$  in PPAR $\alpha$  KO mice [30], however in contrast to these previous findings we did not find a significant upregulation of PPAR $\gamma$  gene expression in the KO mice. This does not rule out a compensatory mechanism by PPAR $\gamma$  per se, as an enhanced activation is not necessarily accompanied by an increased gene expression. Activation of PPAR $\gamma$  was hard to study as the overlap between PPAR target genes is high and currently no specific target genes in colon are known to discriminate between the activation of the different PPARs. A compensatory mechanism by PPARs might explain why lipid metabolism-related genes are still highly upregulated by dietary heme in the PPAR $\alpha$  KO mice.

The five PPAR $\alpha$  target genes of which the induction by heme was blocked in the PPAR $\alpha$  KO animals were *Fabp1*, *Cyp4a10*, *Ascl1*, *Slc27a2* and *Acaa1a*. Therefore, these genes do not play a role in the heme-induced hyperproliferation. The exposure of the epithelial surface to lipid peroxidation products and to cytotoxic molecules in the WT and KO heme-fed mice must be similar as TBARS and cytotoxicity measurements show no differences between WT and KO heme-fed mice. However, there is more oxidative damage in surface cells of the KO mice, as shown by the alkaline phosphatase activity

staining and Vanin-1 induction. In line with this, there is a reduced antioxidant defense in the KO mice, which is reflected by the lower induction of Nrf2 target genes, such as Nqo1 and Cat, upon heme feeding in the KO mice. Together these data suggest that there is less protection against oxidative stress and/or lipid peroxidation in the heme-fed KO mice, indicating that PPAR $\alpha$  plays a protective role in the heme-induced oxidative stress response. This attenuated antioxidant response did not lead to an increased cell proliferation as hypothesized, and it is therefore unlikely that oxidative stress induces signaling to the crypt to initiate hyperproliferation. It is more plausible that cytotoxic stress induces hyperproliferation and hyperplasia in the colon of heme-fed mice. We have shown earlier that dietary antioxidants prevent all detrimental effects of dietary heme in the colon [32]. However, that study could not differentiate between causal effects of oxidative and cytotoxic stress, because heme induced cytotoxicity was also prevented by antioxidants. This is consistent with other studies [4,21] showing that cytotoxicity is due to a covalently modified porphyrin formed from heme, probably by radical-mediated addition reactions in the gastrointestinal tract. It can be speculated that this complex radical-mediated formation of the cytotoxic heme factor lags behind the instantaneous generation of oxygen radicals by heme. Whether this is the case requires investigations of the possible differential time course of the heme-induced oxidative and cytotoxic stress. The induction of Vanin-1 is slightly higher in the KO heme-fed mice compared to the control heme-fed mice (4-fold vs. 3-fold). This might suggest that there is slightly more oxidative stress in the KO mice, which could be the result of a lower antioxidant response in the KO mice. From our previous study [5] in which we separated colonic surface and crypt cell gene expression, expression of Vanin-1 was 2 times higher at the surface epithelium compared to the crypt under control conditions. Upon heme feeding, Vanin-1 expression increased 3-fold at the surface epithelium, while the expression remained unchanged in the crypt (results can be found in the Gene Expression Omnibus, accession number GSE27849). This implies that the oxidative stress is exclusively induced at the surface epithelium. Besides its role as oxidative stress marker, Vanin-1 is recently proposed as a causal factor in colonic hyperproliferation [33]. As mentioned above, the expression of Vanin-1 is induced in the surface epithelium and proliferation occurs from the stem cells in the crypt. This implies that if Vanin-1 plays a role in the heme-induced hyperproliferation Vanin-1 should signal from the surface to the crypt to initiate this hyperproliferation. This is not supported in this study, as the levels of Vanin-1 expression are 3 times higher in WT heme-fed mice compared to KO heme-fed mice while proliferation rates are similar. Thus, in our study we could not correlate the gene expression level of Vanin-1 to the level of proliferation in the colon. Nrf2 is the prominent transcription factor that regulates the antioxidant response. Nrf2 is essential for the antioxidant response element (ARE)-mediated induction of many cytoprotective enzymes, such as Cat and Nqo1. Nrf2 activity is controlled by Keap1.

Oxidative stress (generated e.g. by heme-rich diet) can oxidize critical cysteine residues in Keap1, resulting in inactivation of Keap1 and accumulation of Nrf2 in the nucleus, where it binds to ARE in the promoter region of many antioxidative genes, initiating their transcription (reviewed in [34]). Although the antioxidant response is predominantly regulated by Nrf2, there is an overlap in target genes between this transcription factor and PPAR $\alpha$  [9,18]. Bunger et al. [18] showed that in the intestine, known Nrf2-target genes Cat and glutathione-related genes, are also regulated by PPAR $\alpha$ . This might explain the lower induction of Cat and glutathione-related genes in the heme-fed KO mice compared to the heme-fed WT mice. However, as other antioxidant response genes, such as Sod1 and Nqo1 are no PPAR $\alpha$  target genes an additional mechanism must be present by which PPAR $\alpha$  indirectly influences the Nrf2-driven antioxidant response. This possible additional mechanism by which PPAR $\alpha$  can be protective involves regulation of Fosl1. Fosl1 is significantly upregulated only in the PPAR $\alpha$  KO mice. Fosl1 represses the Nrf2-dependent expression of antioxidant response element (ARE) containing genes such as Nqo1 and Gclc [19,20]. How PPAR $\alpha$  influences Fosl1 expression is largely unknown. Direct regulation of Fosl1 by PPAR $\alpha$  is not likely because its expression is not modulated by the PPAR $\alpha$ -specific ligand WY14643 [18]. We propose that Fatty acid binding protein 1 (Fabp1) acts as an intermediate in the PPAR $\alpha$ -dependent regulation of Fosl1. In contrast to Fabp2, Fabp1 has a large hydrophobic pocket and can bind toxic hydrophobic molecules such as (oxidized) long chain fatty acids, bile acids and heme [35]. There is a heme-induced upregulation of Fabp1 expression in the WT mice, but this induction is blocked in the KO mice. The absence of Fabp1 in the KO might lead to more unbound hydrophobic toxicants in colon cells of these KO mice. Fosl1 can be induced by toxic compounds [36], and we hypothesize that unbound toxicants present in the KO mice can induce the expression of Fosl1. The expression of Fabp2 was induced by heme in both the WT and the KO with 1.5-fold, but Fabp2 cannot bind toxic molecules such as heme in its small pocket. It is therefore unlikely that Fabp2 plays a role in the induction of Fosl1. The hypothesized mechanism suggests that PPAR $\alpha$  plays its protective role in the colon via its target Fabp1 which can bind large hydrophobic molecules and thereby preventing the induction of Fosl1 (Figure 5). This mechanism predicts that Fabp1 KO mice should have higher Fosl1 levels and an attenuated antioxidant response compared to WT mice. Whether this is the case requires further investigation, but our mechanism is corroborated by studies showing that cells transfected with Fabp1 have lower intracellular ROS levels and a reduction of oxidative stress compared to untransfected cells [37,38]. The PPAR $\alpha$  KO and WT mice have a SV129 background. Our previous studies carried out with heme-rich diets were performed in C57Bl6/J mice and we see similar effects on luminal cytotoxicity and epithelial proliferation. Besides proliferation, also similar effects were found on gene expression as similar genes were induced in the SV129 WT heme compared to the C57Bl6/J (Pearson correlation coefficient of 0.881, n=3673 genes). This

shows that there is a similar response to dietary heme in these two mouse stains. These results are also similar to results observed in rats [21], indicating that the heme effect is species and strain-independent.

Taken together, we conclude that the heme-induced hyperproliferation is not mediated by PPAR $\alpha$ . As only 5 PPAR $\alpha$  target genes did not respond to heme in the KO mice, a possible role in the heme induced hyperproliferation for other PPAR $\alpha$  target genes and lipid metabolism-related genes in general cannot be excluded. Our data do suggest that PPAR $\alpha$  plays a protective role against oxidative stress induced by dietary heme in the colonic epithelial cells. Moreover, our results indicate that most probably not ROS-induced stress, but cytotoxicity-induced stress initiates colonic hyperproliferation.

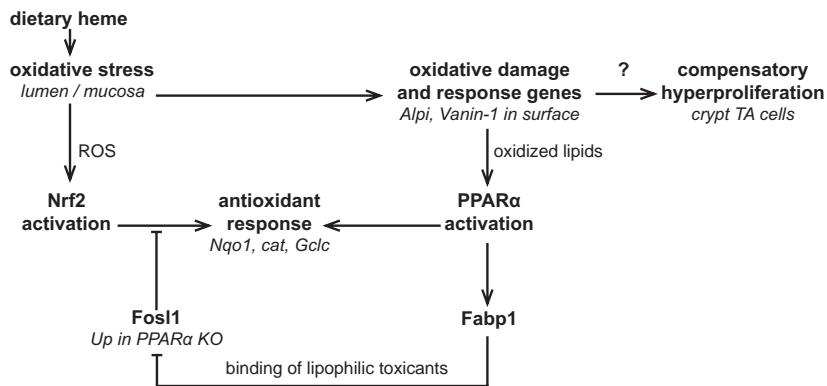


**Figure 5.** Hypothesized mechanism by which heme induces PPAR $\alpha$  and modulates the antioxidant response. Dietary heme induces oxidative stress by generating reactive oxygen species (ROS) and the production of lipid peroxidation products. ROS induces Nrf2 activation and oxidized lipids activate PPAR $\alpha$  leading to an antioxidant response. In PPAR $\alpha$  KO mice Fosl1 is upregulated which can inhibit the Nrf2 antioxidant response. Fosl1 upregulation might occur via lipophilic toxicants. The free concentration of these toxicants is probably higher in the KO mice due to the absence of the toxicants-binding Fabp1. As there was no role of PPAR $\alpha$  in the heme induced compensatory hyperproliferation of transit amplifying (TA) crypt cells, the question mark indicates a dubious relationship.

## ACKNOWLEDGEMENTS

The authors would like to thank Sander Kersten for critically reviewing the manuscript; Mechteld Grootte Bromhaar, Jenny Jansen, Philip de Groot and Mark Boekschoten for microarray analysis and Shohreh Keshtkar, Arjan Schonewille and Bert Weijers for technical assistance.

## REFERENCES

- 1 Jemal A, Siegel R, et al. Cancer statistics, 2010. *CA: a cancer journal for clinicians* 2010;60:277-300.
- 2 Bastide NM, Pierre FH, et al. Heme iron from meat and risk of colorectal cancer: a meta-analysis and a review of the mechanisms involved. *Cancer prevention research* 2011;4:177-84.
- 3 World Cancer Research Fund. Food, Nutrition, Physical Activity and the Prevention of Cancer: a Global Perspective. Washington, DC: American Institute for Cancer Research, 2007.
- 4 Sesink AL, Termont DS, et al. Red meat and colon cancer: the cytotoxic and hyperproliferative effects of dietary heme. *Cancer Res* 1999;59:5704-9.
- 5 IJssennagger N, Rijnierse A, et al. Dietary haem stimulates epithelial cell turnover by downregulating feedback inhibitors of proliferation in murine colon. *Gut* 2012;61:1041-9.
- 6 Kinzler KW, Vogelstein B. Lessons from hereditary colorectal cancer. *Cell* 1996;87:159-70.
- 7 Giovannucci E, Rimm EB, et al. Intake of fat, meat, and fiber in relation to risk of colon cancer in men. *Cancer Res* 1994;54:2390-7.
- 8 Larsson SC, Rafter J, et al. Red meat consumption and risk of cancers of the proximal colon, distal colon and rectum: the Swedish Mammography Cohort. *Int J Cancer* 2005;113:829-34.
- 9 Abdelmegeed MA, Moon KH, et al. Role of peroxisome proliferator-activated receptor- $\alpha$  in fasting-mediated oxidative stress. *Free Radic Biol Med* 2009;47:767-78.
- 10 de Vogel J, Jonker-Termont DS, et al. Green vegetables, red meat and colon cancer: chlorophyll prevents the cytotoxic and hyperproliferative effects of haem in rat colon. *Carcinogenesis* 2005;26:387-93.
- 11 Ohkawa H, Ohishi N, et al. Assay for lipid peroxides in animal tissues by thiobarbituric acid reaction. *Analytical biochemistry* 1979;95:351-8.
- 12 Gentleman RC, Carey VJ, et al. Bioconductor: open software development for computational biology and bioinformatics. *Genome biology* 2004;5:R80.
- 13 Lin K, Kools H, et al. MADMAX - Management and analysis database for multiple ~omics experiments. *J Integr Bioinform* 2011;8:160.
- 14 Bolstad BM, Irizarry RA, et al. A comparison of normalization methods for high density oligonucleotide array data based on variance and bias. *Bioinformatics* 2003;19:185-93.
- 15 Irizarry RA, Bolstad BM, et al. Summaries of Affymetrix GeneChip probe level data. *Nucleic Acids Res* 2003;31:e15.
- 16 Dai M, Wang P, et al. Evolving gene/transcript definitions significantly alter the interpretation of GeneChip data. *Nucleic Acids Res* 2005;33:e175.
- 17 Bunger M, van den Bosch HM, et al. Genome-wide analysis of PPAR $\alpha$  activation in murine small intestine. *Physiological genomics* 2007;30:192-204.
- 18 Venugopal R, Jaiswal AK. Nrf1 and Nrf2 positively and c-Fos and Fra1 negatively regulate the human antioxidant response element-mediated expression of NAD(P)H:quinone oxidoreductase1 gene. *Proc Natl Acad Sci U S A* 1996;93:14960-5.
- 19 Yang HP, Magilnick N, et al. Nrf1 and Nrf2 regulate rat glutamate-cysteine ligase catalytic subunit transcription indirectly via NF- $\kappa$ B and AP-1. *Molecular and Cellular Biology* 2005;25:5933-46.
- 20 de Vogel J, van-Eck WB, et al. Dietary heme injures surface epithelium resulting in hyperproliferation, inhibition of apoptosis and crypt hyperplasia in rat colon. *Carcinogenesis* 2008;29:398-403.
- 21 Harada T, Koyama I, et al. Heat shock induces intestinal-type alkaline phosphatase in rat IEC-18 cells. *American journal of physiology Gastrointestinal and liver physiology* 2003;284:G255-62.
- 22 Berruyer C, Martin FM, et al. Vanin-1 $^{-/-}$  mice exhibit a glutathione-mediated tissue resistance to oxidative stress. *Mol Cell Biol* 2004;24:7214-24.
- 23 Rakhshandehroo M, Knoch B, et al. Peroxisome proliferator-activated receptor  $\alpha$  target genes. *PPAR Res* 2010;2010.
- 24 Andrews GK. Regulation of metallothionein gene expression by oxidative stress and metal ions. *Biochem Pharmacol* 2000;59:95-104.
- 25 Anton PM, Theodorou V, et al. Pathways involved in mild gastrointestinal inflammation induced by a low level exposure to a food contaminant. *Digestive diseases and sciences* 2002;47:1308-15.

- 26 Pialoux V, Mounier R, et al. Relationship between oxidative stress and HIF-1 alpha mRNA during sustained hypoxia in humans. *Free Radic Biol Med* 2009;46:321-6.
- 27 Lee SJ, Kim CE, et al. 4-Hydroxynonenal enhances MMP-9 production in murine macrophages via 5-lipoxygenase-mediated activation of ERK and p38 MAPK. *Toxicology and Applied Pharmacology* 2010;242:191-8.
- 28 Zoete V, Grosdidier A, et al. Peroxisome proliferator-activated receptor structures: ligand specificity, molecular switch and interactions with regulators. *Biochim Biophys Acta* 2007;1771:915-25.
- 29 Patsouris D, Reddy JK, et al. Peroxisome proliferator-activated receptor alpha mediates the effects of high-fat diet on hepatic gene expression. *Endocrinology* 2006;147:1508-16.
- 30 Muoio DM, MacLean PS, et al. Fatty acid homeostasis and induction of lipid regulatory genes in skeletal muscles of peroxisome proliferator-activated receptor (PPAR) alpha knock-out mice. Evidence for compensatory regulation by PPAR delta. *J Biol Chem* 2002;277:26089-97.
- 31 Pierre F, Tache S, et al. Meat and cancer: haemoglobin and haemin in a low-calcium diet promote colorectal carcinogenesis at the aberrant crypt stage in rats. *Carcinogenesis* 2003;24:1683-90.
- 32 Pouyet L, Roisin-Bouffay C, et al. Epithelial vanin-1 controls inflammation-driven carcinogenesis in the colitis-associated colon cancer model. *Inflamm Bowel Dis* 2010;16:96-104.
- 33 Nguyen T, Nioi P, et al. The Nrf2-antioxidant response element signaling pathway and its activation by oxidative stress. *J Biol Chem* 2009;284:13291-5.
- 34 Thompson J, Ory J, et al. The liver fatty acid binding protein--comparison of cavity properties of intracellular lipid-binding proteins. *Mol Cell Biochem* 1999;192:9-16.
- 35 Reddy SP, Mossman BT. Role and regulation of activator protein-1 in toxicant-induced responses of the lung. *Am J Physiol Lung Cell Mol Physiol* 2002;283:L1161-78.
- 36 Wang G, Gong Y, et al. Antioxidative function of L-FABP in L-FABP stably transfected Chang liver cells. *Hepatology* 2005;42:871-9.
- 37 Yamamoto T, Noiri E, et al. Renal L-type fatty acid-binding protein in acute ischemic injury. *J Am Soc Nephrol* 2007;18:2894-902.





## Chapter 4

### Dietary heme induces acute oxidative stress but delayed cytotoxicity and compensatory hyperproliferation in mouse colon

Noortje IJssennagger, Anneke Rijnierse, Nicole de Wit, Mark Boekschoten, Jan Dekker, Arjan Schonewille, Michael Müller and Roelof van der Meer

*Submitted*

## ABSTRACT

Red meat consumption is associated with an increased colon cancer risk. Heme, present in red meat, injures the colon surface epithelium by luminal cytotoxicity and reactive oxygen species. This surface injury is compensated by hyperproliferation and hyperplasia of crypt cells, which was induced by a changed surface to crypt signalling, as recently described. It is unknown whether the change in signaling is caused by cytotoxic stress and/or by oxidative stress, as these processes were never studied separately. Therefore, the aim of this study was to determine the possible differential effects of dietary heme on these luminal stressors and their impact on the colonic mucosa after 2, 4, 7, and 14 days of heme feeding.

Mice received a purified, humanized, control diet or this diet supplemented with 0.2  $\mu\text{mol}$  heme/g. Oxidative stress was measured as Thiobarbituric Acid Reactive Substances (TBARS) in fecal water. Cytotoxicity of fecal water was quantified with a bioassay. Epithelial cell proliferation was determined by Ki67 immunohistochemistry and mucosal responses were further studied in detail by whole genome transcriptomics. Dietary heme caused acute as well as delayed changes in the luminal contents, which were reflected in the mucosa. Very early after the start of heme ingestion, there was an increase in reactive oxygen species leading to increased levels of lipid peroxidation products. Mucosal gene expression showed at the earliest time point antioxidant response and PPAR target gene activation. After day 4, cytotoxicity of the colonic contents was increased and hyperproliferation was initiated, indicating that cytotoxicity was causal for the initiation of hyperproliferation. Simultaneously, several oncogenes were activated, whereas the tumor suppressor P53 was inhibited. In conclusion, dietary heme caused an acute production of reactive oxygen species in mouse colon. A lag time was observed in the formation of cytotoxicity, which coincided with the initiation of hyperproliferation and the differential expression of oncogenes and tumor suppressor genes.

## INTRODUCTION

Colon cancer is an important health problem in Western countries [1]. Diets high in red meat are associated with an increased risk of colon cancer [2,3,4], whereas diets high in white meat do not increase this risk [5,6]. Kinzler and Vogelstein [7] argued that dietary factors increasing the risk of colon cancer are probably not mutagens, but rather luminal irritants that damage colonic epithelial cells. The iron porphyrin pigment heme, which is such a luminal irritant, is present at much higher levels in red meat than in white meat. Several epidemiological studies show that the intake of dietary heme is associated with an increased cancer risk [8,9].

When rodents receive a diet supplemented with heme, increased reactive oxygen species (ROS) are found in the fecal water (described in chapter 3 and by Sesink et al. [10]), leading to oxidative stress responses in the mucosa. In addition, the colonic contents become more cytotoxic on the heme diet [10,11]. Consequently, the colonic surface epithelium is damaged and compensatory hyperproliferation is initiated in the crypts. We showed recently, that dietary heme initiated this hyperproliferation and hyperplasia by downregulating feedback inhibitors of proliferation, such as Wnt inhibitory factor 1 (Wif1), Interleukin-15 (IL-15), Indian Hedgehog (Ihh) and Bone morphogenetic protein 2 (Bmp2) in the surface epithelium [11].

The increases in ROS, cytotoxicity and proliferation were observed after 14 days of heme feeding. So far, the time dependency of the heme-induced ROS stress and cytotoxic stress on the initiation of hyperproliferation was not studied. It is currently unknown whether the described changes in surface to crypt signaling [11] were caused by cytotoxic stress and/or by oxidative stress. Therefore, we now studied the time course of the possible differential luminal and mucosal effects of dietary heme. Our results show that acute effects, which were already established within 2 days of heme feeding, were the formation of ROS and lipid peroxidation products and the activation of many PPAR target genes. The more delayed effects, occurring after day 4 of heme feeding, were a significantly increase in cytotoxicity of the colon contents and the concomitant induction of compensatory hyperproliferation and hyperplasia in the mucosa.

## MATERIALS AND METHODS

### Animals and diets

Experiments were approved by the Ethical Committee on Animal Testing of Wageningen University and were in accordance with national law. Eight week-old male C57Bl6/J mice (Harlan, Horst, the Netherlands) similar in weight were housed individually in a room with controlled temperature (20- 24°C), relative humidity (55%  $\pm$  15%) and a 12 h light dark cycle. Mice were fed the diet and demineralized water ad libitum.

In a previous experiment the concentration of 0.5  $\mu$ mol heme/g diet was used [11]. A pilot study is performed to study whether a lower dose of heme (0.2  $\mu$ mol heme/g diet)

has similar effects as observed before on heme-induced hyperproliferation. Thereto, mice received a Westernized purified control diet (40 en% fat (mainly palm oil) low calcium (30  $\mu\text{mol/g}$ ) as described previously [12], or this diet supplemented with either 0.2 or 0.5  $\mu\text{mol heme/g}$  diet (Sigma-Aldrich Chemie, St. Louis) for 14 days ( $n=8$  per group).

To study the time-dependent effects of heme on the colonic epithelium, mice received either the Westernized control diet [12] or this diet supplemented with 0.2  $\mu\text{mol heme/g}$ . Before the start of the intervention all mice received the control diet for 1 week. Thereafter, mice received the control or the heme-diet for 2, 4, 7, or 14 days ( $n=4$ , per time point, per diet). One control mouse died for unknown reason at day 2 and this group thus contained three mice. 24-Hour feces were quantitatively collected at day 2, 4, 7, and 14 of the experiment, frozen at  $-20^{\circ}\text{C}$  and subsequently freeze-dried. Mice were anesthetized with isoflurane (1.5% in 70% nitrous oxide and 30% oxygen). After sacrifice, the colon was excised, mesenteric fat was removed and the colon was opened longitudinally. The colon was washed in PBS and cut into three parts. The middle 1.5 cm tissue was formalin-fixed and paraffin embedded for histology. The remaining proximal and distal parts were scraped. Scraped mucosa was pooled per mouse, snap-frozen in liquid nitrogen and stored at  $-80^{\circ}\text{C}$  until further analysis.

## **Fecal analyses**

Fecal water was prepared and the cytotoxicity of this fecal water was measured as described previously [11]. To determine lipid peroxidation products in the lumen, Thiobarbituric Acid Reactive Substances (TBARS) in fecal water were quantified, according to Ohkawa et al. [13]. Briefly, fecal water was diluted 4-fold with double-distilled water. To 100  $\mu\text{l}$  of this dilution, 100  $\mu\text{l}$  of 8.1% SDS and 1 ml of 0.11 mol/L 2,6-di-tert-butyl-p-cresol, 0.5% thiobarbituric acid in 10% acetic acid (pH 3.5) was added. To correct for background, TBA was omitted from the assay. TBARS were extracted, after heating for 75 minutes at  $82^{\circ}\text{C}$ , with 1.2 ml n-butanol. The absorbance of the extracts was measured at 540 nm. The amount of TBARS was calculated as malondialdehyde equivalents using 1,1,3,3-tetramethoxypropane as standard.

## **Immunohistochemistry**

Paraffin embedded colon sections of 5  $\mu\text{m}$  were deparaffinized. Hematoxylin and Eosin staining was performed to assess the morphology of the tissue. To stain proliferating cells, sections were stained with an anti-mouse Ki67-antibody as described previously [11]. Colonocytes from 15 well-oriented crypts (longitudinal sections) were counted for each animal. A cell was scored Ki67-positive when the nucleus of the cell was distinctly brown. The number of Ki67-positive cells per crypt, the total number of cells per crypt and the labeling index (% of Ki67-positive cells per crypt) were determined. For Ki67 quantification, only colons of time point 0 and 14 days ( $n=4$  per time point) were included

for the control mice. Regarding the heme-fed mice, all animals from all time points (day 2, 4, 7, 14; n=4 per time point) were included.

### **RNA isolation**

Total RNA was isolated by using TRIzol reagent (Invitrogen, Breda, the Netherlands) according to the manufacturer's protocol. For microarray hybridization the isolated RNA was further column purified (SV total RNA isolation system Promega, Leiden, the Netherlands). RNA concentration was measured on a Nanodrop ND-1000 UV-Vis spectrophotometer (Isogen, Maarssen, the Netherlands) and analyzed on an Agilent 2100 bioanalyzer (Agilent Technologies, Amsterdam, the Netherlands) with 6000 Nano Chips, according to the supplier's protocol. RNA was judged as suitable for array hybridization only if samples exhibited intact bands corresponding to the 18S and 28S ribosomal RNA subunits, and displayed no chromosomal peaks or RNA degradation products (RNA Integrity Number > 8.0).

### **Array hybridization and microarray data analysis**

For the pilot study using different heme concentrations, RNA was isolated from scrapings of three groups receiving 0, 0.2 or 0.5  $\mu\text{mol}$  heme/g diet (n=8 per group) and pooled per group. To determine the optimal heme concentration there were thus 3 arrays performed. With regard to the time course study, RNA of colon scrapings was isolated and pooled per time point and treatment group. Nine arrays were performed; 1 at time point 0, 2 for all other time points). RNA from both studies was analyzed using Affymetrix Mouse Gene 1.0 ST arrays (Affymetrix). Labeling was performed with 'Affymetrix Whole Transcript Sense Labeling without rRNA reduction step' according to the WT Sense Target Labeling Assay Manual (Affymetrix Santa Clara, CA). Scanned microarrays were analyzed as described [14]. Arrays were normalized using the Robust Multi-array Average method [15,16]. Probe sets were defined according to Dai et al. [17]. Only genes with more than 10 probes on the array, and genes with a signal intensity >20 in at least one of the arrays were included in the analysis. A fold change of 1.3 was set as cut-off for differential regulation. Array data have been submitted to the Gene Expression Omnibus, accession number GSE40671.

### **Statistical analysis**

Physiological data are presented as mean  $\pm$  SEM. Differences in weight and proliferating cells between the different heme concentrations were tested by a one-way ANOVA with a Bonferroni's Multiple Comparison Test. For the time course experiment, differences between heme and control at a certain time point were tested for statistical significance by a two-tailed Student t-test. P-values <0.05 were considered to be significant.

# RESULTS

## Both 0.2 and 0.5 $\mu\text{mol}$ heme per gram food induce hyperproliferation

We previously showed that dietary heme induced hyperproliferation in mouse colon by downregulating feedback inhibitors of proliferation [11]. In that study, using a heme concentration of 0.5  $\mu\text{mol/g}$  diet, body weight was decreased. To prevent weight loss of mice we wanted to use a lower concentration of dietary heme. Moreover, we hypothesized that for studying the heme-induced effects in time, a low concentration of heme is preferred to separate possible differential time-dependent effects. Thereto, we first tested the effects of the more physiological concentration of 0.2  $\mu\text{mol}$  heme/g on proliferation and gene expression at day 14 and compared these effects to the effects of 0.5  $\mu\text{mol}$  heme/g.

After 2 weeks of feeding, mice fed the 0.2  $\mu\text{mol}$  heme/g diet had a similar weight compared to the controls (Table 1). Mice on the 0.5  $\mu\text{mol}$  heme/g diet however, had a significantly lower body weight after 14 days of intervention (Table 1). Colonic proliferation was investigated by Ki67 staining for  $n=4$  mice per group. The amount of proliferating cells and the total number of cells were quantified and presented in Table 1. Proliferation was significantly induced by both 0.2 and 0.5  $\mu\text{mol}$  heme/g diets. The total number of cells per crypt and the number of Ki67-positive cells per crypt were significantly higher in the 0.5 compared to the 0.2  $\mu\text{mol}$  heme/g diet, but the labeling index, which is the percentage of proliferating cells per crypt, was similar in both heme-fed groups.

**Table 1.** Effects of different heme concentrations on physiological parameters.

	control	0.2 $\mu\text{mol}$ heme/g	0.5 $\mu\text{mol}$ heme/g
Weight (g)	25.9 $\pm$ 0.7 <sup>a</sup>	26.0 $\pm$ 0.7 <sup>a</sup>	20.5 $\pm$ 0.6 <sup>b</sup>
Total number of cells per crypt	40.6 $\pm$ 2.1 <sup>a</sup>	58.1 $\pm$ 2.8 <sup>b</sup>	81.4 $\pm$ 1.6 <sup>c</sup>
Number of Ki67-positive cells per crypt	14.3 $\pm$ 1.4 <sup>a</sup>	35.7 $\pm$ 3.6 <sup>b</sup>	46.8 $\pm$ 2.2 <sup>c</sup>
Labeling index (%) <sup>#</sup>	34.9 $\pm$ 1.6 <sup>a</sup>	60.7 $\pm$ 4.3 <sup>b</sup>	57.5 $\pm$ 2.0 <sup>b</sup>

Data are represented as mean  $\pm$  SEM, ( $n=8$  for weight,  $n=4$  for other parameters) after 14 days of intervention.

<sup>#</sup> Labeling index is calculated as percentage Ki67-positive cells per crypt. Statistical significant ( $p<0.05$ ) results are indicated with a different letter (a, b or c) and were tested by one-way ANOVA with a Bonferroni's Multiple Comparison Test.

Mucosal gene expression levels were investigated by microarray on pooled scrapings for the control, the 0.2 and the 0.5  $\mu\text{mol}$  heme/g diets. To determine whether mucosal changes were similar in both heme groups, changes in gene expression on the 0.5  $\mu\text{mol}$  heme/g diet were correlated to the fold changes for significant changed genes ( $n=3,663$ ,  $q<0.01$ ) found in our previous identically designed mice study with individual arrays ( $n=7-9$  per group) [11]. This yielded a Pearson correlation coefficient of 0.832 ( $p<0.000$ , not shown), implying that gene expression changes were highly similar and reproducible between both studies. When comparing the expression levels of these 3,663 genes within

this experiment, comparing 0.2 and 0.5  $\mu\text{mol heme/g}$ , a Pearson correlation coefficient of 0.881 was obtained ( $p < 0.000$ , Figure 1). This implies that both 0.2 and 0.5  $\mu\text{mol heme/g}$  modulate the expression of similar genes to a similar extent.

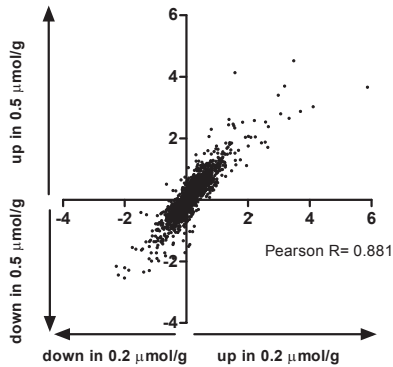


**Figure 1.** Fold changes of genes induced by the 0.5  $\mu\text{mol heme/g}$  concentration are correlated to fold changes of the same genes induced by 0.2  $\mu\text{mol heme/g}$ . Correlation analysis includes fold changes of genes which were differentially expressed ( $n=3663$ ,  $q < 0.01$ ) in a recent, identical study [11], using individual arrays ( $n=7$  for controls and  $n=9$  for heme). Pearson  $R=0.881$  with  $p < 0.000$ .

### Differential time course of heme-induced oxidative and cytotoxic stress in the colonic lumen

Next, a time course study was performed to investigate the causality of heme-induced changes. In this study mice received a heme diet for 2, 4, 7, or 14 days ( $n=4$  per time point). For this study, the concentration of 0.2  $\mu\text{mol heme/g}$  diet was used as it increased cell proliferation, without affecting body weight, and induced similar gene expression changes as 0.5  $\mu\text{mol heme/g}$  (see above). Before the start of the experiment, all mice received the control diet for 1 week. Also in this study, body weight was not significantly different in the heme group compared to the control throughout the experiment (final weights (mean  $\pm$  SEM):  $26.6 \pm 1.0$  versus  $28.1 \pm 1.2$  g for heme and control, respectively). The overall morphology of the colonic tissue was visualized by an H&E staining (Figure 2). There were no signs of inflammation, as there was no infiltration of neutrophils or macrophages in the lamina propria.

Heme induced oxidative stress in the colonic lumen of mice by generating reactive oxygen species (ROS), reflected by a heme-dependent increase in fecal thiobarbituric acid reactive substances (TBARS) (chapter 3). TBARS were measured in fecal waters at all time points included in the study. TBARS were significantly higher in the heme-fed mice compared to the controls at day 2 of heme-feeding and stayed higher than controls throughout the study (Figure 3A). This implies that dietary heme induced ROS production acutely, that is within the first 2 days of heme exposure. Besides ROS production, we previously found that dietary heme also induces cytotoxicity of the colonic contents [11]. This increase in cytotoxicity is caused by the covalently modified heme metabolites of which the exact structure is unknown [12]. In our time course study, cytotoxicity of fecal water was low in control animals and was stable over time (Figure 3B). Remarkably, there

was a lag time in the induction of cytotoxicity of the colonic contents of the heme-fed mice. Cytotoxicity increased after day 4 and was significantly higher on heme compared to the controls on day 7 and 14. The Ki67 staining for proliferation (Figure 2) revealed that heme mice increased their proliferation of colonic epithelial cells from day 4, and the difference was significant on day 7 and 14 (Figure 3C). Together these physiological changes show that oxidative stress is a very early heme-induced effect whereas the induction of both cytotoxicity and hyperproliferation are delayed effects.

### **Time course of differential heme-modulated transcription factors and processes in colon mucosa**

To get more insight into the heme-modulated cellular processes in time, gene expression patterns were investigated by using whole genome microarrays. Based on the physiological changes described above there were 2 main effects in time; acute effects from day 2 that persisted till day 14, and delayed effects which were initiated after day 4 and lasted till day 14. Ingenuity software (Ingenuity® Systems, [www.ingenuity.com](http://www.ingenuity.com)) was used to get more insight into the processes and transcription factors which were involved in these heme-induced acute or delayed effects. Thereto, differentially expressed genes (fold change >1.3 or -1.3) for each time point were uploaded and analyzed. Ingenuity software showed that the majority of the differentially expressed genes at day 2 played a role in lipid metabolism (Figure 4A). The genes changed after day 4 however, were related to neoplasia/cancer and proliferation. Based on differentially expressed genes, Ingenuity indicates which transcription factors are involved in the induction or repression of these genes. For day 2, these were PPAR $\alpha$  and PPAR $\gamma$ , two important transcription factors in lipid metabolism, which were activated (Figure 4B). After day 4, the heme diet activated several oncogenes, such as Myc, Tbx2, Foxm1 and Jun, and inhibited the tumor suppressor TP53 (Figure 4B). Thus, this Ingenuity analysis indicated acute activation of PPAR $\alpha$  and PPAR $\gamma$  targets and lipid-related processes and a more delayed induction of tumor-related processes, which is line with the physiological findings described above.

### **Heme instantaneously changed the expression of lipid and oxidative stress-related genes**

Gene expression levels were determined to see which genes contributed to the acute or delayed heme-induced effects (Figure 5). In line with the Ingenuity results, many of the genes that were up or downregulated at day 2 were involved in fatty acid metabolism according to their GO annotations. Of all the genes changed at day 2, 64% were PPAR $\alpha$  target genes (Figure 5A). For the colon, several PPAR $\gamma$  targets were identified [18], but these PPAR $\gamma$  target genes show a large overlap with the PPAR $\alpha$  targets [19]. Therefore in Figure 5 expression levels of defined PPAR $\alpha$  targets were shown [19]. Dietary heme catalyzed the production of ROS which results in the production of oxidized lipids.



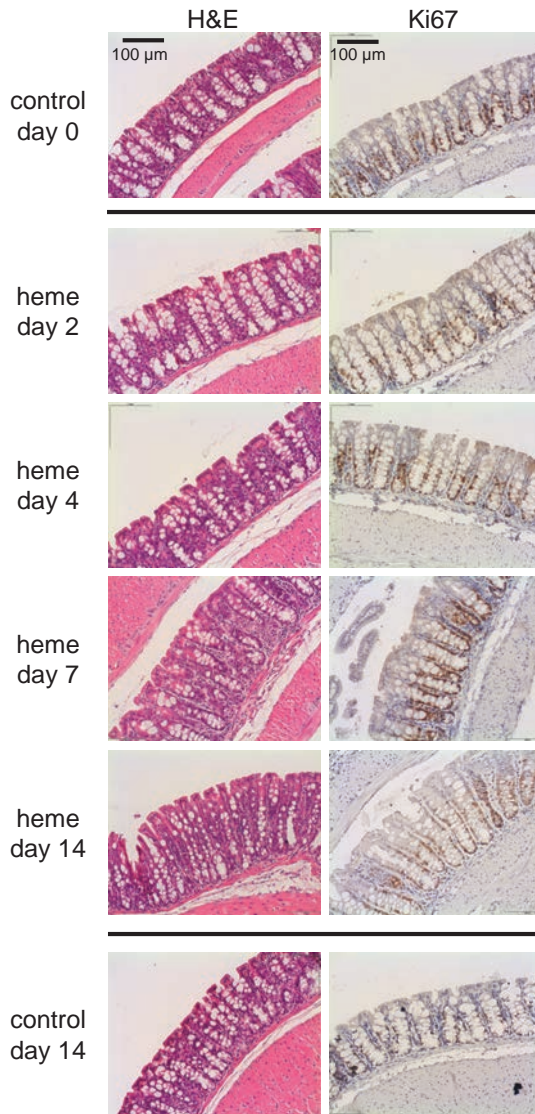


**Figure 2.** Stainings of mouse colonic mucosa in time on control or heme diet. Histological staining was performed for H&E. Ki67 immunohistochemistry was performed using a Ki67-specific antibody.

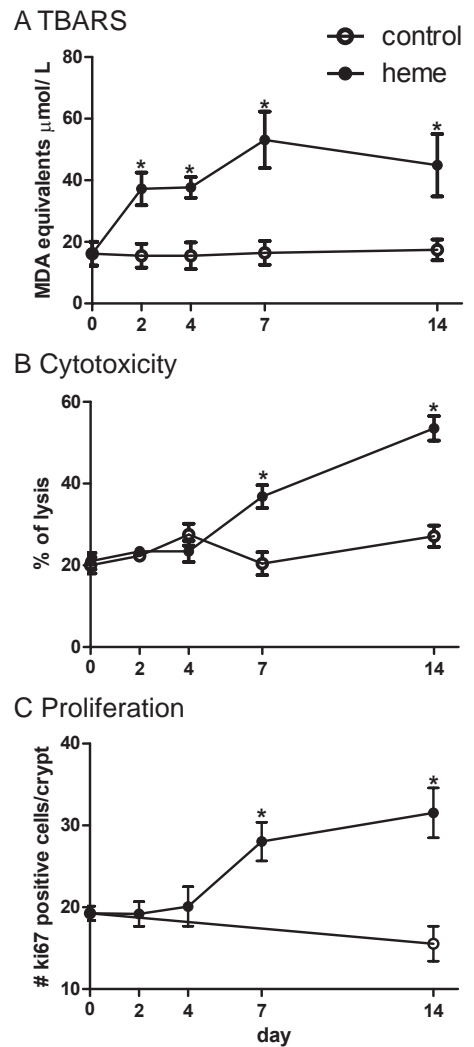


**Figure 3.** The effects of the heme diet on TBARS (A), cytotoxicity (B) and proliferation (C) in time. TBARS and cytotoxicity measurements were performed in triplo. Ki67-positive cells were counted for all heme-fed mice and for controls on day 0 and day 14. Data are represented as mean  $\pm$  SEM (n=4). \* indicates significant difference with  $p < 0.05$ .

These oxidized lipids are ligands for PPARs, and most probably induced the expression of PPAR target genes on the heme diet. Besides PPARα targets, 11% of differentially expressed genes were upregulated Nrf2-target genes, such as catalase. Nrf2 was also present in the Ingenuity results as involved transcription factor at day 2 with a p-value of 0.0013. However, Nrf2 had a z-score lower than 2 and was therefore not presented in Figure 4B. Vanin-1 (Vnn1), which is a PPARα target and a marker of oxidative stress [20], was also instantaneously upregulated (Figure 5A).

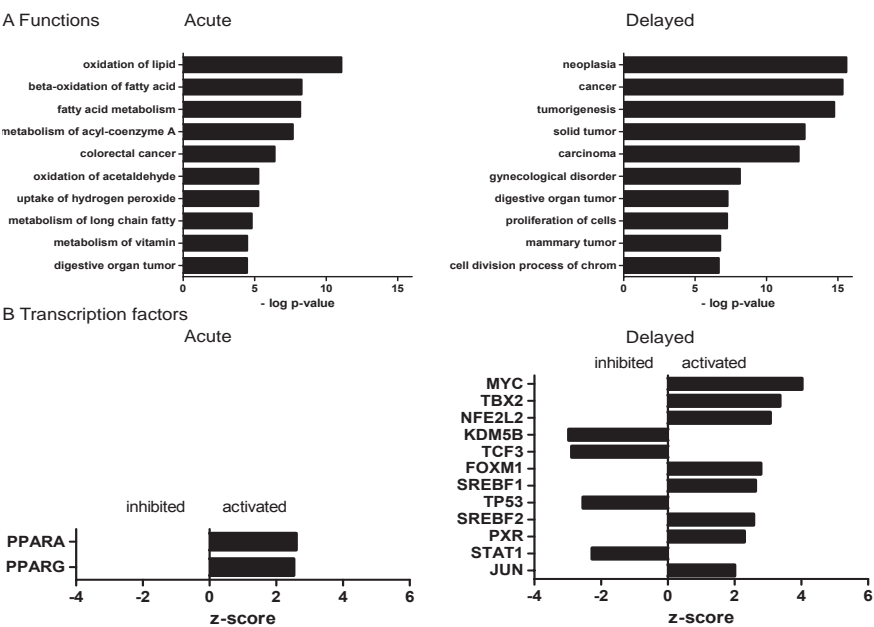


**Figure 4.** (A) Top 10 of significantly changed functional annotations affected acutely and delayed upon a heme diet. P-value ranges for instantaneous effects are:  $8.8 \times 10^{-12}$ - $2.8 \times 10^{-4}$  and for delayed effects:  $2.6 \times 10^{-14}$ - $5.3 \times 10^{-6}$ . (B) Transcription factors that control in the instantaneous and delayed differential gene expression. Only transcription factors which have a z-score higher than 2 or lower than -2 and were significantly regulated (day 2:  $p < 7.45 \times 10^{-12}$ , day 7:  $p < 5.30 \times 10^{-3}$ ) were included.

### Delayed mucosal sensing of heme and cytotoxicity coincided with hyperproliferation

Gene expression levels for the delayed effects are shown in Figure 5B. In total there were more delayed than acute differentially expressed genes (381 versus 44), and the delayed differentially expressed genes were involved in a broad range of processes. Heme-sensing genes were generally changed after day 4, such as the enzyme Hmox1 which is induced by its substrate heme [21]. The putative heme transporter Slc46a1 [22] and the heme and bilirubin exporter Abcg2 [23] were also significantly changed after day 4. The delayed differential expression of these heme metabolism-related genes after day 4 suggests that the cells did not sense dietary heme immediately after ingestion. This delayed heme

sensing was also illustrated by the downregulation of *Ppargc1α*, which is an important target gene of the heme sensor *Nr1d1* (*Rev-erba*). Wu et al. [24] showed that heme-activated *Nr1d1* represses the transcription of *Ppargc1α* and this occurred in our study after day 4. Eventually, the expression of *Nr1d1* itself was downregulated after day 7.

As luminal cytotoxicity was increased after day 4 we determined when the increased cytotoxicity affected the epithelial surface cells. Therefore, cytotoxic stress- and cell death-related genes were investigated and are shown in Figure 5B. In our previous study we showed that dietary heme induced surface specific inhibition of cap-dependent protein translation by increasing surface epithelial cell levels of the ER stress marker *Eif4ebp1* (4E-BP1) [11]. In this time course study we found that 4E-BP1 was upregulated after day 4, which coincides with the increased cytotoxic stress. The induced expression of glutathione metabolism-related genes between day 4 and 7 indicated an increased need for protection against noxious compounds. With regard to cell death we found that the apoptosis inhibitor survivin (*Birc5*) was upregulated at day 4. Recently, we determined that this is a crypt-specific upregulation [11]. Another apoptosis inhibitor, Immediate early response 3 (*Ier3*), was also upregulated after day 4, and this is a surface cell-specific upregulation [11]. Besides apoptosis inhibitors, the necrosis inducer Receptor interacting protein kinase-3 (*Ripk3*) was significantly upregulated upon heme feeding after day 4. This indicated that after 4 days of heme-feeding, there was a shift in type of cell death from apoptosis to luminal necrosis, which is in line with our earlier studies [11,25].

As the mucosa sensed cytotoxicity after day 4, signals from the damaged surface cells had to trigger the transit-amplifying crypt cells for compensatory hyperproliferation. We showed recently that dietary heme initiated this hyperproliferation, resulting in hyperplasia, by downregulating feedback inhibitors of proliferation, such as *Wif1*, *Ihh*, *Bmp2* and *IL-15*, in the surface epithelium [11]. When investigating gene expression changes of these genes in time, we found a downregulation of *Wif1*, *Bmp2* and *IL-15* after day 4, whereas *Ihh* remained constant (Figure 5B). The downregulation of these three signaling molecules coincided with the increase in cell proliferation (Figure 3C) and with the upregulation of cell cycle-related genes (Figure 5B). The *Ki67* gene expression levels were significantly higher in heme-fed mice compared to controls after day 4, which is in line with their protein levels (Figure 2). *Plk1*, *Mad2l1* and *Cdc20*, belonging to the KEGG cell cycle pathway, were upregulated after day 4 (Figure 5B). Moreover, cyclins A2 and B2 were significantly higher expressed in heme than control after day 4.

Taken together, these gene expression results show that the mucosal response to luminal oxidative and cytotoxic stress coincided with the differential time course of the luminal stressors. This is illustrated for selected marker genes in Figure 6A. Catalase expression showed that cytotoxic stress was sensed acutely. However, sensing of oxidative stress (e.g. *Ripk3*) occurred after day 4. This coincided with the downregulation of the surface to crypt signaling proliferation inhibitors (e.g. *IL-15*) and upregulation of cell turnover

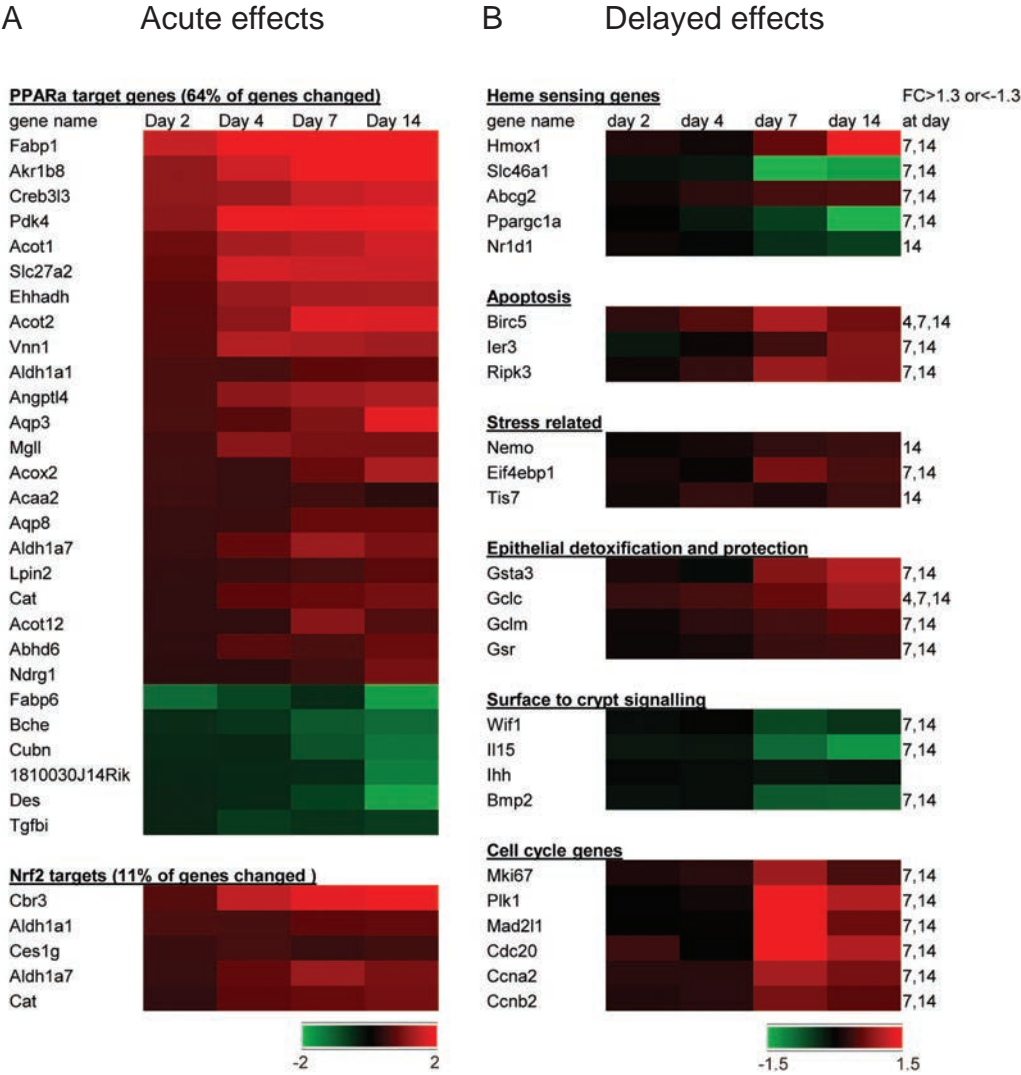


**Figure 5.** Heat map showing heme-induced acute (A) and delayed (B) response genes. Expression is based on pooled arrays of  $n=4$  mice per group, and represented as signal log ratios. Panel A contains differentially expressed genes ( $FC>1.3$  or  $FC<-1.3$ ) at day 2, of which many were involved in lipid metabolism and oxidative stress based on KEGG pathways. Red indicates upregulation and green indicated downregulation. Color scale ranges from a signal log ratio of -2 (green) to 2 (red). Panel B contains delayed heme-induced genes. The day on which these genes were differentially expressed ( $FC>1.3$  or  $FC<-1.3$ ) is indicated in the last column. Color scale ranges from a signal log ratio of -1.5 (green) to 1.5 (red).

genes (e.g. Ki67). Remarkably, there was also delayed heme sensing (Hmox1). This raised the question why heme was sensed only after day 4, whereas heme is present in the colon at day 1, as the oral fecal transit time in rodents is much less than 24 hours. This implies that there was a barrier between the heme present in the luminal contents and the surface epithelial cells. The continuous mucus layer in the colon protects the surface cells against the luminal heme contents. We investigated whether there were time-dependent changes in the expression of mucin and O-glycosylation genes. Only the expression of the cell surface mucin 1 (Muc1) and the core-2 glucosaminyl (N-acetyl) transferase 1 (Gcnt1) was downregulated after day 4 (Figure 6A). Analysis of the expression database from our recent laser capture microdissection study [11] showed that the heme-induced downregulation of these genes occurs exclusively in the surface epithelium (Figure 6B). This indicates that there might be a reduced mucus barrier function after day 4 on the heme diet.

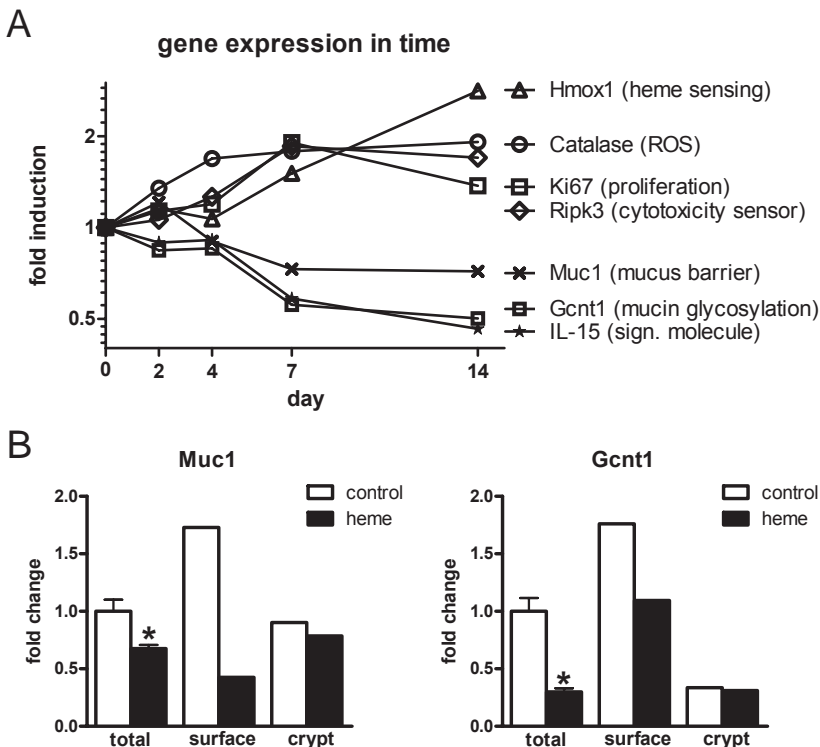


**Figure 6.** (A) Expression of selected marker genes indicating the differential mucosal response in time. (B) Expression levels of Muc1 and Gcnt1 in total scrapings, in surface cells and crypt cells. Expression levels of total scrapings are based on microarray analysis of individual mice ( $n=7$  control and  $n=9$  heme-fed mice) as described in [11]. Data are represented as mean  $\pm$  SEM,  $*q<0.01$ . Surface- and crypt-specific microarray gene expression profiles are obtained from pooled tissue samples obtained by laser capture microdissection ( $n=4$  controls,  $n=3$  heme-fed mice) [11]. Surface and crypt expression values are normalized for the expression of total scrapings from control mice.

## DISCUSSION

To our knowledge this is the first study showing that the effect of dietary heme on the colon epithelium can be separated into an acute ROS stress and a delayed cytotoxic stress. The increased ROS production, which was present within the first 2 days of heme feeding, induced the formation of lipid peroxidation products. These lipid peroxidation products are ligands for PPARs [26,27,28], and may thus explain the acute activation of PPAR target genes. Besides, ROS can activate Nrf2, which is a transcription factor regulating the antioxidant response via the antioxidant response element (ARE)-mediated induction of many cytoprotective enzymes, such as catalase. Several Nrf2-targets were induced at day 2 after heme consumption and stayed higher expressed throughout the experiment. Vanin-1 is an oxidative stress marker [20], which was upregulated from day 2. Besides an oxidative stress marker, Vanin-1 is recently proposed as a causal factor in colonic hyperproliferation [29]. However, this is not corroborated by our study as no increase in proliferation is observed concomitant with Vanin-1 upregulation. Besides Vanin-1, expression levels of Metallothionein-1 (MT1) [30] and alkaline phosphatase (Alpi) [31] are known to be induced by oxidative stress and these genes were upregulated significantly from day 4 (data not shown). Together, these gene expression changes and the changes in TBARS show that shortly after heme consumption increased oxidative stress is present. However, there were no acute changes in cell cycle genes observed, indicating that luminal ROS does not directly cause hyperproliferation. Remarkable is the expression of Birc5 (survivin), which was increased at day 4. Survivin is an apoptosis inhibitor and its upregulation implies that apoptosis is decreased. As the total numbers of cells per crypt is similar at day 2 and 4 we speculate that a possible inhibition of apoptosis might compensate for a slightly increased necrosis, induced by oxidative damage.

After day 4 the expression of several cytotoxic stress markers is upregulated, which coincides with the induction in luminal cytotoxicity. We have shown before that the immediate early response gene *Tis7* is upregulated by dietary heme especially at the surface epithelium [11]. In the current study we show that this upregulation is a delayed effect. The induction of the necrosis inducer *Ripk3* and the stress-related gene *Nemo* was also delayed. From our previous study we also know that protein translation is inhibited in heme-fed mice specifically at the surface epithelium, shown by an upregulation of the translation inhibitor 4E-BP1 [11]. Here we show that 4E-BP1 was upregulated after day 4 and thus coincides with the increased cytotoxic stress. It is most probable that cytotoxicity damages the surface cells, which subsequently inhibit their protein translation to prevent energy dissipation. The induction of 4E-BP1 inhibits protein translation which implies that protein levels of the identified signaling molecules involved in proliferation are lower than would be expected based on gene expression changes. Although there were no significant changes found at gene expression level for the signaling molecule *Ihh*, *Ihh* protein levels can actually be lower under heme conditions due to the translation inhibition of 4E-BP1.



Besides the increased cytotoxicity, also hyperproliferation and hyperplasia is induced by heme after day 4 both at gene expression level as well as for the Ki67 counts. In line with this, there was activation of several oncogenes and inhibition of the tumor suppressor TP53. Previous dietary interventions with bile acids [32] or calcium [33] showed that luminal cytotoxicity is causal for hyperproliferation. The present study supports this causality as both the heme-induced cytotoxicity and hyperproliferation originate simultaneously.

The delayed luminal cytotoxicity observed in the present study is in line with our proposed mechanism for the formation of the cytotoxic heme factor (CHF). As described earlier [10], we believe that CHF is formed in the colonic lumen via covalent addition of reactive lipid peroxides to the protoporphyrin ring of heme, resulting in very lipophilic products with a molecular weight higher than that of heme [12]. This implies that lipid peroxides, measured as TBARS, must first accumulate in the colonic lumen before substantial CHF formation can occur. With the low heme concentration in the present study this apparently requires about 4 days. This lag time is dependent on the heme dosage and should be shorter with higher heme intake. Indeed, an earlier pilot experiment in our laboratory showed that cytotoxicity was already increased at the earliest time point, i.e. day 3, using a diet with 0.6  $\mu\text{mol}$  heme/g in rats (Sesink & van der Meer, unpublished observation). Unfortunately, final proof for this mechanism is lacking as the precise structure of CHF remains unknown. We could not obtain its mass spectrum in different types of mass spectrometers, because CHF could not be ionized, which is a known problem with complex lipophilic compounds. However, there are several dietary interventions which support our mechanism. For instance, heme-induced TBARS and cytotoxicity are almost completely prevented by antioxidants [34], replacement of polyunsaturated fat by monounsaturated fat [34], and by the heme antagonist chlorophyll, mimicking intake of vegetables [12,35]. It should be noted that these interventions also prevented heme-induced hyperproliferation [12,35] and aberrant crypt formation [34], illustrating the causal role of luminal cytotoxicity. Taken together, these studies show that formation of CHF in the colonic lumen is critically dependent on the presence of lipid peroxides. Thus, whereas lipid peroxides themselves do not cause hyperproliferation, they are indirectly causal via de formation of CHF.

We speculate that this heme  $\rightarrow$  CHF  $\rightarrow$  cytotoxicity  $\rightarrow$  hyperproliferation sequence in colon may be modulated by other luminal factors such as the microbiota. This is because bacteria are able to catabolize heme [36] and other porphyrins [37] which may interfere with the formation of CHF. In addition, the colon microbiota metabolizes the protective mucus layer and modulates the expression of the genes controlling the mucin barrier [38]. With regard to this, it may be of significance that the downregulation of Muc1 and Gcnt1 (Fig 6B) coincides with the increase in cytotoxicity. This is not due to a generic cytotoxic effect as the expression of other mucin genes was not changed.

Therefore this may indicate a specific change in luminal signals reflecting a change in microbiota composition. Using classical plating techniques we have shown recently that heme increases enterobacteria and decreases lactobacilli [39]. Therefore we will first more specifically study whether heme induces changes in the microbiota by using phylogenetic microarrays. If these changes are substantial we will study whether they are causally related to the mechanistic heme sequence by using antibiotics.

In this study we used heme as a proxy for the consumption of red meat. The results show that a low concentration of heme (0.2  $\mu\text{mol heme/g}$ ) already induces cytotoxicity and epithelial hyperproliferation. This is in line with earlier studies in rats showing that 0.16 and 0.25  $\mu\text{mol heme/g}$  induce cytotoxicity leading to hyperproliferation [40] and aberrant crypt formation [34], respectively. As an average human diet consists of about 400 g dry weight per day, 0.2  $\mu\text{mol heme/g}$  diet corresponds to 80  $\mu\text{mol heme/day}$ . As beef contains 0.5  $\mu\text{mol heme/g}$  wet weight [41], this implies that 0.2  $\mu\text{mol heme/g}$  used in our study mimics a daily intake of 160 g red meat for humans.

In conclusion, dietary heme causes an acute luminal ROS production and oxidative stress response in the mucosa. Delayed, dietary heme increases the cytotoxicity of the colonic content and simultaneously heme-induced hyperproliferation is observed. Therefore, heme-induced hyperproliferation is related to cytotoxic stress rather than oxidative stress. Whether changes in colon microbiota play a role in the delayed cytotoxicity and hyperproliferation will be investigated further.

## **ACKNOWLEDGEMENTS**

The authors would like to thank Mechteld Grootte Bromhaar, Jenny Jansen and Philip de Groot for microarray analysis and Bert Weijers for technical assistance.



## REFERENCES

- 1 Jemal A, Siegel R, et al. Cancer statistics, 2010. *CA: a cancer journal for clinicians* 2010;60:277-300.
- 2 World Cancer Research Fund. Food, Nutrition, Physical Activity and the Prevention of Cancer: a Global Perspective. Washington, DC: American Institute for Cancer Research, 2007.
- 3 Larsson SC, Wolk A. Meat consumption and risk of colorectal cancer: a meta-analysis of prospective studies. *Int J Cancer* 2006;119:2657-64.
- 4 Norat T, Bingham S, et al. Meat, fish, and colorectal cancer risk: the European Prospective Investigation into cancer and nutrition. *J Natl Cancer Inst* 2005;97:906-16.
- 5 Giovannucci E, Rimm EB, et al. Intake of fat, meat, and fiber in relation to risk of colon cancer in men. *Cancer Res* 1994;54:2390-7.
- 6 Larsson SC, Rafter J, et al. Red meat consumption and risk of cancers of the proximal colon, distal colon and rectum: the Swedish Mammography Cohort. *Int J Cancer* 2005;113:829-34.
- 7 Kinzler KW, Vogelstein B. Lessons from hereditary colorectal cancer. *Cell* 1996;87:159-70.
- 8 Balder HF, Vogel J, et al. Heme and chlorophyll intake and risk of colorectal cancer in the Netherlands cohort study. *Cancer Epidemiol Biomarkers Prev* 2006;15:717-25.
- 9 Lee DH, Anderson KE, et al. Heme iron, zinc, alcohol consumption, and colon cancer: Iowa Women's Health Study. *J Natl Cancer Inst* 2004;96:403-7.
- 10 Sesink AL, Termont DS, et al. Red meat and colon cancer: the cytotoxic and hyperproliferative effects of dietary heme. *Cancer Res* 1999;59:5704-9.
- 11 IJssennagger N, Rijnierse A, et al. Dietary haem stimulates epithelial cell turnover by downregulating feedback inhibitors of proliferation in murine colon. *Gut* 2012;61:1041-9.
- 12 de Vogel J, Jonker-Termont DSM, et al. Green vegetables, red meat and colon cancer: chlorophyll prevents the cytotoxic and hyperproliferative effects of haem in rat colon. *Carcinogenesis* 2005;26:387-93.
- 13 Ohkawa H, Ohishi N, et al. Assay for lipid peroxides in animal tissues by thiobarbituric acid reaction. *Analytical biochemistry* 1979;95:351-8.
- 14 Lin K, Kools H, et al. MADMAX – Management and analysis database for multiple -omics experiments. *Journal of integrative bioinformatics* 2011;8:160.
- 15 Bolstad BM, Irizarry RA, et al. A comparison of normalization methods for high density oligonucleotide array data based on variance and bias. *Bioinformatics* 2003;19:185-93.
- 16 Irizarry RA, Bolstad BM, et al. Summaries of Affymetrix GeneChip probe level data. *Nucleic Acids Res* 2003;31:e15.
- 17 Dai M, Wang P, et al. Evolving gene/transcript definitions significantly alter the interpretation of GeneChip data. *Nucleic Acids Res* 2005;33:e175.
- 18 Su W, Bush CR, et al. Differential expression, distribution, and function of PPAR-gamma in the proximal and distal colon. *Physiol Genomics* 2007;30:342-53.
- 19 Rakhshandehroo M, Knoch B, et al. Peroxisome proliferator-activated receptor alpha target genes. *PPAR Res* 2010;2010.
- 20 Berruyer C, Martin FM, et al. Vanin-1-/- mice exhibit a glutathione-mediated tissue resistance to oxidative stress. *Mol Cell Biol* 2004;24:7214-24.
- 21 Loboda A, Jazwa A, et al. Heme oxygenase-1 and the vascular bed: from molecular mechanisms to therapeutic opportunities. *Antioxid Redox Signal* 2008;10:1767-812.
- 22 West AR, Oates PS. Mechanisms of heme iron absorption: current questions and controversies. *World J Gastroenterol* 2008;14:4101-10.
- 23 Latunde-Dada GO, Simpson RJ, et al. Recent advances in mammalian haem transport. *Trends Biochem Sci* 2006;31:182-8.
- 24 Wu N, Yin L, et al. Negative feedback maintenance of heme homeostasis by its receptor, Rev-erbalpha. *Genes Dev* 2009;23:2201-9.
- 25 de Vogel J, van-Eck WB, et al. Dietary heme injures surface epithelium resulting in hyperproliferation, inhibition of apoptosis and crypt hyperplasia in rat colon. *Carcinogenesis* 2008;29:398-403.
- 26 Delerive P, Furman C, et al. Oxidized phospholipids activate PPARalpha in a phospholipase A2-dependent manner. *FEBS Lett* 2000;471:34-8.

- 27 Sethi S, Ziouzenkova O, et al. Oxidized omega-3 fatty acids in fish oil inhibit leukocyte-endothelial interactions through activation of PPAR alpha. *Blood* 2002;100:1340-6.
- 28 Pizzimenti S, Laurora S, et al. Synergistic effect of 4-hydroxynonenal and PPAR ligands in controlling human leukemic cell growth and differentiation. *Free Radic Biol Med* 2002;32:233-45.
- 29 Pouyet L, Roisin-Bouffay C, et al. Epithelial vanin-1 controls inflammation-driven carcinogenesis in the colitis-associated colon cancer model. *Inflamm Bowel Dis* 2010;16:96-104.
- 30 Andrews GK. Regulation of metallothionein gene expression by oxidative stress and metal ions. *Biochem Pharmacol* 2000;59:95-104.
- 31 Harada T, Koyama I, et al. Heat shock induces intestinal-type alkaline phosphatase in rat IEC-18 cells. *American journal of physiology Gastrointestinal and liver physiology* 2003;284:G255-62.
- 32 Lapre JA, Van der Meer R. Diet-induced increase of colonic bile acids stimulates lytic activity of fecal water and proliferation of colonic cells. *Carcinogenesis* 1992;13:41-4.
- 33 Lapre JA, De Vries HT, et al. The antiproliferative effect of dietary calcium on colonic epithelium is mediated by luminal surfactants and dependent on the type of dietary fat. *Cancer Res* 1993;53:784-9.
- 34 Pierre F, Tache S, et al. Meat and cancer: haemoglobin and haemin in a low-calcium diet promote colorectal carcinogenesis at the aberrant crypt stage in rats. *Carcinogenesis* 2003;24:1683-90.
- 35 de Vogel J, Jonker-Termont DS, et al. Natural chlorophyll but not chlorophyllin prevents heme-induced cytotoxic and hyperproliferative effects in rat colon. *J Nutr* 2005;135:1995-2000.
- 36 Frankenberg-Dinkel N. Bacterial heme oxygenases. *Antioxid Redox Signal* 2004;6:825-34.
- 37 Young GP, St John DJ, et al. Haem in the gut. Part II. Faecal excretion of haem and haem-derived porphyrins and their detection. *J Gastroenterol Hepatol* 1990;5:194-203.
- 38 McGuckin MA, Linden SK, et al. Mucin dynamics and enteric pathogens. *Nature reviews Microbiology* 2011;9:265-78.
- 39 Schepens MA, Vink C, et al. Dietary heme adversely affects experimental colitis in rats, despite heat-shock protein induction. *Nutrition* 2011;27:590-7.
- 40 Sesink AL, Termont DS, et al. Red meat and colon cancer: The cytotoxic and hyperproliferative effects of low concentrations of dietary heme. *Gastroenterology* 2000;118:A282-A.
- 41 Schwartz S, Ellefson M. Quantitative fecal recovery of ingested hemoglobin-heme in blood: comparisons by HemoQuant assay with ingested meat and fish. *Gastroenterology* 1985;89:19-26.

## Chapter 5

### Dietary heme alters microbiota and mucosa of mouse colon without functional changes in host-microbe cross-talk

Noortje IJssennagger\*, Muriel Derrien\*, Gerdien van Doorn, Anneke Rijnierse, Bartholomeus van den Bogert, Michael Müller, Jan Dekker, Michiel Kleerebezem and Roelof van der Meer

*\*both authors contributed equally*

*Under revision in PLoS ONE*

## ABSTRACT

Colon cancer is a major cause of cancer deaths in Western countries and is associated with diets high in red meat. Heme, the iron-porphyrin pigment of red meat, induces cytotoxicity of gut contents which injures surface cells leading to compensatory hyperproliferation of crypt cells. This hyperproliferation results in epithelial hyperplasia which increases the risk of colon cancer. In humans, a high red-meat diet increases *Bacteroides* spp. in feces. Therefore, we simultaneously investigated the effects of dietary heme on colonic microbiota and on the host mucosa of mice.

Whole genome microarrays showed that heme injured the colonic surface epithelium and induced hyperproliferation by changing the surface to crypt signaling. Using 16S rRNA phylogenetic microarrays, we investigated whether bacteria play a role in this changed signaling. Heme increased Bacteroidetes and decreased Firmicutes in colonic contents. This shift was most likely caused by a selective susceptibility of Gram-positive bacteria to heme cytotoxic fecal water, which is not observed for Gram-negative bacteria, allowing expansion of the Gram-negative community. The increased amount of Gram-negative bacteria most probably increased LPS exposure to colonocytes, however, there is no appreciable immune response detected in the heme-fed mice. There was no functional change in the sensing of the bacteria by the mucosa, as changes in inflammation pathways and Toll-like receptor signaling were not detected. This unaltered host-microbe cross-talk indicates that the changes in microbiota do not play a causal role in the observed hyperproliferation and hyperplasia.

## INTRODUCTION

Colon cancer is a leading cause of cancer deaths in Western countries [1]. The risk to develop colon cancer is associated with diets high in red meat [2], but not with diets high in white meat, such as poultry and fish [3,4]. Heme, the iron porphyrin pigment, is present at much higher levels in red- compared to white meat. Epidemiological studies show that increased heme intake is related to increased colon cancer risk [5,6].

Our previous studies show that when rodents consume heme, their colonic contents become more cytotoxic [7,8]. This increased cytotoxicity injures colon surface epithelial cells and leads to initiation of hyperproliferation from stem cells in the crypts to compensate for the injured surface cells. Recently, we showed that dietary heme changed the surface to crypt signaling by downregulating feedback inhibitors of proliferation such as Wnt inhibitory factor 1 (Wif1), Interleukin-15 (IL-15), Indian hedgehog (Ihh) and Bone morphogenetic protein 2 (Bmp2) in the surface epithelium [8]. The resulting compensatory hyperproliferation and hyperplasia increases the risk of mutations in oncogenes and tumor suppressor genes and thereby increases the risk to develop colon cancer.

Dietary heme is poorly absorbed in the small intestine, and approximately 90% of dietary heme proceeds to the colon where it can be used by colonic bacteria as a growth factor [9]. The relationship between intestinal microbiota and development of colon cancer has long been suspected [10], especially since the colon is the most densely bacteria-populated intestinal region. Cultivation-based studies from individuals with a high colon cancer risk showed distinct fecal microbiota compared to healthy individuals [11]. Besides beneficial components such as short chain fatty acids, microbiota can also produce deleterious components, such as secondary bile acids [12], hydrogen sulfide from sulfate and sulfur-amino acids [13], and N-nitroso-compounds (NOC) from nitrite [14], which all might play a role in development of colon cancer [15,16].

Recently, we showed by classical culturing methods that a heme diet increases the colonic enterobacteria in rats, but decreases lactobacilli [17]. Because of that we now repeat our mice study described above, to explore how heme affects the overall composition of the gut microbiota by using a phylogenetic microarray specific for mouse gut-phylotypes. Whole genome microarrays were used to validate the simultaneous effects of heme on mouse colonic mucosa. Subsequently, we investigated whether the changes in microbiota can be related to the heme-induced epithelial hyperproliferation and hyperplasia.

## **MATERIALS AND METHODS**

### **Ethics statement**

The institutional and national guidelines for the care and use of animals were followed and the experiment was approved by the Local Committee for Care and Use of Laboratory Animals at Wageningen University.

### **Animals and diets**

Eight-week-old male C57Bl6/J mice (Harlan, Horst, the Netherlands) similar in weight were individually housed in a room with controlled temperature (20- 24°C), relative humidity (55%  $\pm$  15%) and a 12 h light-dark cycle. Mice were fed diets and demineralized water ad libitum. To study the effects of heme on the colonic epithelium, mice (n=8/group) received either a Westernized control diet (40 % fat (mainly palm oil) low calcium (30  $\mu$ mol/g)) or this diet supplemented with 0.5  $\mu$ mol/g heme (Sigma-Aldrich Chemie, St. Louis, USA) for 14 days, as previously described [18]. Feces were quantitatively collected during days 11-14, frozen at -20°C and freeze-dried. After 14 days of diet intervention the colon was excised, mesenteric fat was removed and the colon was opened longitudinally. Luminal colonic contents were collected and stored at -80°C for microbiome analysis. The colon was washed in PBS and cut into three parts. The middle 1.5 cm tissue was formalin-fixed and paraffin embedded for histology. The remaining proximal and distal parts were scraped. Scrapings were pooled per mouse, snap-frozen in liquid nitrogen and stored at -80°C until further analysis. The present study was an exact repetition of our recently described study [8], except for the microbiome analysis.

### **Fecal analyses**

Cytotoxicity of fecal water was determined as described before [8]. The procedure to measure host DNA in feces was described in [19]. To determine lipid peroxidation products in the colonic lumen, thiobarbituric acid reactive substances (TBARS) in fecal water were quantified (see supplement).

### **Histology**

Immunohistochemical and immunofluorescent stainings were performed on paraffin embedded colon sections (details in supplement). Ki67 immunohistochemistry was performed to stain proliferating cells, as described previously [8]. Colonocytes from 15 well-oriented crypts (longitudinal section) were counted for each animal.

### **RNA isolation and microarrays**

As the present study was a repetition of our recent study [8], we ascertained whether the reported changes in mucosal gene expression were reproducible in this experiment. RNA from scrapings (n=8 per group) was isolated, pooled and analyzed by using

Affymetrix Mouse Gene 1.0 ST arrays (details in supplement). These array data have been submitted to the Gene Expression Omnibus, accession number GSE34253. Gene expression profiling in the present and the earlier study yielded highly similar results (Pearson correlation coefficient of 0.871,  $n=3663$  genes) indicating that the heme-induced differential gene expression was reproducible and robust between different experiments. For the analysis of the mucosal gene expression response in this experiment we therefore rely on the previously created dataset, as in this dataset individual gene expression profiling was performed and statistics was applied. The pooled arrays from the current experiment were thus only used to confirm that the heme induced gene expression profile was reproducible.

Regarding the previously described individual microarray analysis, RNA of the colon of mice ( $n=7$  controls,  $n=9$  heme) was isolated and hybridized to Affymetrix Mouse genome 430 2.0 arrays (Affymetrix, Santa Clara, CA, USA) [8]. Genes that satisfied the criterion of false discovery rate  $< 1\%$  ( $q\text{-value} < 0.01$ ) were considered to be significantly differentially expressed. Genes with signal intensities below 20 in both treatments were considered absent. The microarray procedure applied on LCM-isolated surface and crypt cells is also previously described [8]. These array data were earlier submitted to the Gene Expression Omnibus, accession number GSE27849.

### **Bacterial DNA extraction and MITChip procedure**

DNA was extracted from 0.1 g of fresh colonic sample using the repeated bead beating method [20]. Microarray analyses were conducted by using the Mouse Intestinal Tract Chip (MITChip) produced by Agilent technologies (Agilent Technologies, Palo Alto, CA, USA) in analogy to the (previously developed) human HITChip [21]. Details about DNA extraction and MITChip can be found in the supplement. A customized classification was introduced based on three levels of taxonomic resolution; level 0 (phylum), level 1 (class or *Clostridium* cluster) and level 2 (including sequences with  $\geq 90\%$  sequence similarity, reflecting a genus-like level). The pre-processing was performed using in-house MySQL and R scripts. Ward's minimum variance method was used to generate hierarchical clustering of the total microbiota probe profiles by calculating a distance matrix between the samples based on the Pearson's distance [22].

### **Quantitative PCR**

qPCR included quantification of total bacteria using 16S rRNA-specific primers and gene specific qPCR, targeting functional genes representing bacterial groups with the following capacity: sulfate or nitrate reduction. For detailed method see supplement. Primer sequences can be found in Supplementary Table 1.

## Bacterial incubations with fecal water

Gram-negative *Escherichia coli* (ABLE K) was cultivated in Luria-Bertani (LB) broth and Gram-positive *Lactobacillus plantarum* WCFS1 [23] was grown in MRS liquid medium (Becton Dickinson, Breda, the Netherlands). Bacteria from overnight cultures were pelleted by centrifugation for 15 min at 4800 rpm and washed 2 times with PBS. Cell-pellets were resuspended to an OD600 of 1, and 5 µl of the resulting suspension was mixed with 10 µl PBS or deoxycholate (final concentrations of 0.7, 1.3 and 2.7 mM) as controls, or with control or heme fecal water from 4 biologically independent, but identical experiments. Each mixture was made in triplicate, and incubated for 2 h at 37°C. Subsequently, bacteria present in the suspensions were stained with the live/death BacLight Bacterial Viability and Counting Kit (Molecular Probes, Leiden, the Netherlands) and analyzed by flow cytometry (FACS) analysis.

## Statistical analysis

Physiological responses, and levels 0, 1 and 2 taxonomic groups were compared using an unpaired, two-tailed t-test. Statistical analysis was carried out in SPSS Statistics 17.0 (SPSS Inc., Chicago, IL). A p-value < 0.05 was considered as statistically significant. All values are presented as mean ± SEM. Statistical considerations for microarray analysis are described above.

## RESULTS

### Effects of dietary heme on colon physiology

Addition of heme to the diet for 2 weeks increased cytotoxicity of fecal water (Table 1). Besides cytotoxic stress, heme-fed mice suffered from reactive oxygen species (ROS) stress in their colon, as shown by the increase of thiobarbituric acid reactive substances (TBARS) (Table 1). Dietary heme increased epithelial cell proliferation as shown by the Ki67 staining (Figure 1 and Table 1). Mucosal gene expression changes induced by heme were similar to those described into detail previously [8] and show that stress response genes were upregulated (e.g. Hmox1, Catalase and Glutathione-related genes). Signaling from the injured surface epithelium to the proliferative crypt to initiate compensatory hyperproliferation occurs via downregulation of feedback inhibitors such as Wif1, IL-15, Ihh and Bmp2. Cell cycle genes were induced (e.g. Ki67, Cyclins) and apoptosis inhibitors were upregulated (Birc5, Ier3).

In line with the earlier described inhibition of apoptosis [19], we found that heme upregulated the necrosis inducer receptor interacting protein kinase-3 (Ripk3) by 2.4-fold (not shown), indicating that epithelial cells die predominantly by necrosis [24]. If cells die by necrosis, apoptosis will be inhibited to compensate for the cells lost by necrosis, as apoptosis is required for cell shedding [25]. This would result in diminished cell shedding and thus decreased levels of host DNA in feces. Therefore we measured



host DNA levels of the feces of control and heme fed mice. The amount of host DNA in the feces of heme-fed mice was significantly lower compared to controls (Table 1). Taken together, the effects of heme on the colonic lumen and mucosa in the present study are in very good agreement with those reported earlier [8,19].

**Table 1.** Differential effects of dietary heme on fecal and mucosal parameters.

	Control	Heme
<b>Feces</b>		
Cytotoxicity of fecal water (% lysis)	2 ± 2	106 ± 4 *
Fecal host DNA (µg/d)	1.31 ± 0.25	0.48 ± 0.09 *
Fecal TBARS (µmol/L malondialdehyde equivalents)	20.9 ± 1.7	55.8 ± 3.7 *
<b>Mucosa</b>		
Total number of cells per crypt	48.0 ± 3.1	75.4 ± 4.3 *
Number of Ki67-positive cells per crypt	19.7 ± 2.6	44.3 ± 3.5 *
Labeling index (% Ki67-positive cells per crypt)	40.5 ± 2.2	58.8 ± 1.6 *

Data are represented as mean ± SEM (n=8). \*Significantly different from respective controls at  $p < 0.05$ .

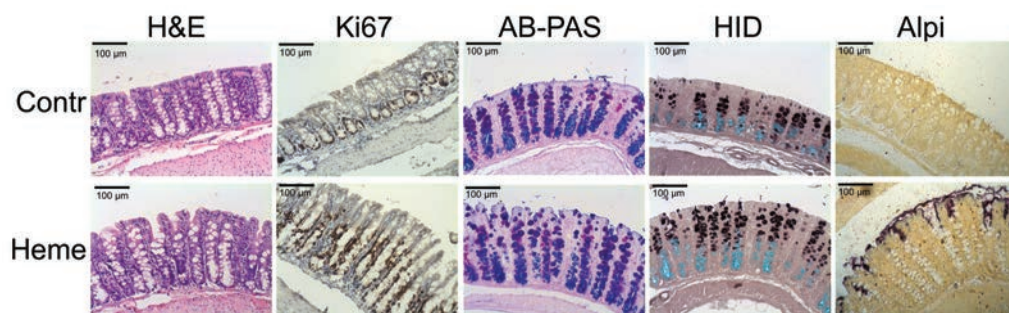


**Figure 1.** Histological staining of mouse colonic mucosa after 14 days on control or heme diet. Histological staining was performed for H&E, AB-PAS, HID and Alpi. Ki67 immunohistochemistry was performed using a Ki67-specific antibody.

## Effects of dietary heme on microbial composition

Until now, the effect of heme or red meat on colonic bacteria was studied only by classical culturing methods [17]. Therefore, we now investigate whether the overall composition of colonic microbiota of heme-fed mice differed from that of control mice by using 16S rRNA phylogenetic microarrays, targeting murine phylotypes (MITChip). The MITChip has previously been used to study the microbiota from mouse intestinal samples [26]. In our study, MITChip analysis indicated that samples of heme-fed mice clustered separately from control mice (Figure 2), because of major changes in bacterial phyla (Supplementary Figure 1) and classes (Table 2). Upon heme consumption,

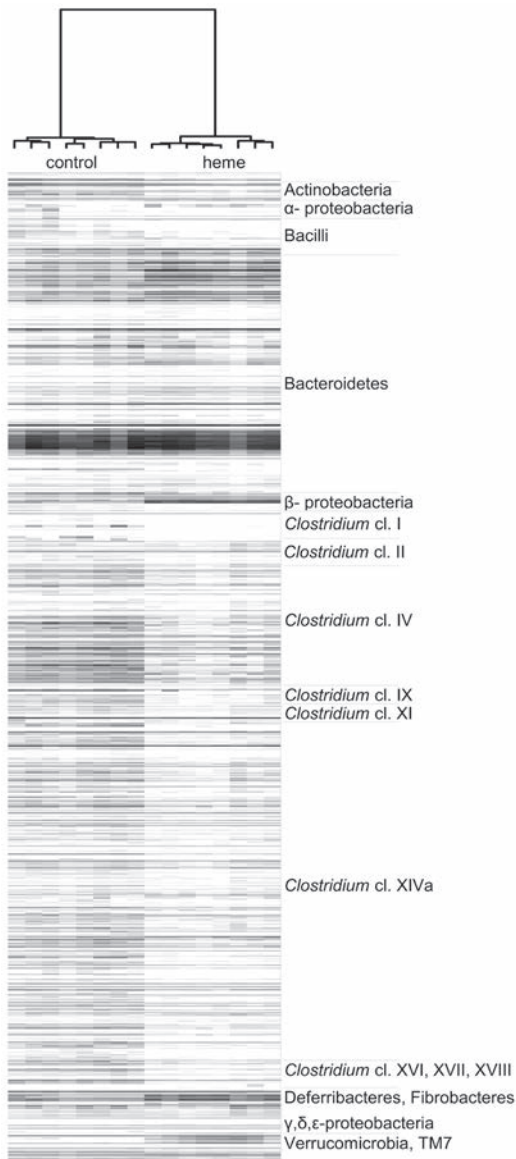


**Figure 2.** Phylogenetic fingerprints of the colonic microbiota of the control group and heme group. Gel-view figure of the intensity of 3,580 probes covered by MITChip and assigned to the phylogenetic class-like groups (level 1) depicted on the right side. Ward's minimum variance method was used to generate hierarchical clustering of the total microbiota probe profiles, whereas the distance matrix between the samples was based on the Pearson's product moment correlation.

12 bacterial classes were significantly changed. Amongst them, the Gram-negative Bacteroidetes, Proteobacteria and Verrucomicrobia were increased, while the Gram-positives such as the Actinobacteria and Firmicutes, including Bacilli, and *Clostridium* cluster XIVa, were decreased in heme-fed mice. A further analysis of the bacterial composition was carried out at genus-level (designated level-2 in the chip data; Supplementary Table 2). Genera such as *Bacteroides*, *Alistipes*, *Prevotella*, *Helicobacter*, *Sphingomonas* and *Akkermansia* were significantly increased upon heme-feeding. Based on MITChip data, Gram-negative bacteria (i.e. Bacteroidetes, Deferribacteres, Fibrobacteres, Fusobacteria, Proteobacteria and Verrucomicrobia) accounted for  $40.7 \pm 3.5$  % of the total bacteria in the controls, while the heme diet promoted an increase ( $p < 0.001$ ) of relative abundance of Gram-negative bacteria to  $66.6 \pm 3.2$  % of the total bacteria detected. The total bacterial density was similar between the heme and control group (Table 3), indicating that a heme-diet induced drastic changes in the ratio of Gram-negative to Gram-positive bacteria from 0.7 to 2.2 (Table 3) without influencing the overall community density. Analogously, the ratio between the most dominant Gram-negative and Gram-positive phyla, Bacteroidetes and Firmicutes, was also strongly increased (Table 3).

**Table 2.** Relative contribution of bacterial classes- Clostridium clusters (level 1) detected by MITChip in control and heme-fed mice.

Phylum	Class	Control	Heme
Actinobacteria	Actinobacteria	2.46 ± 0.32	1.26 ± 0.04**
Bacteroidetes	Bacteroidetes	33.48 ± 3.71	53.11 ± 4.77**
Firmicutes	Bacilli	1.15 ± 0.13	0.80 ± 0.06*
	Clostridium cluster I	0.97 ± 0.19	0.67 ± 0.05
	Clostridium cluster II	1.55 ± 0.11	1.17 ± 0.18
	Clostridium cluster IV	10.83 ± 0.79	5.01 ± 0.67***
	Clostridium cluster IX	0.28 ± 0.04	0.03 ± 0.00***
	Clostridium cluster XI	3.01 ± 0.38	2.20 ± 0.47
	Clostridium cluster XIVa	25.76 ± 1.71	12.33 ± 1.87***
	Clostridium cluster XVI	4.24 ± 0.80	1.98 ± 0.09*
	Clostridium cluster XVII	1.60 ± 0.20	1.63 ± 0.14
	Clostridium cluster XVIII	3.66 ± 0.51	3.23 ± 0.28
	Mollicutes	2.93 ± 0.41	2.62 ± 0.24
Deferribacteres	Deferribacteres	1.40 ± 0.35	1.38 ± 0.38
Fibrobacteres	Fibrobacteres	0.19 ± 0.03	0.15 ± 0.02
Fusobacteria	Fusobacteria	0.80 ± 0.07	0.70 ± 0.12
Proteobacteria	Proteobacteria (alpha)	0.74 ± 0.05	1.26 ± 0.23*
	Proteobacteria (beta)	0.57± 0.08	2.05 ± 0.22***
	Proteobacteria (delta)	0.21±0.06	0.10 ± 0.04
	Proteobacteria (epsilon)	0.26 ± 0.02	0.56 ± 0.06***
	Proteobacteria (gamma)	2.83 ± 0.20	4.99 ± 1.38
TM7	TM7	0.88 ± 0.07	0.48 ± 0.09**
Verrucomicrobia	Verrucomicrobia	0.18 ± 0.07	2.28 ± 0.63**

Data are represented as mean ± SEM, (n=8) \*  $p < 0.05$ , \*\*  $p < 0.01$ , \*\*\*  $p < 0.001$ , significance indicated between the control group and the heme group.

Next we investigated whether heme can act as a selective growth factor involved in the modulation of the ratio of Gram-negative to Gram-positive bacteria. Notably, several members of the Gram-negative Bacteroidetes can use heme as a growth factor [27]. However, such a generic growth stimulating effect of heme was unlikely, since several Gram-positive bacteria able to use heme [28], such as *Corynebacterium diptheriae* et rel. (fold change=0.8), and *Streptococcus* (fold change=0.13), were decreased. Alternatively, various bacteria can use heme as electron carrier in cytochrome- catalyzed anaerobic respiration, like sulfate and nitrate reduction in anaerobic bacteria. Therefore, putative changes in sulfate and nitrate reduction capacity in the microbiota were assessed by quantification of the corresponding functional gene copy-numbers within the total microbiota community. This was done by qPCR for dissimilatory sulfate reductase

**Table 3.** Quantification of total bacteria and specific functional genes in colonic samples from control and heme-fed mice. Results are expressed in log10 of gene copy-nr/g fecal dry weight. Genes used for quantification are mentioned between brackets.

	Control	Heme
Total bacteria (16S rRNA)	11.20 ±0.08	11.30 ±0.17
Ratio Gram-negative to Gram-positive bacteria	0.72 ± 0.09	2.16 ± 0.27 **
Ratio Bacteroidetes to Firmicutes	0.64 ± 0.09	1.88 ± 0.30*
Sulfate reducers ( <i>dsrA</i> )	7.92 ±0.15	8.29 ±0.15
Nitrate reducers ( <i>narG</i> )	9.45 ±0.16	10.50 ±0.13*

Data are represented as mean ± SEM, (n=8). \* indicates significant change between control and heme ( $p<0.05$ ),

\*\* indicates significant change between control and heme ( $p<0.001$ ).

(*dsrA*) and the membrane-bound nitrate reductase (*narG*) encoding genes. There was no significant difference in abundance of the *dsrA* gene between the control and heme-fed group (Table 3), suggesting an unaltered sulfate-reduction capacity of the microbiota. In contrast, the abundance of the *narG* gene was significantly higher in the microbiota of the heme-fed mice, indicating an enhanced microbial nitrate reduction capacity. However, nitrate reduction occurs in various Gram-negative and -positive bacteria, indicating that increased nitrate reduction capacity in the microbiota encountered on the heme diet cannot be correlated directly with the increased number of Gram-negative bacteria. Taken together, these results make it unlikely that heme itself acts as a bacterial growth factor and thereby changes the ratio of Gram-negative to Gram-positive bacteria. Another possibility is that the ratio of Gram-negative to Gram-positive bacteria is directly affected by the toxic heme, which may act as a lytic surfactant to which Gram-positive bacteria are more susceptible, thereby selectively decreasing the Gram-positive bacterial populations, and allowing expansion of the Gram-negative community [29]. To evaluate whether the cytotoxic heme had a differential impact on the viability of Gram-negative and Gram-positive bacteria, the exemplary Gram-negative *Escherichia coli* (ABLE K), and Gram-positive *Lactobacillus plantarum* WCFS1 were incubated with fecal water of heme or control mice, or with deoxycholate as a positive control. There was a clear concentration-dependent decrease of viability of Gram-positive *L. plantarum* cells when these were incubated with deoxycholate (Figure 3A). However, the percentage of viable Gram-negative *E. coli* cells was barely affected by deoxycholate treatment. Similarly, *L. plantarum* was more sensitive to fecal water from heme-fed mice as compared to the control, whereas the viability of *E. coli* was equally affected by heme and control fecal water (Figure 3B). These differential sensitivity effects were consistently found for fecal water pools from four biologically independent, but similar diet-interventions in mice, indicating that heme fecal water has a more pronounced antimicrobial effect on Gram-positive bacteria. This may explain the observed modulation of the ratio between Gram-negative and Gram-positive bacteria in the colon microbiota of heme- and control-fed mice.

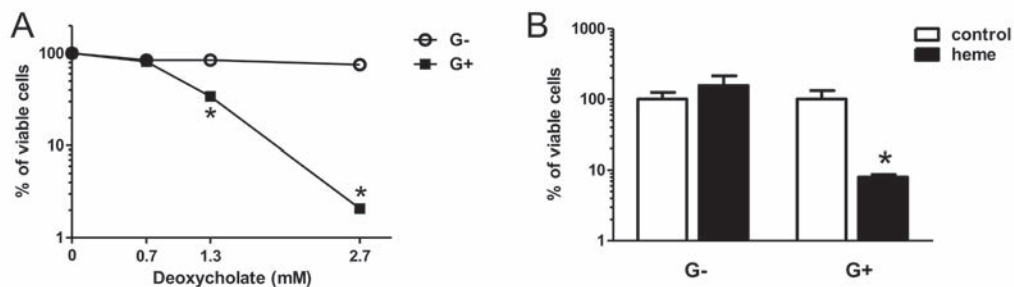


**Figure 3.** Differential effect of deoxycholate (A) and of control and heme fecal water (B) on viability of Gram-negative (G-) *E.coli* and Gram-positive (G+) *L. plantarum*. Fecal water pools from four separate, but identical, animal experiments were used in triplicate. Viability is measured relative to PBS (A) and control fecal water (B). Data are presented as mean  $\pm$  SEM, (n=4) \* $p$ <0.05.

### Heme did not change microbe-sensing pathways in colonic mucosa

Because of these drastic changes in colon microbiota we queried the mucosa for heme-induced differences in inflammation markers, mucin dynamics and Toll-like receptor (Tlr) signaling pathways. The surface epithelium of the heme fed mice was ruffled, because of luminal necrosis [19], but there were no signs of inflammation, as there was no infiltration of neutrophils or macrophages observed in the lamina propria (Figure 1). This is supported by the finding that mucosal myeloperoxidase (Mpo) activity is negligible low in control animals and not affected by dietary heme [17]. Moreover, the expression of inflammation markers for macrophages (CD14, CD68, CD11b, and F4/80 not changed, data not shown) and for neutrophils (Mpo, lactoferrin, neutrophil elastase, and Emr4 not changed, data not shown) is unaltered by dietary heme. Mucins protect the surface epithelium against bacteria and toxic luminal factors and are increased by inflammation [30]. Furthermore, on a purified diet such as used in this study, mucins serve as an important substrate for bacteria. There were no clear differences in presence and distribution of neutral and acidic mucins between the heme-fed animals and the control animals as shown by AlcianBlue/PAS staining (Figure 1). The same holds for the sulfated and carboxylated mucins shown by HID staining (Figure 1). Also the expression of Muc genes was not upregulated (Table 4), showing that heme did not increase the mucin dynamics.

Colonocytes can also directly respond to bacterial cell components via Tlr-signaling pathways. The strong increase in Gram-negative bacteria in colon microbiota of heme-fed mice suggests an increased exposure of the mucosa to lipopolysaccharide (LPS). However, the expression of Tlr4, which recognizes LPS, was not changed by heme (Table 4). Tlr2 can form heterodimers with Tlr1 or with Tlr6 to detect different ligands (reviewed in [31]). Tlr2/1 recognizes triacyl lipoproteins found mainly in Gram-negative bacteria, while Tlr2/6 recognizes diacyl groups on lipoteichoic acid and lipoproteins of Gram-

positive bacteria. The heme intervention downregulated the expression of Tlr1 and Tlr2 (fold change resp. -1.2 and -1.9, Table 4), but Tlr6 remained unchanged. Downstream targets of TLRs, such as MyD88, Traf6 and Tirap, were not changed, except for the NF- $\kappa$ B activator Nemo (Ikbky), which was induced by heme (Table 4).

**Table 4.** Heme-modulated mucosal gene expression.

Gene name	Symbol	Signal intensity control	Signal intensity heme
<b>Mucins</b>			
Mucin 2	Muc2	32474 $\pm$ 598	27798 $\pm$ 375*
Mucin 3	Muc3	18870 $\pm$ 427	15016 $\pm$ 301*
Mucin 4	Muc4	596 $\pm$ 45	673 $\pm$ 23
Mucin 13	Muc13	6412 $\pm$ 179	5087 $\pm$ 128*
<b>Anti-microbial response</b>			
Alkaline phosphatase, intestinal	Alpi	854 $\pm$ 133	2144 $\pm$ 135*
Secretory leukocyte peptidase inhibitor	Slpi	6 $\pm$ 3	2961 $\pm$ 498*
Regenerating islet-derived 3 beta	Reg3 $\beta$	4662 $\pm$ 1458	4746 $\pm$ 1071
Regenerating islet-derived 3 gamma	Reg3 $\gamma$	498 $\pm$ 195	881 $\pm$ 272
Lysozyme	Lyzs	483 $\pm$ 214	378 $\pm$ 43
<b>Toll-like receptor signaling</b>			
Toll-like receptor 1	Tlr1	768 $\pm$ 37	631 $\pm$ 18*
Toll-like receptor 2	Tlr2	362 $\pm$ 52	187 $\pm$ 20*
Toll-like receptor 4	Tlr4	127 $\pm$ 8	116 $\pm$ 9
Toll-like receptor 6	Tlr6	6 $\pm$ 0	6 $\pm$ 0
Toll-like receptor 9	Tlr9	22 $\pm$ 1	21 $\pm$ 1
Inhibitor of kappaB kinase gamma	Ikbky	85 $\pm$ 3	324 $\pm$ 22*
Tnf receptor-associated factor 6	Traf6	11 $\pm$ 1	12 $\pm$ 1
Toll-interleukin 1 receptor (TIR) domain-containing adaptor protein	Tirap	24 $\pm$ 1	32 $\pm$ 2
Myeloid differentiation primary response gene 88	Myd88	198 $\pm$ 9	231 $\pm$ 8
Tumor necrosis factor	Tnf $\alpha$	6 $\pm$ 0	6 $\pm$ 0
Interleukin 1 beta	Il-1 $\beta$	7 $\pm$ 0	7 $\pm$ 0
Interleukin 6	Il-6	3 $\pm$ 0	3 $\pm$ 0
Interleukin 12a	Il-12a	4 $\pm$ 0	4 $\pm$ 0
Interleukin 12b	Il-12b	5 $\pm$ 0	5 $\pm$ 0

\* indicates significant fold change ( $q < 0.01$ ), genes with signal intensities below 20 are considered not expressed.



Although the heme diet led to, (i) increased exposure to Gram-negative bacteria, (ii) altered expression of Tlr1 and Tlr2, as well as (iii) Nemo, these changes did not elicit significant modulation of the transcription of downstream genes associated with inflammatory cytokine production, such as TNF $\alpha$ , IL-1 $\beta$ , IL-6 and IL-12. This indicated that the heme diet did not induce functional changes in the Tlr-signaling pathways (Table 4). Moreover, Serum Amyloid A3 (Saa3), a gene encoding a protein involved in acute phase response, is 8-fold downregulated in the mucosa of the heme-fed animals (data not shown), supporting the lack of innate immune responses in heme-fed mice. In a recent study of a rat model of colitis, heme feeding decreased mucosal Mpo and IL-1 $\beta$  levels, showing that heme even inhibited inflammation in that model [17]. Finally, plasma IgM against core endotoxin was measured in this study and its concentration was similar in heme-fed and control mice (not shown), indicating that also a systemic marker for immune activation was unaffected by heme. Taken together these results show an unaltered innate immune system in the heme-fed mice as compared to the controls.

The absence of a heme-induced innate immune response is in good agreement with the observation that the heme diet did not increase macrophage and neutrophil recruitment in the mucosa (see above), and is also in line with the unchanged expression of well-known anti-microbial peptides (defensins (not shown), lysozyme and regenerating islet-derived 3 (Table 4)). Interestingly, the heme diet led to a drastic increase of expression of Secretory Leukocyte Protease Inhibitor (Slpi), which was especially prominent in the surface epithelium (Figure 4A). Western blot analysis confirmed the elevated Slpi levels in colon homogenates obtained from heme-fed mice as compared to control-fed mice (Figure 4A). Slpi is induced upon cell or tissue injury and suppresses excessive inflammatory responses [32] and therefore might play a role in prevention of innate immune reactions in the heme-fed mice. Notably, Slpi was not detected in fecal water (not shown), indicating that a direct effect of Slpi in the lumen of the colon is not likely. Finally, we evaluated whether the mucosal surface did not sense the increased number of Gram-negative bacteria due to LPS inactivation by Alkaline phosphatase (Alpi), which can dephosphorylate LPS and thereby preventing its induction of Tlr4-signaling [33]. Indeed mucosal Alpi is 2.5-fold upregulated in the epithelium of heme-fed mice, specifically in the surface epithelium (Figure 4B). This transcriptional effect is validated by histochemical analysis showing that heme increases the activity of this apical ectoenzyme, especially in the surface epithelium (Figure 1). Alpi expression can be induced by thyroid hormone or cellular stress, reviewed in [34]. It is unlikely that thyroid hormone activation occurred in this study, because the heme diet led to decreased surface expression of the dioxygenase-enzyme (Dio1), which converts inactive thyroxine into locally active thyroid hormone. In-vitro studies show that induced Alpi expression through cellular stress co-occurs with Heat Shock Protein (Hsp)72 induction in enterocytes [35]. This is

corroborated by our finding that heme also induced the expression of Hsp72 (Hspa1a), exclusively in the surface epithelium (Figure 4B), indicating that the induction of Alpi and Hsp72 can be part of the heme-induced stress response in the surface epithelium, which we recently described in detail [8]. The oxidative stress-induced Alpi may inactivate LPS and thus protect the epithelium against luminal LPS exposure.

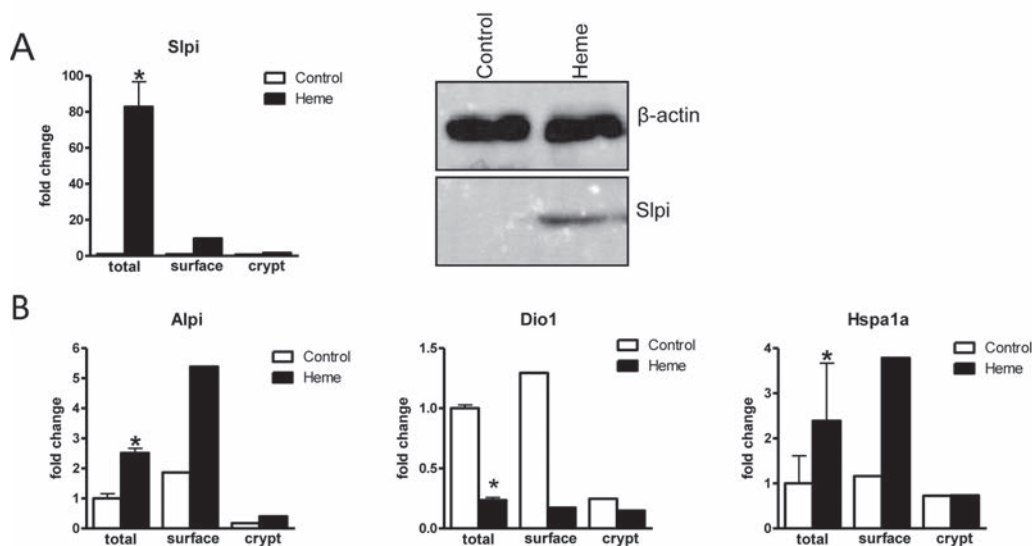


**Figure 4.** Gene expression and protein levels of *Slpi* and gene expression levels of *Alpi*, *Dio1* and *Hspa1a*. Western blot (A) shows the presence of *Slpi* protein colon scraping homogenate pools ( $n=8$  for both groups) of heme-fed mice. *Slpi* is not detectable in controls.  $\beta$ -actin serves as a loading control. (B) Gene expression levels (A and B) in total scrapings are based on microarray analysis on individual mice ( $n=7$  controls,  $n=9$  heme-fed mice). Relative gene expression changes (fold changes) on heme were calculated by setting RNA levels of control mice to 1 (mean  $\pm$  SEM,  $*q<0.01$ ). Surface- and crypt-specific microarray gene expression profiles are from pooled tissue samples obtained by LCM ( $n=4$  controls,  $n=3$  heme-fed mice). In this LCM experiment also total scrapings were again collected and analyzed by microarray. Surface and crypt expression values are normalized for the expression in total scrapings.

## DISCUSSION

This study shows that dietary heme not only impacts the colonic mucosa by inducing epithelial surface injury and compensatory hyperproliferation and hyperplasia, but also drastically changed the microbiota composition in mouse colon. This change is characterized by an increased ratio of Gram-negative to Gram-positive bacteria on the heme diet, which was predominantly caused by increased abundance of the Gram-negative bacteria *Bacteroides*, *Prevotella* (Bacteroidetes), *Helicobacter* (Gamma-proteobacteria), *Akkermansia* (Verrucomicrobia) and *Mucispirillum* (Deferribacteres). Interestingly, an increase in *Bacteroides* spp. on a high-red meat diet has been previously reported in humans, which coincided with reduced abundance of lactobacilli and clostridia [36].



Moreover, *Bacteroides* spp. were also more abundant in the colon of humans eating meat compared to vegetarians [37]. Thus, the findings of this study are in agreement with the changes observed in humans, implying that heme-consumption in mice elicits similar microbiota modulations as those seen in humans consuming a high red-meat diet.

We studied functional bacterial genes previously reported to be linked with colon cancer, such as sulfate- and nitrate reduction. Sulfate reducing bacteria produce sulfide which is associated with an increased risk to develop colon cancer [38,39]. However, changes in sulfate reduction capacity were not observed in our study, neither by changed abundance of the major genus of colonic sulfate reducers (*Desulfovibrio*) in the MITChip, nor by qPCR targeting the conserved gene involved in sulfate reduction. Nitrate reducing bacteria are also associated with colon cancer, as nitrite is a precursor in the production of the putatively carcinogenic N-nitrosocompounds (NOC). Diets high in red meat increased apparent NOC, which are able to form alkylating DNA adducts in the colon [14]. If these adducts are not repaired, this increases the risk of colon cancer. Microbiota may play a role in NOC formation as nitrate reduction is a common activity of the GI tract microbiota [40]. The nitrate reducing capacity was significantly increased in microbiota of heme-fed mice as shown by the elevated copy numbers of the conserved gene involved. This indicates that dietary heme, besides the previously reported cytotoxic and hyperproliferative effect [8], may have an additional carcinogenic effect in the colon that is mediated via the microbiota.

Our results suggest that the cause for the increased ratio of Gram-negative to Gram-positive bacteria is most probably related directly to the presence of toxic heme in fecal water of heme-fed mice. The in-vitro experiments presented support a selective susceptibility of Gram-positive bacteria to heme fecal water, which is not observed for Gram-negative bacteria, and is in agreement with the general higher susceptibility of Gram-positives to surfactants. There are no indications that factors such as anti-microbial peptides produced by the host mucosa influence this ratio directly. We speculate that the heme lipophilic moiety can enter the membrane of the Gram-positive bacteria and exerts its toxic effect through typical surfactant activity leading to loss of membrane integrity and viability, which also occurs during treatment with other cytotoxic surfactants such as bile acids [29]. Consequently, the selective reduction of Gram-positive members of the microbiota by the heme-derived surfactant activity, allows the generally more resistant Gram-negative bacteria to thrive and expand their relative (and absolute) abundance in heme-fed mice. It was suggested that Gram-positive bacteria are particularly vulnerable to the luminal surfactant concentration as they are lacking the outer LPS-containing membrane [29]. Our observed heme effect is in line with classical culture studies showing that heme preferentially kills Gram-positive bacteria [41].

More Gram-negative bacteria in the colon microbiota of heme-fed mice would expose the colonic epithelium to increased amounts of LPS, which is known to elicit innate immune

responses (reviewed in [42]). However, despite the increased exposure to Gram-negative bacterial communities, there was no appreciable innate immune response detected in the colon of heme-fed mice. Plasma IgM against core endotoxin levels remained unaffected by the heme diet, whereas its elevation is a marker for general activation of the immune system. The downregulation of Saa3, involved in acute phase response, in the mucosa of heme-fed mice suggests that the immune responses in the mucosa are repressed rather than activated by heme. This is in agreement with the finding that heme inhibits the inflammatory response in TNBS-treated rats [17].

The suppression of an immune response might be attributed to Slpi induction exclusively found in heme-fed mice. Slpi may act as an antimicrobial peptide as well as a modulator of the response to LPS stimulation [43,44]. Furthermore, Slpi is also shown to counteract excessive inflammatory responses [32]. Therefore, Slpi could play a major role in maintaining mucosal homeostasis to protect the host against the drastic changes in Gram-negative bacteria and thus LPS exposure after heme consumption. Slpi can be induced upon tissue injury [32] and therefore might be triggered by heme-induced surface damage in this study. The antimicrobial effect of Slpi has been shown with the Gram-negative target organisms *Salmonella typhimurium* and *E. coli* [45]. However, this contrasts with our observation that heme drastically increased the abundance of Gram-negative bacteria. Furthermore, although Slpi has been reported to be secreted apically [45], we were unable to detect Slpi in fecal water (not shown), suggesting that the effect of Slpi is exerted basolaterally (immune suppression), which would be in agreement with the previously reported lack of detectable Slpi in the colonic mucus layer of mice [46].

It was suggested that Alpi acts as a microbiota controlled LPS-detoxifying mechanism functioning at the apical surface [47]. This was based on the finding that in zebrafish Alpi was absent in germ-free animals, and its expression was induced following exposure to bacteria [48]. However, this induction may be zebrafish-specific since Alpi activation was not observed in germ-free mice and rats during conventionalization (reviewed in [34]). In our study, Alpi induction co-occurs with increased expression of Hsp72, indicating that Alpi induction is most probably part of the heme-induced epithelial stress response [8].

In conclusion, our study shows that dietary heme changed the microbiota with a major increase in the ratio of Gram-negative to Gram-positive bacteria, which is most likely explained by the selective susceptibility of the Gram-positives to toxic heme fecal water. Furthermore, heme changed the colon mucosa of the host by inducing hyperproliferation and subsequently hyperplasia. It is especially remarkable that the increased amount of Gram-negative bacteria, which coincides with increased mucosal exposure to LPS, did not elicit a detectable immune reaction in the host mucosa. This may be due to the strong upregulation of Slpi which is able to suppress excessive immune reactions. We did not detect any sign of heme-dependent inflammation or functional change in epithelial microbe sensing. This indicates that the change in microbiota does not cause the

observed hyperproliferation and hyperplasia via inflammation pathways. Whether this may occur via alternative mechanisms in colon lumen, such as modulation of oxidative and cytotoxic stress, will be studied using broad-spectrum antibiotics.

## **ACKNOWLEDGEMENTS**

The authors would like to thank Mechteld Grootte Bromhaar, Jenny Jansen, Philip de Groot and Mark Boekschoten for microarray analysis; Denise Jonker-Termont, Dicky Lindenberg-Kortleve, Rolien Raatgeep, Patrick Janssen and Bert Weijers for technical assistance; Hans Snel and Saskia van Schalkwijk for implementation and validation of the *dsrA* and *narG* qPCR method.

## REFERENCES

- 1 Jemal A, Siegel R, et al. Cancer statistics, 2008. *CA Cancer J Clin* 2008;58:71-96.
- 2 World Cancer Research Fund. Food, Nutrition, Physical Activity and the Prevention of Cancer: a Global Perspective. Washington, DC: American Institute for Cancer Research, 2007.
- 3 Giovannucci E, Rimm EB, et al. Intake of fat, meat, and fiber in relation to risk of colon cancer in men. *Cancer Res* 1994;54:2390-7.
- 4 Larsson SC, Rafter J, et al. Red meat consumption and risk of cancers of the proximal colon, distal colon and rectum: the Swedish Mammography Cohort. *Int J Cancer* 2005;113:829-34.
- 5 Lee DH, Anderson KE, et al. Heme iron, zinc, alcohol consumption, and colon cancer: Iowa Women's Health Study. *J Natl Cancer Inst* 2004;96:403-7.
- 6 Balder HF, Vogel J, et al. Heme and chlorophyll intake and risk of colorectal cancer in the Netherlands cohort study. *Cancer Epidemiol Biomarkers Prev* 2006;15:717-25.
- 7 Sesink AL, Termont DS, et al. Red meat and colon cancer: the cytotoxic and hyperproliferative effects of dietary heme. *Cancer Res* 1999;59:5704-9.
- 8 IJssennagger N, Rijnierse A, et al. Dietary haem stimulates epithelial cell turnover by downregulating feedback inhibitors of proliferation in murine colon. *Gut* 2012;61:1041-9.
- 9 Young G, Rose I, et al. Haem in the gut. I. Fate of haemoproteins and the absorption of haem. *J Gastroenterol Hepatol* 1989;4:537-45.
- 10 McGarr SE, Ridlon JM, et al. Diet, Anaerobic Bacterial Metabolism, and Colon Cancer: A Review of the Literature. *Journal of Clinical Gastroenterology* 2005;39:98-109.
- 11 Moore W, Moore L. Intestinal floras of populations that have a high risk of colon cancer. *Appl Environ Microbiol* 1995;61:3202-7.
- 12 Ridlon JM, Kang D-J, et al. Bile salt biotransformations by human intestinal bacteria. *J Lipid Res* 2006;47:241-59.
- 13 O'Keefe SJ. Nutrition and colonic health: the critical role of the microbiota. *Current opinion in gastroenterology* 2008;24:51-8.
- 14 Lewin MH, Bailey N, et al. Red meat enhances the colonic formation of the DNA adduct O6-carboxymethyl guanine: implications for colorectal cancer risk. *Cancer research* 2006;66:1859-65.
- 15 Attene-Ramos MS, Nava GM, et al. DNA damage and toxicogenomic analyses of hydrogen sulfide in human intestinal epithelial FHs 74 Int cells. *Environmental and Molecular Mutagenesis* 2010;51:304-14.
- 16 Bernstein H, Bernstein C, et al. Bile acids as carcinogens in human gastrointestinal cancers. *Mutation Research/Reviews in Mutation Research* 2005;589:47-65.
- 17 Schepens MA, Vink C, et al. Dietary heme adversely affects experimental colitis in rats, despite heat-shock protein induction. *Nutrition* 2011;27:590-7.
- 18 de Vogel J, Jonker-Termont DSML, et al. Green vegetables, red meat and colon cancer: chlorophyll prevents the cytotoxic and hyperproliferative effects of haem in rat colon. *Carcinogenesis* 2005;26:387-93.
- 19 de Vogel J, van-Eck WB, et al. Dietary heme injures surface epithelium resulting in hyperproliferation, inhibition of apoptosis and crypt hyperplasia in rat colon. *Carcinogenesis* 2008;29:398-403.
- 20 Salonen A, Nikkila J, et al. Comparative analysis of fecal DNA extraction methods with phylogenetic microarray: effective recovery of bacterial and archaeal DNA using mechanical cell lysis. *Journal of microbiological methods* 2010;81:127-34.
- 21 Rajilic-Stojanovic M, Heilig H, et al. Development and application of the human intestinal tract chip, a phylogenetic microarray: analysis of universally conserved phylotypes in the abundant microbiota of young and elderly adults. *Environmental Microbiology* 2009;11:1736-51.
- 22 Carter RL, Morris R, et al. On the Partitioning of Squared Euclidean Distance and Its Applications in Cluster-Analysis. *Psychometrika* 1989;54:9-23.
- 23 Kleerebezem M, Boekhorst J, et al. Complete genome sequence of *Lactobacillus plantarum* WCFS1. *Proceedings of the National Academy of Sciences of the United States of America* 2003;100:1990-5.
- 24 Vandenabeele P, Declercq W, et al. The role of the kinases RIP1 and RIP3 in TNF-induced necrosis. *Science signaling* 2010;3:re4.

- 25 Marchiando AM, Shen L, et al. The epithelial barrier is maintained by in vivo tight junction expansion during pathologic intestinal epithelial shedding. *Gastroenterology* 2011;140:1208-18 e1-2.
- 26 Geurts L, Lazarevic V, et al. Altered gut microbiota and endocannabinoid system tone in obese and diabetic leptin-resistant mice: impact on apelin regulation in adipose tissue. *Frontiers in microbiology* 2011;2:149.
- 27 Aljalili TAR, Shah HN. Protoheme, a Dispensable Growth-Factor for *Bacteroides-Fragilis* Grown by Batch and Continuous Culture in a Basal Medium. *Current Microbiology* 1988;17:13-8.
- 28 Nobles CL, Maresso AW. The theft of host heme by Gram-positive pathogenic bacteria. *Metallomics : integrated biometal science* 2011;3:788-96.
- 29 Bovee-Oudenhoven IM, Wissink ML, et al. Dietary calcium phosphate stimulates intestinal lactobacilli and decreases the severity of a salmonella infection in rats. *The Journal of nutrition* 1999;129:607-12.
- 30 McGuckin MA, Linden SK, et al. Mucin dynamics and enteric pathogens. *Nature reviews Microbiology* 2011;9:265-78.
- 31 Meijerink M, Wells JM. Probiotic modulation of dendritic cells and T cell responses in the intestine. *Benef Microbes* 2010;1:317-26.
- 32 Nakamura A, Mori Y, et al. Increased susceptibility to LPS-induced endotoxin shock in secretory leukoprotease inhibitor (SLPI)-deficient mice. *The Journal of experimental medicine* 2003;197:669-74.
- 33 Poelstra K, Bakker WW, et al. Dephosphorylation of endotoxin by alkaline phosphatase in vivo. *The American journal of pathology* 1997;151:1163-9.
- 34 Lalles JP. Intestinal alkaline phosphatase: multiple biological roles in maintenance of intestinal homeostasis and modulation by diet. *Nutrition reviews* 2010;68:323-32.
- 35 Harada T, Koyama I, et al. Heat shock induces intestinal-type alkaline phosphatase in rat IEC-18 cells. *American journal of physiology Gastrointestinal and liver physiology* 2003;284:G255-62.
- 36 Maier BR, Flynn MA, et al. Effects of a high-beef diet on bowel flora: a preliminary report. *Am J Clin Nutr* 1974;27:1470-4.
- 37 Zimmer J, Lange B, et al. A vegan or vegetarian diet substantially alters the human colonic faecal microbiota. *European journal of clinical nutrition* 2011.
- 38 Huycke MM, Gaskins HR. Commensal Bacteria, Redox Stress, and Colorectal Cancer: Mechanisms and Models. *Exp Biol Med* 2004;229:586-97.
- 39 Levitt MD, Furne J, et al. Detoxification of hydrogen sulfide and methanethiol in the cecal mucosa. *The Journal of clinical investigation* 1999;104:1107-14.
- 40 Parham NJ, Gibson GR. Microbes involved in dissimilatory nitrate reduction in the human large intestine. *FEMS Microbiology Ecology* 2000;31:21-8.
- 41 Nitzan Y, Wexler HM, et al. Inactivation of anaerobic bacteria by various photosensitized porphyrins or by hemin. *Curr Microbiol* 1994;29:125-31.
- 42 Aderem A, Ulevitch RJ. Toll-like receptors in the induction of the innate immune response. *Nature* 2000;406:782-7.
- 43 Williams SE, Brown TI, et al. SLPI and elafin: one glove, many fingers. *Clin Sci* 2006;110:21-35.
- 44 Xu W, He B, et al. Epithelial cells trigger frontline immunoglobulin class switching through a pathway regulated by the inhibitor SLPI. *Nat Immunol* 2007;8:294-303.
- 45 Si-Tahar M, Merlin D, et al. Constitutive and regulated secretion of secretory leukocyte proteinase inhibitor by human intestinal epithelial cells. *Gastroenterology* 2000;118:1061-71.
- 46 Johansson ME, Phillipson M, et al. The inner of the two Muc2 mucin-dependent mucus layers in colon is devoid of bacteria. *Proceedings of the National Academy of Sciences of the United States of America* 2008;105:15064-9.
- 47 Vaishnava S, Hooper LV. Alkaline phosphatase: keeping the peace at the gut epithelial surface. *Cell host & microbe* 2007;2:365-7.
- 48 Bates JM, Akerlund J, et al. Intestinal alkaline phosphatase detoxifies lipopolysaccharide and prevents inflammation in zebrafish in response to the gut microbiota. *Cell host & microbe* 2007;2:371-82.

## **SUPPLEMENTARY METHODS**

### **Histology**

Haematoxylin and eosin (H&E) staining was performed on colon tissue of all animals to investigate tissue morphology. Furthermore, an Alcian blue/PAS staining (staining neutral and acidic mucins), and a High Iron Diamine staining (HID, staining sulfated and carboxylated mucins), were performed. For both stainings, colon sections were deparaffinized and rehydrated in a series of graded alcohols. For the Alcian blue/PAS staining, the sections were incubated with Alcian blue (pH=2.5) for 30 min, then with periodic acid for 10 min and subsequently in Schiff's reagent for 10 min. For the HID staining, deparaffinized sections were incubated overnight in diamine solution in a dark and humid atmosphere. Then the sections were incubated with Alcian blue (pH=2.5) for 30 min. Between all incubations, sections were rinsed with water. Before mounting, sections were dehydrated in a series of graded alcohols and xylene. For the detection of Alkaline phosphatase, colon tissue slides were deparaffinized and incubated with the alkaline-dye mixture (Alkaline phosphatase kit 85L2-1KT Sigma-Aldrich) for 90 min at 37°C. Slides were rinsed with water and mounted.

### **Thiobarbituric Acid Reactive Substances (TBARS) assay**

The assay used determines lipid peroxidation by quantifying the concentration of malondialdehyde (MDA) in fecal water [1]. Fecal water was diluted 4-fold with double-distilled water. To 100 µl of this dilution, 100 µl of 8.1% SDS and 1 ml of 0.11 mol/L 2,6-di-tert-butyl-p-cresol, 0.5% TBA in 10% acetic acid (pH 3.5) was added. To correct for background, TBA was omitted from the assay. TBARS were extracted, after heating for 75 minutes at 82°C, with 1.2 ml n-butanol. The absorbance of the extracts was measured at 540 nm. The amount of TBARS was calculated as MDA equivalents using 1,1,3,3,-tetramethoxypropane as standard.

### **Bacterial DNA extraction**

Approximately 0.1 g fresh colonic sample was used for mechanical and chemical lysis using 0.5 ml buffer (500 mM NaCl, 50 mM Tris-HCl (pH 8), 50 mM EDTA, 4% SDS) and 0.25 g of 0.1 mm zirconia beads and 3 mm glass beads. Nucleic acids were precipitated by addition of 130 µl, 10 M ammonium acetate, using one volume of isopropanol. Subsequently, DNA pellets were washed with 70% ethanol. Further purification of DNA was performed using the QiaAmp DNA Mini Stool Kit (Qiagen, Hilden, Germany). Finally, DNA was dissolved in 200 µl Tris/EDTA buffer and its purity and quantity were checked spectrophotometrically (ND-1000, nanoDrop technologies, Wilmington, USA).

### Quantitative qPCR

qPCR was performed using an IQ5 Cyclor apparatus (Bio-Rad, Veenendaal, the Netherlands). Reactions were performed in triplicate in a single run. Samples were analyzed in a 25 ml reaction mixture consisting of 12.5 ml Bio-Rad master mix SYBR Green (50 mM KCl, 20 mM Tris-HCl, pH 8.4, 0.2 mM of each dNTP, 0.625 U *iTaq* DNA polymerase, 3 mM MgCl<sub>2</sub>, 10 nM fluorescein), 0.1 μM of each primer and 5 ml of template faecal DNA diluted 100- or 1000-fold. Standard curves of 16 S rRNA or specific gene PCR product from pure culture were created using serial 10-fold dilution of the purified PCR product. Standards included *Lactobacillus casei* (total bacteria), *Desulfovibrio* sp. (sulfate reducer) and *Pseudomonas aeruginosa* (nitrate reducer). The following qPCR conditions were used: 95°C for 10 min, followed by 35 cycles of denaturation at 95°C for 15 sec, annealing temperature of 60°C for 20 sec, extension at 72°C for 30 sec and a final extension step at 72°C for 5 min. A melting curve was determined at the end of each run to verify the specificity of the PCR amplicons. Data analysis was performed using the Bio-Rad software.

### Array hybridization and microarray data analysis

Pooled samples were analyzed using Affymetrix Mouse Gene 1.0 ST arrays. Labeling was performed with 'Affymetrix Whole Transcript Sense Labeling without rRNA reduction step' according to the WT Sense Target Labeling Assay Manual (Affymetrix Santa Clara, CA). Arrays were normalized using the Robust Multi-array Average (RMA) method. [2,3]. Genes with signal intensities below 20 were considered absent.

### MITChip procedure

The full length 16S rRNA gene was amplified using primers T7prom-Bact-27-forward and Uni-1492-reverse [4]. The PCR products were transcribed into RNA and the resulting RNA was labeled with Cy3 and Cy5 prior to fragmentation and hybridization to the array. Arrays were scanned with Agilent DNA Microarray Scanner to collect fluorescence data, which were then extracted from the generated images by using the Agilent Extraction Software 9.1. The array normalization was performed as described earlier [5]. In summary, each scanner channel of each of the arrays was first spatially normalized with polynomial regression, after which the outliers in each set of probes were detected with a chi-squared test and discarded. The logarithmic intensities from the spatially normalized, reproducible, and sample-wise quantile-normalized hybridizations were then averaged to a single value for each probe and each sample in the data set.

**Supplementary Table 1.** Primers sequences used in this study.

Primer name	Primer sequence (5'-3')	References
<b>16S Total bacteria (MITChip)</b>		
T7 prom-Bact-27-F	TGAATTGTAATACGACTCACTATAGGGGTTTGATCCTGGCTCAG	[4]
Uni-1492-R	CGGCTACCTTGTTACGAC	
<b>16S Total bacteria (qPCR)</b>		
Bact-1369-F	CGGTGAATACGTTC	[6]
Prok-1492-R	GGWTACCTTGTTAC	
<b>Sulfate reducers</b>		
RH1dsr-F	GCCGTTACTGTGACCAGCC	[7]
RH3-dsr-R	GGTGGAGCCGTGCATGTT	
<b>Nitroreductors</b>		
narG-F	TCGCCSATYCCGGCSATGTC	[8]
narG-R	GAGTTGTACCAGTCRCGSGAYTCSG	

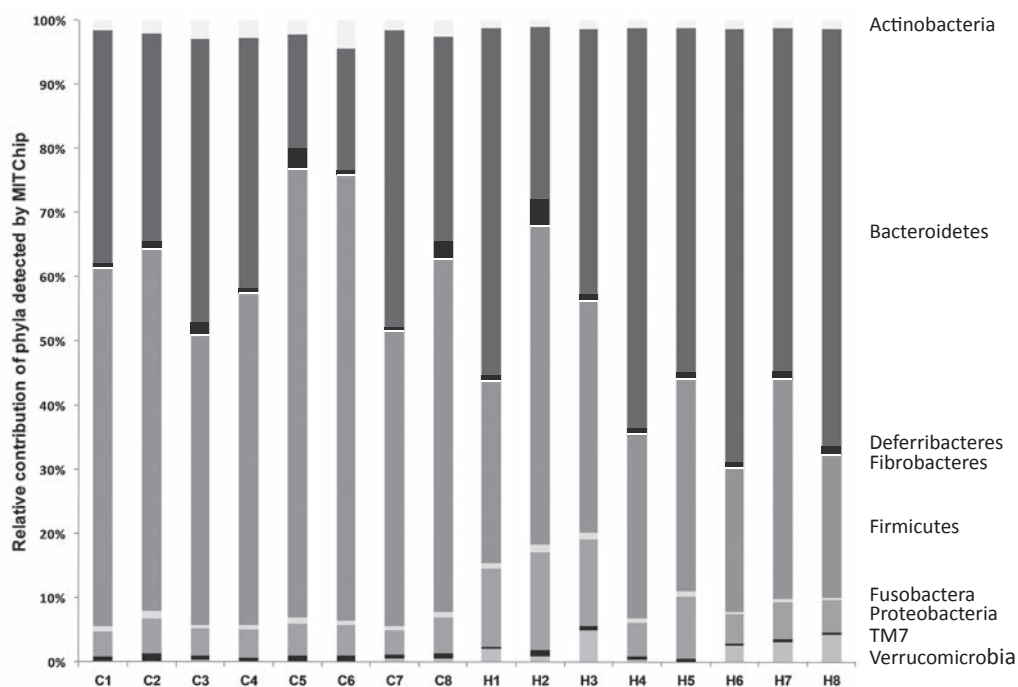
**Supplementary Table 2.** Averaged relative contribution of significantly changed genus-like groups (levels 2) detected by MITChip in control and heme-fed mice. Genera are ranked by their highest ratio heme/control.

Higher taxonomy level	Genus level	Relative abundance		Ratio heme/control	p-value
		Control	Heme		
Verrucomicrobia	<i>Akkermansia</i>	0.18 ± 0.07	2.28 ± 0.63	12.69	0.005
Bacteroidetes	<i>B. distasonis et rel.</i>	0.19 ± 0.03	2.29 ± 0.18	12.13	0.000
Bacteroidetes	<i>B. vulgatus et rel.</i>	0.43 ± 0.10	3.56 ± 0.39	8.24	0.000
Bacteroidetes	<i>Un. Cyanobacteria</i>	0.00 ± 0.00	0.01 ± 0.00	6.63	0.008
Bacteroidetes	<i>Prevotella</i>	0.40 ± 0.05	2.52 ± 0.19	6.37	0.000
Proteobacteria	<i>Sphingomonas et rel.</i>	0.23 ± 0.04	0.97 ± 0.24	4.22	0.009
Bacteroidetes	Un. Bacteroidetes	0.00 ± 0.00	0.01 ± 0.00	4.01	0.000
Bacteroidetes	<i>B. plebeius et rel.</i>	0.18 ± 0.04	0.69 ± 0.08	3.90	0.000
Proteobacteria	<i>Sutterella wadsorthia et rel.</i>	0.57 ± 0.08	2.05 ± 0.22	3.60	0.000
Bacteroidetes	<i>B. fragilis et rel.</i>	1.47 ± 0.31	4.88 ± 0.60	3.33	0.000
Bacteroidetes	<i>Alistipes</i>	2.42 ± 0.37	5.86 ± 0.46	2.42	0.000
Bacteroidetes	<i>Rikenella</i>	0.43 ± 0.09	0.99 ± 0.07	2.30	0.000
Proteobacteria	<i>Helicobacter</i>	0.26 ± 0.02	0.56 ± 0.06	2.17	0.000
Bacteroidetes	<i>B. splanchnicus et rel.</i>	0.65 ± 0.17	1.35 ± 0.19	2.06	0.017
Bacilli	<i>Propionibacterium</i>	0.01 ± 0.00	0.01 ± 0.00	1.59	0.001
Clostridium cl. XVII	<i>Coprobacillus cateniformis et rel</i>	0.89 ± 0.09	1.22 ± 0.12	1.37	0.048
Bacilli	<i>L. paracasei et rel.</i>	0.83 ± 0.06	0.60 ± 0.03	-1.38	0.005
Proteobacteria	<i>Acitenobacter</i>	0.01 ± 0.00	0.00 ± 0.00	-1.38	0.026



Actinobacteria	<i>Bifidobacterium</i>	0.49 ± 0.03	0.34 ± 0.04	-1.45	0.007
Clostridium cl. XIVa	<i>Butyrivibrio crossotus et rel.</i>	1.42 ± 0.13	0.92 ± 0.13	-1.54	0.017
Clostridium cl. IV	<i>Ruminobacter amylophilus et rel.</i>	0.00 ± 0.00	0.00 ± 0.00	-1.64	0.001
Clostridium cl. IV	<i>Un. Cl. IV</i>	0.01 ± 0.00	0.00 ± 0.00	-1.69	0.000
Clostridium cl. XVII	<i>Catenibacterium</i>	0.70 ± 0.12	0.41 ± 0.04	-1.72	0.038
Clostridium cl. XIVa	<i>Eub. plexicaudatus et rel.</i>	4.10 ± 0.31	2.36 ± 0.39	-1.74	0.004
Proteobacteria	<i>Labrys methylaminiphilus et rel.</i>	0.51 ± 0.04	0.29 ± 0.09	-1.76	0.037
Actinobacteria	<i>Eggerthella</i>	1.59 ± 0.28	0.88 ± 0.06	-1.80	0.026
TM7	<i>Un. TM7</i>	0.88 ± 0.07	0.48 ± 0.09	-1.83	0.003
Mollicutes	<i>Solobacterium moorei et rel.</i>	0.67 ± 0.11	0.35 ± 0.02	-1.91	0.013
Clostridium cl. XIVa	<i>Cl. symbiosum et rel.</i>	0.06 ± 0.01	0.03 ± 0.01	-2.17	0.023
Clostridium cl. IV	<i>Dorea</i>	2.33 ± 0.24	1.04 ± 0.24	-2.24	0.002
Actinobacteria	<i>Atopobium</i>	0.01 ± 0.00	0.00 ± 0.00	-2.39	0.001
Clostridium cl. XIVa	<i>Lachnospira pectinoschiza et rel.</i>	0.70 ± 0.06	0.29 ± 0.09	-2.39	0.001
Clostridium cl. XIVa	<i>Uncl. Clostridium cl XIVa</i>	11.7 ± 0.95	4.85 ± 0.71	-2.42	0.000
Clostridium cl. XIVa	<i>Bryantella</i>	2.20 ± 0.30	0.85 ± 0.16	-2.59	0.002
Clostridium cl. IV	<i>Sporobacter termitidis et rel.</i>	8.47 ± 0.73	3.22 ± 0.52	-2.63	0.000
Clostridium cl. II	<i>Cl. lactifermentans et rel.</i>	0.35 ± 0.06	0.12 ± 0.04	-3.07	0.004
Clostridium cl. XIVa	<i>Lachnobacillus bovis et rel.</i>	0.94 ± 0.09	0.22 ± 0.03	-4.32	0.000
Clostridium cl. XVI	<i>Allobaculum</i>	1.64 ± 0.37	0.25 ± 0.03	-6.54	0.002
Bacilli	<i>L. salivarius et rel.</i>	0.05 ± 0.02	0.01 ± 0.00	-6.65	0.031
Bacilli	<i>Streptococcus intermedius et rel.</i>	0.04 ± 0.01	0.01 ± 0.00	-7.24	0.003
Clostridium cl. IX	<i>Peptococcus niger et rel.</i>	0.28 ± 0.04	0.02 ± 0.00	-12.13	0.000
Mollicutes	<i>Acholeplasma</i>	0.18 ± 0.04	0.01 ± 0.00	-15.66	0.001
Actinobacteria	<i>Olsenella et rel.</i>	0.31 ± 0.11	0.00 ± 0.00	-169.08	0.012

Data are represented as mean ± SEM, (n=8). P-value is based on Student t-test.



**Supplementary Figure 1.** Relative contribution of phylum levels of the individual control (C) and heme-fed (H) mice. *n*=8 mice per group.

## SUPPLEMENTARY REFERENCES

- 1 Ohkawa H, Ohishi N, et al. Assay for lipid peroxides in animal tissues by thiobarbituric acid reaction. *Analytical biochemistry* 1979;95:351-8.
- 2 Bolstad BM, Irizarry RA, et al. A comparison of normalization methods for high density oligonucleotide array data based on variance and bias. *Bioinformatics* 2003;19:185-93.
- 3 Irizarry RA, Bolstad BM, et al. Summaries of Affymetrix GeneChip probe level data. *Nucleic Acids Res* 2003;31:e15.
- 4 Frank JA, Reich CI, et al. Critical Evaluation of Two Primers Commonly Used for Amplification of Bacterial 16S rRNA Genes. *Appl Environ Microbiol* 2008;74:2461-70.
- 5 Rajilic-Stojanovic M, Heilig H, et al. Development and application of the human intestinal tract chip, a phylogenetic microarray: analysis of universally conserved phylotypes in the abundant microbiota of young and elderly adults. *Environmental Microbiology* 2009;11:1736-51.
- 6 Suzuki MT, Taylor LT, et al. Quantitative Analysis of Small-Subunit rRNA Genes in Mixed Microbial Populations via 5'-Nuclease Assays. *Appl Environ Microbiol* 2000;66:4605-14.
- 7 Ben-Dov E, Brenner A, et al. Quantification of Sulfate-reducing Bacteria in Industrial Wastewater, by Real-time Polymerase Chain Reaction (PCR) Using *dsrA* and *apsA* Genes. *Microbial Ecology* 2007;54:439-51.
- 8 Bru D, Sarr A, et al. Relative Abundances of Proteobacterial Membrane-Bound and Periplasmic Nitrate Reductases in Selected Environments. *Appl Environ Microbiol* 2007;73:5971-4.

## Chapter 6

### Microbiota facilitates dietary heme-induced epithelial hyperproliferation and hyperplasia by breaking the mucus barrier

Noortje IJssennagger, Clara Belzer, Guido Hooiveld, Jan Dekker, Michael Müller, Michiel Kleerebezem and Roelof van der Meer

*In preparation*

## ABSTRACT

Colorectal cancer risk is associated with diets high in red meat. Heme, the iron porphyrin pigment of red meat, induces cytotoxicity of the colonic contents and epithelial cell damage. A compensatory hyperproliferation and inhibition of apoptosis lead to epithelial hyperplasia, which eventually can develop into colorectal cancer. A heme-rich diet changed the host microbiota, with a major increase in the Gram-negative bacteria (mainly Bacteroidetes, Proteobacteria and Verrucomicrobia). We now investigate whether bacteria play a causal role in the heme-induced cytotoxicity and epithelial hyperproliferation, by giving antibiotics (Abx) simultaneously with the heme diet.

During 2 weeks, C57Bl6/J mice received a control or a heme diet with or without broad-spectrum Abx (ampicillin, neomycin and metronidazole) via their drinking-water. Abx reduced bacterial abundance in colon 100 to 1,000-fold. Heme induced luminal oxidative as well as cytotoxic stress in heme and heme plus Abx fed mice, indicating that there was no major role for the microbiota in the formation of reactive oxygen species and the toxic heme metabolite. Heme induced hyperproliferation and hyperplasia, but this is blocked completely by Abx. Whole genome transcriptomics showed that Abx blocked the heme-induced differential expression of oncogenes, tumor suppressors and cell turnover genes. Moreover, Abx blocked the mucosal sensing of luminal cytotoxicity indicating that Abx increased the mucus barrier. Abx eliminated mucin-degrading bacteria, such as *Akkermansia*, and sulfate-reducing bacteria (SRBs) that produce sulfide. In-vitro studies showed that sulfide is more potent than N-acetylcysteine and cysteine in reducing, and thus splitting, disulfide bonds. This indicates that SRB generated sulfide can denature mucins and thus open the mucus barrier.

In conclusion, this study shows that the microbiota plays an important facilitating role in the heme-induced hyperproliferation and hyperplasia by breaking the mucus barrier and thereby decreasing the protection against luminal irritants such as the toxic heme metabolite.

## INTRODUCTION

Colorectal cancer, the second leading cause of cancer death in Western countries, is associated with the consumption of diets high in red meat [1]. Heme, the iron porphyrin pigment of red meat, is known to induce cytotoxicity of the gut contents and epithelial cell damage [2,3]. A compensatory hyperproliferation together with inhibition of apoptosis leads to epithelial hyperplasia [3], which eventually can develop into colorectal cancer. Besides its effect on the colonic mucosa of mice, dietary heme changed the microbiota drastically, with a major increase in the Gram-negative bacteria (mainly Bacteroidetes, Proteobacteria and Verrucomicrobia) (chapter 5). The increased amount of Gram-negative bacteria most probably increased LPS exposure to colonocytes. However, there was no appreciable innate immune response evoked in the heme-fed mice. There was no functional change in the sensing of the bacteria by the mucosa, as changes in inflammation pathways and Toll- like receptor signaling were not detected. This indicated that the change in microbiota does not cause the observed hyperproliferation and hyperplasia via inflammation pathways (chapter 5). However, bacteria can still play a role in the heme induced compensatory hyperproliferation via alternative mechanisms in colon lumen, such as modulation of oxidative and cytotoxic stress. Oxidative stress induced the formation of peroxidized lipids and these lipids react with heme to form the cytotoxic heme factor (CHF) which subsequently increased cytotoxic stress (chapter 4). In a time course study we showed that there is a lag time in the formation of CHF as well as in the induction of hyperproliferation (chapter 4) which could be due to a time-dependent adaptation of the colon microbiota to the heme diet. Moreover, dietary heme does not increase cytotoxicity and epithelial hyperproliferation in the small intestine [4] indicating that formation of CHF only occurs in the colon where bacterial density is high. Therefore, the aim of this study was to investigate whether bacteria play a crucial role in the heme-induced cytotoxicity and hyperproliferation.

## MATERIALS AND METHODS

### Animals and diets

Experiments were approved by the Ethical Committee on Animal Testing of Wageningen University and were in accordance with national law. Eight week-old male C57Bl6/J mice (Harlan, Horst, the Netherlands) were housed individually in a room with controlled temperature (20-24°C), relative humidity (55%±15%) and a 12h light dark cycle. Mice were fed diets and demineralized water ad libitum. To study the role of microbiota in the heme-induced hyperproliferation, mice (n=9/group) received either a 'Westernized' control diet (40 en% fat (mainly palm-oil), low calcium (30 µmol/g)) or this diet supplemented with 0.5 µmol/g heme (Sigma-Aldrich, St. Louis, USA) for 14 days, as previously described [5]. Mice received the control or the heme diet with or without broad spectrum antibiotics (Abx) in their drinking water during the time of diet intervention. The mixture contained

ampicillin (1 g/L), neomycin (1 g/L), and metronidazole (0.5 g/L) (Sigma-Aldrich). In total there were thus 4 experimental groups; control, heme, control plus Abx and heme plus Abx. Feces were quantitatively collected during days 11-14, frozen at -20°C and subsequently freeze-dried. After 14 days of intervention, the colon was excised, mesenteric fat was removed and the colon was opened longitudinally, washed in PBS, and cut into three parts. The middle 1.5 cm colon tissue was formalin-fixed and paraffin embedded for histology. The remaining proximal and distal parts were scraped. Scrapings were pooled per mouse, snap-frozen in liquid nitrogen and stored at -80°C until further analysis. Colonic contents were sampled for microbiota analysis.

### **Fecal analyses**

Fecal water was prepared by reconstituting freeze-dried feces with double distilled water to obtain a physiological osmolarity of 300 mOsm/l, as described previously [2]. The cytotoxicity of fecal water was quantified by potassium release from human erythrocytes after incubation with fecal water [2]. The relevance of this bioassay was validated with human colon carcinoma-derived Caco-2 cells [6]. To determine lipid peroxidation products in the gut lumen Thiobarbituric Acid Reactive Substances (TBARS) in fecal water were quantified. The assay determines lipid peroxidation by quantifying the concentration of malondialdehyde (MDA) in fecal water [7]. Briefly, fecal water was diluted 4-fold with double-distilled water. To 100 µl of this dilution, 100 µl of 8.1% SDS and 1 ml of 0.11 mol/L 2,6-di-tert-butyl-p-cresol, 0.5% TBA in 10% acetic acid (pH 3.5) was added. To correct for background, TBA was omitted from the assay. TBARS were extracted, after heating for 75 minutes at 82°C, with 1.2 ml n-butanol. The absorbance of the extracts was measured at 540 nm. The amount of TBARS was calculated as MDA equivalents using 1,1,3,3,-tetramethoxypropane as standard.

Bile acids were determined in fecal water of n=3 mice per treatment. Fecal waters were evaporated under nitrogen and resolubilized in 20% (v/v) acetonitrile in water. Samples were analyzed using reversed-phase HPLC combined with simultaneous amperometric detection of free and conjugated bile acids, as described in [8].

### **Immunohistochemistry**

H&E staining was performed to assess the morphology of the tissue. To stain proliferating cells, paraffin embedded colon sections of 5 µm were deparaffinized and stained with an anti-mouse Ki67 antibody as described previously [3]. Colonocytes from 15 well-oriented crypts (longitudinal section, displaying the total crypt) were counted per animal. These crypts were equally distributed over the middle 1.5 cm of the colon. A cell was scored Ki67-positive when the nucleus of the cell was distinctly brown. The number of Ki67-positive cells per crypt, the total number of cells per crypt and the labeling index (percentage of Ki67-positive cells per crypt) were determined.

## **RNA isolation**

Total RNA was isolated by using TRIzol reagent (Invitrogen, Breda, the Netherlands) according to the manufacturer's protocol. For microarray hybridization the isolated RNA was further column purified (SV total RNA isolation system Promega, Leiden, the Netherlands). RNA concentration was measured on a Nanodrop ND-1000 UV-Vis spectrophotometer (Isogen, Maarssen, the Netherlands) and analyzed on an Agilent 2100 bioanalyzer (Agilent Technologies, Amsterdam, the Netherlands) with 6000 Nano Chips, according to the manufacturer's protocol. RNA was judged suitable for array hybridization only if samples exhibited intact bands corresponding to the 18S and 28S ribosomal RNA subunits, and displayed no chromosomal peaks or RNA degradation products (RNA Integrity Number > 8.0).

## **Microarray analysis**

The Ambion WT Expression kit (Life Technologies, P/N 4411974) in conjunction with the Affymetrix GeneChip WT Terminal Labeling kit (Affymetrix, Santa Clara, CA; P/N 900671) was used for the preparation of labeled cDNA from 100ng of total RNA without rRNA reduction. Labeled samples were hybridized on Affymetrix GeneChip Mouse Gene 1.1 ST arrays, provided in plate format. Hybridization, washing and scanning of the array plates was performed on an Affymetrix GeneTitan Instrument, according to the manufacturer's recommendations. RNA labeling was performed in two rounds using a complete block design. Array data was analyzed using an in-house, on-line system [9]. Briefly, normalized expression estimates were obtained from the raw intensity values applying the robust multi-array analysis (RMA) preprocessing algorithm [10,11], available in the Bioconductor library AffyPLM with default settings. Next an empirical Bayes method, called ComBat [12] was used to correct for the systematic error (batch effect) introduced during labeling. Probe sets were redefined according to Dai et al. [13]. In this study probes were reorganized based on the Entrez Gene database, build 37, version 1 (remapped CDF v14). Probe sets that satisfied the criterion of a False Discovery Rate (FDR) < 1% (q-value < 0.01) were considered significantly regulated and used for bioinformatics analysis by Ingenuity (Ingenuity® Systems, [www.ingenuity.com](http://www.ingenuity.com)) and Gene set enrichment analysis (GSEA; <http://www.broad.mit.edu/gsea/>). The number included in the array analysis were n=4 per group for control; control plus Abx, heme and n=6 for heme plus Abx. Genes with signal intensities below 20 in all mice from all treatments were considered absent and excluded from further analysis. Array data were submitted to the Gene Expression Omnibus, accession number GSE40670.

## **Bacterial DNA extraction and qPCR**

DNA was extracted from 0.1 g of fresh colonic sample using the method described by Salonen et al [14]. In short, approximately 0.1 g was used for mechanical and chemical

lysis using 0.5 ml buffer (500 mM NaCl, 50 mM Tris-HCl (pH 8), 50 mM EDTA, 4% SDS) and 0.25 g of 0.1 mm zirconia beads and 3 mm glass beads. Nucleic acids were precipitated by addition of 130  $\mu$ l, 10 M ammonium acetate, using one volume of isopropanol. Subsequently, DNA pellets were washed with 70% ethanol. Further purification of DNA was performed using the QiaAmp DNA Mini Stool Kit (Qiagen, Hilden, Germany). Finally, DNA was dissolved in 200  $\mu$ l Tris/EDTA buffer and its purity and quantity were checked spectrophotometrically (ND-1000, nanoDrop technologies, Wilmington, USA). DNA from all bacteria was amplified by real-time PCR using 16S primers: forward Eub338F, ACTCCTACGGGAGGCAGCAG; reverse Eub518R, ATTACCGCGGCTGCTGG [15]. DNA from Bacteroidetes was amplified using primers: forward Bact934F, GGARCATGTGGTTTAATTTCGATGAT; reverse Bact1060R, AGCTGACGACAACCATGCAG [16]. DNA from Firmicutes was amplified by using primers: forward Firm934F, GGAGYATGTGGTTTAATTTCGAAGCA; reverse Firm1060R, AGCTGACGACAACCATGCAC [16]. DNA from *Akkermansia muciniphila* was amplified using S-St-Muc-1129-a-a-20 (AM1): CAGCACGTGAAGGTGGGGAC and S-St-Muc-1437-a-A-20 (AM2) CCTTGCGGTTGGCTTCAGAT. A gene-specific qPCR targeting the *dsrA* gene representing bacterial groups with sulfate-reducing capacity was performed, using the following primers: forward RH1dsr, GCCGTTACTGTGACCAGCC; reverse RH3-dsr GGTGGAGCCGTGCATGTT[17]. Bacterial counts are calculated and expressed in percentages relative to the control without Abx.

### In-vitro splitting of disulfide (S-S) bonds

We determined the S-S splitting potency of sodium sulfide ( $\text{Na}_2\text{S}$ ), N-acetylcysteine (NAC), glutathione (GSH), and cysteine (Cys) using 5,5'-dithiobis-(2-nitrobenzoic acid) (DTNB) as a model disulfide compound. Splitting of its S-S bond can be quantitated by measuring the absorption at 412 nm [18]. This was done at 20°C in a Perkin Elmer spectrophotometer using a 1.5 ml quartz cuvette containing 100 mM potassium phosphate buffer (pH 7.0) and 100  $\mu$ M DTNB. The reaction was started by adding sulfide or the thiols (final concentration 25  $\mu$ M) and its rate was determined as the slope of the progress curve immediately after mixing. The extent of the reaction was calculated from the final, stable, absorption, corrected for blank absorption, using the milimolar extinction coefficient of 14.15. Sodium sulfate ( $\text{Na}_2\text{SO}_4$ ) was used as a negative control.

### Statistics

In-vivo data are presented as mean  $\pm$  SEM. Differences between the mean values of the 4 groups were tested for main effects by a two-way ANOVA. In-vitro data are given as mean  $\pm$  SD and were tested by one-way ANOVA. A Bonferroni's Multiple Comparison Test was used to determine significant differences between groups. P-values <0.05 were considered significant. Statistical considerations for microarray analysis are described above.



## RESULTS

### Heme- and Abx-induced changes in the colonic lumen

To test whether the broad spectrum antibiotics (Abx) decreased the relative abundance of bacteria, qPCR on bacterial DNA was performed with specific primers for total bacteria, Bacteroidetes and Firmicutes (Figure 1A). The Abx treatment significantly reduced the abundance of both total bacteria and Firmicutes by approximately 100-fold and Bacteroidetes by approximately 1,000-fold. Besides, without Abx the heme diet significantly increased the abundance of Bacteroidetes. This is in line with our previous study (chapter 5) in which we also observed a heme-induced increase in Bacteroidetes. Abx thus drastically decreased the number of total bacteria, of the Gram-positive Firmicutes and of the Gram-negative Bacteroidetes.

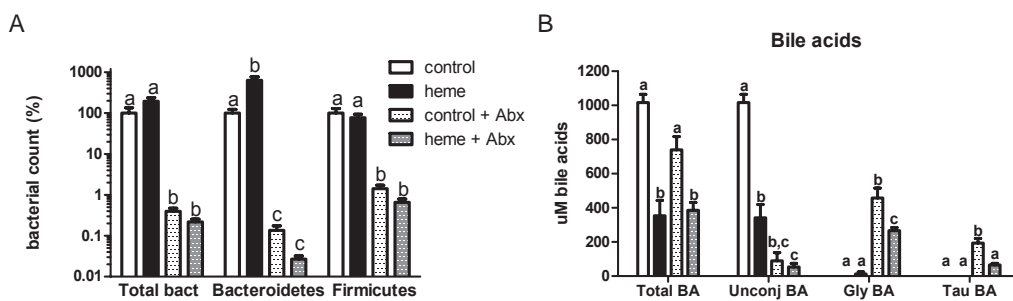


**Figure 1.** (A) Bacterial counts of total bacteria, Bacteroidetes and Firmicutes as measured by qPCR and normalized per gram wet weight. Control bars are set at 100% and the other bars are relative to controls. Data are represented as mean  $\pm$  SEM ( $n=9$  per group) and letters indicate significant different groups ( $p<0.05$ ). (B) Bile acid profiles as determined by HPLC. Data are represented as mean  $\pm$  SEM ( $n=3$  per group) and letters indicate significant different groups ( $p<0.05$ ). Differences were tested by ANOVA with a Bonferroni post-hoc test.

After 2 weeks of intervention the heme-fed mice, both plus and without Abx, had a lower body weight than their controls (Table 1). Cecum sizes of mice receiving Abx in their drinking water were larger than those of mice not receiving Abx (data not shown). Fecal dry and wet weight was significantly increased in the heme plus Abx group (Table 1). A heme diet increases oxidative and cytotoxic stress from the luminal contents (chapters 3, 4 and 5). Reactive oxygen species (ROS) induce the formation of lipid peroxides and these lipid peroxides likely react with heme to form the cytotoxic heme factor (CHF) thereby increasing the cytotoxicity of the luminal contents (chapter 4). Therefore, luminal levels of lipid peroxidation products were determined by measuring TBARS in fecal water. TBARS were low in both control groups (Table 1) and increased significantly on heme as well as on heme plus Abx. This implies that both the heme and the heme plus Abx diet induced ROS stress. A similar pattern was observed for cytotoxicity of the fecal water (Table 1). On the heme and the heme plus Abx diet, cytotoxicity was significantly

increased as compared to their respective controls. The cytotoxicity in the heme plus Abx group was lower than that in the heme group. As there is a drastic reduction in microbiota by Abx, but only a relatively small lowering of cytotoxicity (2-fold) and TBARS (1.3-fold) it is not very likely that bacteria play a major role in the formation of TBARS and cytotoxicity.

Bile acid profiles can influence cytotoxicity levels. Bile acids that are not absorbed in the ileum enter the colon where they are deconjugated by microbiota. It was shown before that glycine- and taurine-conjugation of bile acids decreased the cytotoxicity of mixed bile acid micelles [19] and therefore we determined bile acid profiles in the current study (Figure 1B). On the control and heme diet without Abx hardly any conjugated bile acids were present. Upon Abx treatment, bile acid profiles consisted predominantly of glycine- and taurine-conjugated bile acids.

**Table 1.** Effects of heme and Abx on body weight and fecal parameters

	Control	Heme	Control + Abx	Heme + Abx
Body weight (g)	27.7 ± 0.5 <sup>a</sup>	24.9 ± 0.5 <sup>b</sup>	27.2 ± 0.3 <sup>a</sup>	24.8 ± 0.4 <sup>b</sup>
Fecal wet weight (g/day)	0.49 ± 0.08 <sup>a</sup>	0.60 ± 0.05 <sup>a</sup>	0.62 ± 0.09 <sup>a</sup>	1.20 ± 0.19 <sup>b</sup>
Fecal dry weight (g/day)	0.12 ± 0.01 <sup>a</sup>	0.11 ± 0.01 <sup>a</sup>	0.12 ± 0.01 <sup>a</sup>	0.19 ± 0.02 <sup>b</sup>
TBARS (MDA equivalents, $\mu$ mol/L)	12.70 ± 1.43 <sup>a</sup>	59.84 ± 2.46 <sup>b</sup>	11.06 ± 1.63 <sup>a</sup>	46.06 ± 3.92 <sup>c</sup>
Cytotoxicity (% lysis)	1.09 ± 0.45 <sup>a</sup>	66.90 ± 10.45 <sup>b</sup>	0.05 ± 0.04 <sup>a</sup>	31.30 ± 8.98 <sup>c</sup>

Data are represented as mean ± SEM (n=9 per group). Differences between the groups were tested by ANOVA with a Bonferroni post-hoc test and different indicate significant differences (p<0.05).

### Heme- and Abx-induced changes in the colonic mucosa

To investigate the morphology of the colon tissue an H&E staining was performed (Figure 2A). In the presence of normal microbiota (i.e. no Abx) heme drastically increased crypt depth. This was not due to inflammation as there was no infiltration of neutrophils or macrophages observed in the lamina propria. A Ki67 staining was performed to quantify the effects of heme and Abx on colonic cell proliferation (Figure 2B). The number of Ki67-positive proliferating cells and the total number of cells per crypt were counted, and the percentage of proliferative cells per crypt, the labeling index, was calculated (Figure 2C). The labeling index and the amount of proliferative cells did not differ significantly between the control and the control plus Abx group. The total number of cells per crypt was significantly lower in the control plus Abx compared to the control group. When comparing the heme group to the control group, there was a significantly increased cell proliferation, which resulted in the expansion of the proliferative compartment and in increased crypt depth as found earlier [3]. In contrast, when heme and Abx were given simultaneously, there was no hyperproliferation or hyperplasia observed and the levels of proliferating cells in the heme plus Abx group were similar to that of controls plus

Abx. Heme thus induced hyperproliferation and hyperplasia in mouse colon, but this occurred only in the presence of a normal microbiota.

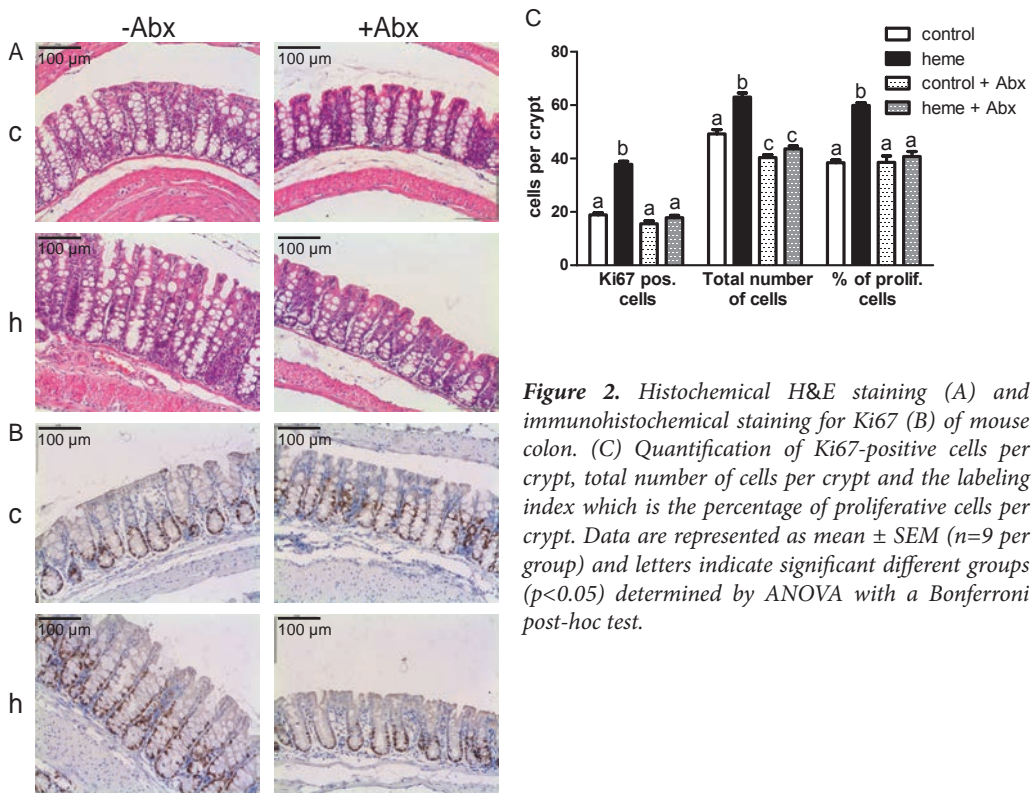


**Figure 2.** Histochemical H&E staining (A) and immunohistochemical staining for Ki67 (B) of mouse colon. (C) Quantification of Ki67-positive cells per crypt, total number of cells per crypt and the labeling index which is the percentage of proliferative cells per crypt. Data are represented as mean  $\pm$  SEM (n=9 per group) and letters indicate significant different groups ( $p < 0.05$ ) determined by ANOVA with a Bonferroni post-hoc test.

### Abx block the heme-induced differential expression of cell cycle genes

To investigate whether the described physiological changes were reflected in gene expression profiles, whole genome transcriptomics was performed. Gene expression profiles of colonic scrapings of mice from the 4 groups were determined. A Venn-diagram (Figure 3A) shows the specific and overlapping genes when comparing the differentially expressed genes on the heme diet versus the heme plus Abx diet. For the comparison heme versus control, there were 5,507 genes differentially expressed with a  $q$ -value  $< 0.01$ . Of those, 4,859 were not changed in the heme-fed mice plus Abx. These 4,859 heme-specific genes were uploaded in Ingenuity to determine the transcription factors involved in the differential gene expression (Figure 3B). The tumor suppressors *Cdkn2a*, *Tp53*, *Smad3*, and *Rb1* were inhibited, while oncogenes such as *Myc* and *Foxm1* were activated in the heme group. Also transcription factors *E2f1* and *Tbx2* playing a role in cell cycle were induced. These transcription factors were not induced when Abx was given simultaneously with the heme-rich diet. With the software Gene Set Enrichment Analysis (GSEA) the cellular processes in which the significantly changed genes were involved were determined. Figure 3C shows

that heme mainly affected cell cycle-related processes but only in the presence of the normal microbiota, which is in line with the increased labeling index (Figure 2C). The heme plus Abx group showed a much lower amount of 369 unique differentially expressed genes. These heme plus Abx-specific genes were also analyzed with the above mentioned software programs. However, responses were much less specific and less significant due to the lower amount of genes present in this comparison. None of the modulated processes in this group was related to the endpoints of our study.

### **Antioxidant response was induced in both heme groups**

There were 648 genes that were significantly regulated both in the heme and in the heme plus Abx group (Figure 3A). Of those overlapping genes 599 genes showed a similar regulation in heme and heme plus Abx. As there is no increased proliferation observed in the heme plus Abx, other processes than cell cycle-related processes should be present in the overlap. Transcription factors that were activated in heme and heme plus Abx groups were predominantly PPARs, involved in fatty acid metabolism, and Nrf2, involved in antioxidant response (Figure 3B and C). This implies that oxidative stress and lipid peroxidation products induced the antioxidant response and the induction of PPAR target genes, respectively, irrespective of the addition of Abx to the diet.

### **Abx block the mucosal sensing of the heme-induced luminal cytotoxicity**

In the heme plus Abx fed mice, there was substantial luminal cytotoxicity but no induction of hyperproliferation, suggesting that the cytotoxic heme factor (CHF) did not reach the surface epithelial cells in these mice. Therefore we investigated the luminal sensing of the cytotoxicity using the marker genes as described earlier (chapter 4). Figure 4A shows that heme upregulated the expression of the anti-apoptosis genes Survivin (Birc5) and Immediately early response 3 (Ier3), and of the necrosis facilitator Ripk3 [20]. However, none of these heme-specific effects occurred in the presence of Abx, indicating that the mucosa did not sense the luminal cytotoxicity after Abx treatment. We hypothesize that the diffusion barrier of the mucus layer in the heme plus Abx mice was increased compared to the heme-fed mice without Abx. This increase in the mucus barrier could be caused by an increase in mucin synthesis, and/or by a decrease in mucin degradation. Therefore, we investigated whether there were differences in mucin (Muc) gene expression between the heme and heme plus Abx treatment that could contribute to the difference in barrier function. Expression levels of the secreted Muc2 and the cell-associated Muc4 were decreased in heme plus Abx compared to heme alone (Figure 4B), whereas the expression of Tff3 is slightly upregulated. The KEGG pathway 'Mucin type O-Glycan biosynthesis' was significantly enriched on the heme diet compared to the heme plus Abx to heme according to the GSEA analysis ( $q < 0.049$ ). Thus, these data indicate that the production of the mucus layer is certainly not increased and may even be decreased.

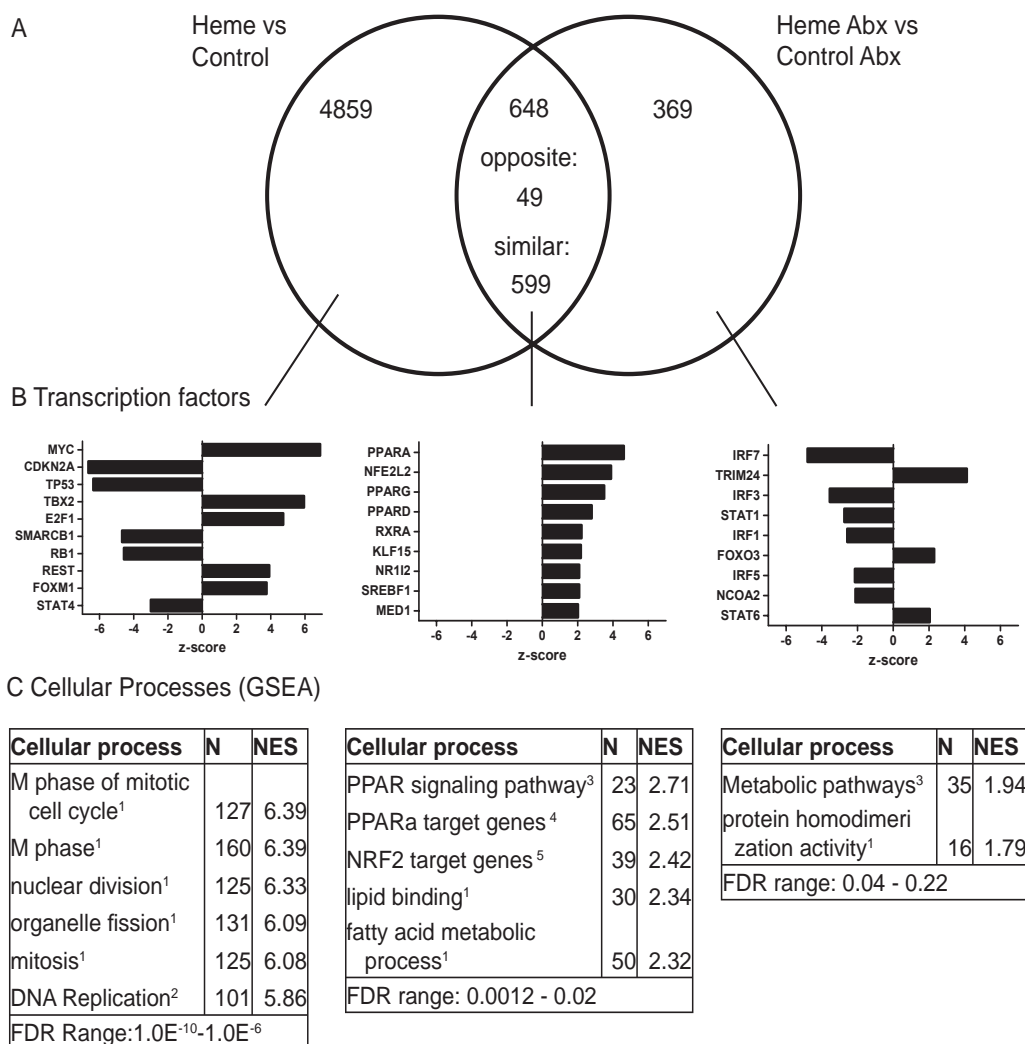


**Figure 3.** (A) Venn-diagram showing the numbers of heme and heme plus Abx specific regulated genes and the number of overlapping genes ( $q < 0.01$ ). (B) Ingenuity analysis showing the activated or inhibited transcription factors (which have a z-score higher than 2 and a p-value  $< 0.05$ ) in both treatments specifically and in the overlapping genes. (C) Gene Set Enrichment Analysis showing the positive enriched processes. Sources of the gene sets are indicated in superscript and represent 1. Gene ontology, 2. Reactome, 3. KEGG, 4. ref [35] and 5. ref [36]. N represents the number of genes in the gene set and NES is the normalized enrichment score, which is the enrichment score for the gene set after it has been normalized to account for variations in gene set size.

Besides an increase in mucin synthesis, also a decrease in mucin degradation could contribute to an increased barrier function. The microbiota breaks down mucins and uses their carbohydrates and amino acids as substrates. In addition, sulfate-reducing bacteria (SRBs) use the mucinous sulfate as an electron acceptor in anaerobic respiration. It is very plausible that due to the Abx treatment the mucus barrier becomes less permeable as only very few bacteria are present. To test this, we investigated the presence

of the mucin- degrading bacterium *Akkermansia muciniphila* after Abx treatment by qPCR (Figure 5A). Heme increased the abundance of *Akkermansia*, but Abx treatment drastically reduced the abundance of this mucin degrader. The Abx treatment could thus lead to an increase in barrier function and protection of the surface epithelial cells by eliminating mucin degraders such as *Akkermansia*.

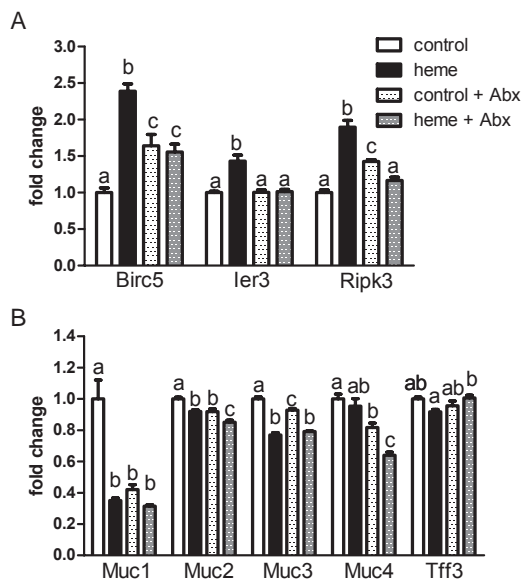


**Figure 4.** Gene expression of cytotoxicity sensing genes *Birc5*, *Ier3* and *Ripk3* (A) and of mucin genes *Muc1* to 4 and *Tff3* (B). Gene expression levels in the control group are set at 1. Expression of the other bars is relative to the controls. Data are represented as mean  $\pm$  SEM ( $n=4$  for control, heme, control plus Abx and  $n=6$  for heme plus Abx) and letters indicate significant differences ( $p<0.05$ ) determined by ANOVA with a Bonferroni post-hoc test.

Colonic mucus is composed primarily of Muc2, and is high in intra- and intermolecular S-S bonds, which stabilizes its structure. When these bonds are broken (reduced), mucins lose their quaternary and tertiary structure, the viscosity of the mucus decreases, and the mucus becomes more available for degradation by the microbiota. SRBs can then use the mucinous sulfate as oxidant in anaerobic respiration thereby producing sulfide. N-acetylcysteine (NAC) and L-cysteine can split S-S bonds and make mucins less viscous [21]. We hypothesized that sulfide can have a similar mucolytic effect. As Abx decreased the abundance of SRBs (Figure 5A), levels of sulfide in the colonic lumen were likely to be much lowered. To test whether sulfide is able to break S-S bonds and decrease the viscosity of mucins we incubated commercially available mucin with NAC and cysteine. We could not reproduce their mucolytic effect [21], probably because of impurity and/or the denatured state of the commercial available mucins. As an alternative we tested the effect of several sulfur-containing compounds on the model compound DTNB (5,5'-dithiobis-(2-nitrobenzoic acid) which has a central S-S bond. When this S-S bond is split by reduction the absorbance at 412 nm increases. The absorbance was followed in time and the initial rate and extent of splitting is presented in Figure 5B.  $\text{Na}_2\text{SO}_4$  was used as negative control. Indeed cysteine, glutathione and NAC splitted the S-S bond



with a similar rate between 24 to 31  $\mu\text{M}/\text{min}$ . However, sulfide gave a significantly higher splitting rate of  $62.4 \pm 5.9 \mu\text{M}/\text{min}$ . This indicates that sulfide, compared to the amino-acid thiols, has a more potent mucolytic effect that may open up the mucus layer to degrading bacteria. The extent of S-S bond splitting was twice as high for sulfide compared to the other amino-acid thiols. Based on Ellman's mechanism [18] this indicates (see scheme Fig. 5C) that a reactive persulfide anion originates from the splitting of the first S-S bond which then splits a second bond thereby creating a trisulfide bond.

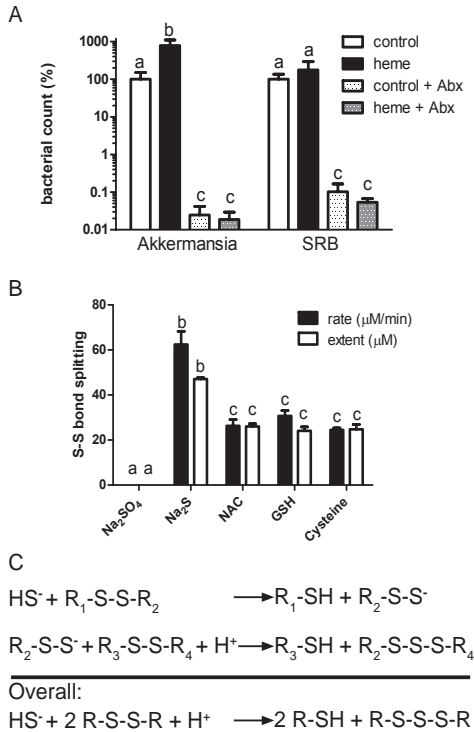


**Figure 5.** (A) bacterial counts of *Akkermansia muciniphila* and sulfate reducing bacteria (SRBs) as determined by qPCR. Control bars are set at 100% and the other bars are relative to controls. Data are represented as mean  $\pm$  SEM ( $n=8-9$  per group) and letters indicate significant different groups ( $p<0.05$ ). (B) Rate and extent of S-S bond splitting. Data are represented as mean  $\pm$  SD ( $n=3-6$  per group) and letters indicate significant different groups ( $p<0.05$ ). Differences between the groups were tested by ANOVA with a Bonferroni post-hoc test. (C) Reaction by which sulfide splits S-S bonds.

# DISCUSSION

In this study we demonstrate that the colonic microbiota facilitates the heme-induced compensatory hyperproliferation and hyperplasia. We show that when there is a drastic reduction of microbiota by Abx, heme does not injure the surface epithelium and there is thus no induction of compensatory hyperproliferation and hyperplasia of the colon crypt cells. The facilitating role of the microbiota is not mediated via the formation of oxidative and cytotoxic stress, as cytotoxicity and ROS levels were significantly higher in both heme and heme plus Abx fed mice compared to their controls. Their slightly lower concentrations in the heme plus Abx group reflect dilution as fecal wet weight was increased (Table 1). Our results indicate that the facilitating effect of the microbiota on heme-induced hyperproliferation is by breaking the mucus barrier by the combined

action of SRB-generated hydrogen sulfide and mucin-degrading bacteria. The crucial steps of this, to our knowledge novel, sulfide hypothesis are schematically depicted in Figure 6. Mucolysis by hydrogen sulfide opens the compact, protective mucus layer to bacterial degradation, and facilitates diffusion of luminal, cytotoxic, micelles to the surface. This way, surface epithelial cells are less protected against luminal cytotoxicity and a compensatory hyperproliferation is induced. Abx eliminates bacteria and thus inhibit HS- production and mucin degradation so that the protective mucus barrier is maintained.

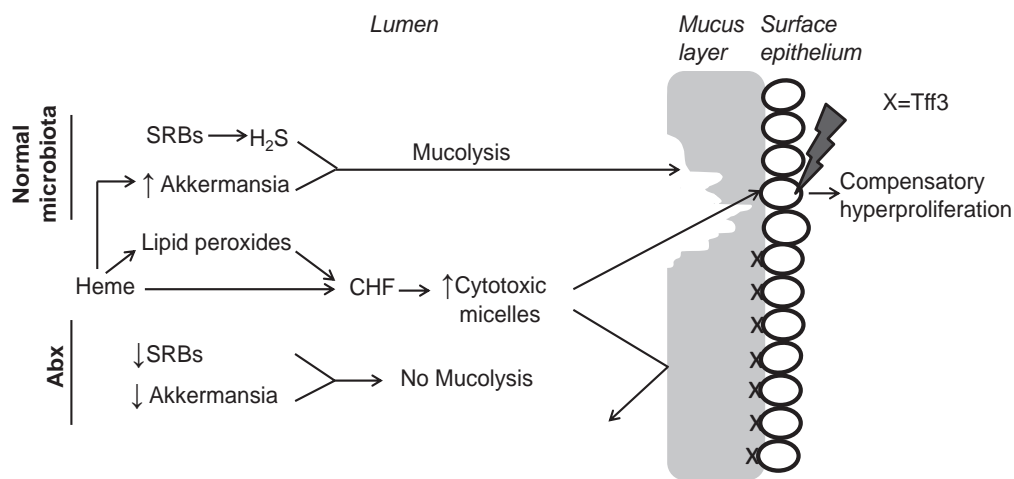


**Figure 6.** Proposed mechanism of how microbiota facilitates heme-induced compensatory hyperproliferation. Upper part represents processes when normal microbiota is present (i.e. without Abx) leading to compensatory hyperproliferation. Lower part represents processes with Abx in which the mucus layer is protective against cytotoxic micelles. SRB is sulfate-reducing bacteria, CHF is cytotoxic heme factor and Tff3 is trefoil factor 3.

Central to our hypothesis is that sulfide can reduce and thus split S-S bonds, which opens the compact mucus layer. The compactness of this layer is determined by intra- and intermolecular S-S bonds in secreted Muc2 and by the intestinal trefoil factor Tff3 [22,23]. Tff3 is a small protein containing 3 S-S bonds and is present in the mucus layer as monomers and S-S bonded dimers, binding mucins in a lectin-like manner [23]. Tff3 binding controls the mucus barrier as this barrier is compromised in knockout mice [24]. Tff3 is produced with Muc2 in goblet cells [25], but in our recent laser capture microdissection study [3], we observed that Tff3 expression is enriched in surface epithelium. The surface to crypt ratio is 4.5 for Tff3 expression and only 0.7 for Muc2 expression. Because of that, we speculate that Tff3 is secreted from the surface epithelial cells and binds secreted Muc2 to the membrane-bound mucins. Splitting of S-S bonds denatures Tff3 and Muc2 monomers, and dissociates their S-S-bonded dimers resulting in reduced viscosity and increased permeability of the mucus layer [22]. Typical S-S



breaking agents are N-acetylcysteine (NAC), used in the treatment of cystic fibrosis, L-cysteine and 2-mercaptoethanol, which all decrease the viscosity of mucus, either in-vivo or in-vitro [21]. We now show that sulfide, compared to these thiols, is at least two-fold more potent in breaking these S-S bonds. This is because the  $pK_a$  of hydrogen sulfide is about one unit lower than that of thiols, implying that the concentration of the nucleophilic agent (i.e. the anion) in the splitting of the S-S is higher with hydrogen sulfide. Moreover, as sulfide donates two electrons it splits two S-S bonds, whereas thiols split only one (Figure 5B). Elaborating Ellman's mechanism of S-S splitting [18] we were surprised to see that the second reaction (see scheme Figure 5C) results in a trisulfide bond. As we were not aware of this bond type we searched the literature for clues and found that this bond is known as an artifact in the biopharmaceutical production of proteins, which can be reproduced by incubating these proteins with sodium sulfide (see [26] for review). Our mechanism is also supported by a recent study of Devkota et al. [27] showing that mono-association of germ-free mice with the sulfite-reducing proteobacterium *Bilophila wardsworthia*, in the presence of taurocholate, results in breaking of the mucus barrier. The authors suggested that this is either due to sulfide (produced from taurine) or to unconjugated deoxycholate. We feel that their results could very well be explained by our proposed mechanism because they did not find barrier breaking in the presence of glycocholate, which is also metabolized to deoxycholate.

Besides SRB, other bacteria play an important role in determining the characteristics of the mucus layer. Bacteria may modulate the synthesis and glycosylation of mucins and thus the thickness, compactness, and permeability of the mucus layer [22,28]. Several bacterial species are known to degrade the mucus layer. For instance, *Akkermansia muciniphila* [29] as well as *Prevotella* [30] are known mucin degraders. Recently, we described that the heme diet drastically increased the abundance of *Akkermansia* and *Prevotella* (chapter 5), which might contribute to increase in mucin degradation leading to a reduced mucus barrier on the heme diet. In this study the heme-induced abundance of *Akkermansia* was confirmed, and we show that *Akkermansia* was eliminated by Abx treatment. Mucin degraders use the abundant carbohydrates in mucin as their main energy source. Because of their metabolic flexibility the microbiota can also use non-digestible carbohydrates as a fermentable substrate [31]. This links the diet of the host to mucin degradation in the digestive tract and thus to the functional efficacy of the mucus barrier. We suggest that foods rich in slow fermentable fibers (such as wheat fiber) might inhibit the mucin degradation activity of the colon microbiota, which is an interesting direction for future research.

In humans 3 main microbial profiles, so-called 'enterotypes' exist [32]. Interestingly, two of those enterotypes are characterized by mucin-degrading bacteria. One of these enterotypes is rich in *Prevotella* and the co-occurring *Desulfovibrio*. *Desulfovibrio* may enhance the rate-limiting sulfatase step by hydrolyzing glycosyl-sulfate

esters and *Prevotella* thus degrades mucin. The second mucin-degrading enterotype is rich in *Ruminococcus* and *Akkermansia*, which are both able to degrade mucins. The third enterotype is rich in *Bacteroides* using carbohydrates and proteins as substrates for fermentation [32]. It would be of interest to see if there are differences in the mucus barrier in these different enterotypes and to investigate whether diseases of the gut, such as cancer and IBD, are more often associated with mucin-degrading enterotypes. In some people the colon microbiota does not reduce sulfate to hydrogen sulfide [33]. We feel that even in that case our mechanism may be of relevance as bacteria can also produce sulfide from taurine-conjugated bile acids, as mentioned above. In humans the glycine/taurine ratio of bile acid conjugation is about 3 [34], which implies that about 25 % of the bile acids spilled over into the colon contains taurine. In addition, we speculate that other bacteria may secrete mucolytic thiols, such as cysteine, instead of the more potent sulfide. We think that this may occur because the colonic milieu is very reducing, but this requires further investigation.

As discussed earlier (chapter 4), the cytotoxic heme factor (CHF) is formed in the colon lumen by covalent addition of lipid peroxides, produced by heme-catalyzed ROS, to the unsaturated bonds of the protoporphyrin ring. This very lipophilic CHF is solubilized in mixed micelles. Our transcriptome data (Figure 4A) show that Abx block the mucosal sensing of these cytotoxic micelles. These data also show that Abx does not block the mucosal sensing of luminal ROS (Figure 3). In both heme and heme plus Abx mice the Nrf2 mediated antioxidant response was initiated and PPARs were activated by oxidized lipids. This differential mucosal sensing indicates that, with Abx, the compact mucus layer is still permeable to small molecules, such as oxidized lipids, but not to large micellar aggregates. As there is no proliferation induced in the heme plus Abx group this shows that mucosal sensing of ROS does not cause compensatory hyperproliferation. This is in line with our previous study showing that ROS is acutely formed after consuming the heme diet, while there is a lag time in the formation of cytotoxicity and the induction of hyperproliferation (chapter 4). Besides, when ROS stress is increasing, there is no higher level of compensatory hyperproliferation observed (chapter 3).

Overall we can conclude that the microbiota plays a facilitating role in the heme-induced hyperproliferation by breaking the mucus barrier. Sulfide, the product of sulfate-reducing bacteria, reduces S-S bonds and thus makes the mucus layer more permeable to degrading bacteria and to cytotoxic micelles.

## ACKNOWLEDGEMENTS

The authors would like to thank Mechteld Grootte Bromhaar, Jenny Jansen, Philip de Groot and Mark Boekschoten for microarray analysis and Shohreh Keshtkar, Arjan Schonewille, Rob Dekker and Bert Weijers for technical assistance.

## REFERENCES

- 1 World Cancer Research Fund. Food, Nutrition, Physical Activity and the Prevention of Cancer: a Global Perspective. Washington, DC: American Institute for Cancer Research, 2007.
- 2 Sesink AL, Termont DS, et al. Red meat and colon cancer: the cytotoxic and hyperproliferative effects of dietary heme. *Cancer Res* 1999;59:5704-9.
- 3 IJssennagger N, Rijnierse A, et al. Dietary haem stimulates epithelial cell turnover by downregulating feedback inhibitors of proliferation in murine colon. *Gut* 2012;61:1041-9.
- 4 Sesink AL, Termont DS, et al. Red meat and colon cancer: dietary haem-induced colonic cytotoxicity and epithelial hyperproliferation are inhibited by calcium. *Carcinogenesis* 2001;22:1653-9.
- 5 de Vogel J, Jonker-Termont DS, et al. Green vegetables, red meat and colon cancer: chlorophyll prevents the cytotoxic and hyperproliferative effects of haem in rat colon. *Carcinogenesis* 2005;26:387-93.
- 6 Lapre JA, Termont DS, et al. Lytic effects of mixed micelles of fatty acids and bile acids. *Am J Physiol* 1992;263:G333-7.
- 7 Ohkawa H, Ohishi N, et al. Assay for lipid peroxides in animal tissues by thiobarbituric acid reaction. *Analytical biochemistry* 1979;95:351-8.
- 8 Dekker R, Vandermeer R, et al. Sensitive Pulsed Amperometric Detection of Free and Conjugated Bile-Acids in Combination with Gradient Reversed-Phase Hplc. *Chromatographia* 1991;31:549-53.
- 9 Lin K, Kools H, et al. MADMAX - Management and analysis database for multiple ~omics experiments. *J Integr Bioinform* 2011;8:160.
- 10 Irizarry RA, Hobbs B, et al. Exploration, normalization, and summaries of high density oligonucleotide array probe level data. *Biostatistics* 2003;4:249-64.
- 11 Irizarry RA, Bolstad BM, et al. Summaries of Affymetrix GeneChip probe level data. *Nucleic Acids Res* 2003;31:e15.
- 12 Johnson WE, Li C, et al. Adjusting batch effects in microarray expression data using empirical Bayes methods. *Biostatistics* 2007;8:118-27.
- 13 Dai M, Wang P, et al. Evolving gene/transcript definitions significantly alter the interpretation of GeneChip data. *Nucleic Acids Res* 2005;33:e175.
- 14 Salonen A, Nikkila J, et al. Comparative analysis of fecal DNA extraction methods with phylogenetic microarray: effective recovery of bacterial and archaeal DNA using mechanical cell lysis. *Journal of microbiological methods* 2010;81:127-34.
- 15 Fierer N, Jackson JA, et al. Assessment of soil microbial community structure by use of taxon-specific quantitative PCR assays. *Appl Environ Microbiol* 2005;71:4117-20.
- 16 Guo X, Xia X, et al. Development of a real-time PCR method for Firmicutes and Bacteroidetes in faeces and its application to quantify intestinal population of obese and lean pigs. *Lett Appl Microbiol* 2008;47:367-73.
- 17 Ben-Dov E, Brenner A, et al. Quantification of Sulfate-reducing Bacteria in Industrial Wastewater, by Real-time Polymerase Chain Reaction (PCR) Using *dsrA* and *apsA* Genes. *Microbial Ecology* 2007;54:439-51.
- 18 Ellman GL. A colorimetric method for determining low concentrations of mercaptans. *Arch Biochem Biophys* 1958;74:443-50.
- 19 Van der Meer R, Termont DS, et al. Differential effects of calcium ions and calcium phosphate on cytotoxicity of bile acids. *Am J Physiol* 1991;260:G142-7.
- 20 Vandenabeele P, Declercq W, et al. The role of the kinases RIP1 and RIP3 in TNF-induced necrosis. *Science signaling* 2010;3:re4.
- 21 Sheffner AL. The reduction in vitro in viscosity of mucoprotein solutions by a new mucolytic agent, N-acetyl-L-cysteine. *Ann N Y Acad Sci* 1963;106:298-310.
- 22 McGuckin MA, Linden SK, et al. Mucin dynamics and enteric pathogens. *Nature reviews Microbiology* 2011;9:265-78.
- 23 Kim YS, Ho SB. Intestinal goblet cells and mucins in health and disease: recent insights and progress. *Curr Gastroenterol Rep* 2010;12:319-30.

- 24 Mashimo H, Wu DC, et al. Impaired defense of intestinal mucosa in mice lacking intestinal trefoil factor. *Science* 1996;274:262-5.
- 25 Taupin D, Podolsky DK. Trefoil factors: initiators of mucosal healing. *Nat Rev Mol Cell Biol* 2003;4:721-32.
- 26 Nielsen RW, Tachibana C, et al. Trisulfides in proteins. *Antioxid Redox Signal* 2011;15:67-75.
- 27 Devkota S, Wang Y, et al. Dietary-fat-induced taurocholic acid promotes pathobiont expansion and colitis in *Il10*<sup>-/-</sup> mice. *Nature* 2012;487:104-8.
- 28 Szentkuti L, Riedesel H, et al. Pre-epithelial mucus layer in the colon of conventional and germ-free rats. *The Histochemical journal* 1990;22:491-7.
- 29 Derrien M, Vaughan EE, et al. *Akkermansia muciniphila* gen. nov., sp. nov., a human intestinal mucin-degrading bacterium. *Int J Syst Evol Microbiol* 2004;54:1469-76.
- 30 Wright DP, Rosendale DI, et al. *Prevotella* enzymes involved in mucin oligosaccharide degradation and evidence for a small operon of genes expressed during growth on mucin. *FEMS Microbiol Lett* 2000;190:73-9.
- 31 Sonnenburg JL, Xu J, et al. Glycan foraging in vivo by an intestine-adapted bacterial symbiont. *Science* 2005;307:1955-9.
- 32 Arumugam M, Raes J, et al. Enterotypes of the human gut microbiome. *Nature* 2011;473:174-80.
- 33 Macfarlane GT, Gibson GR, et al. Comparison of fermentation reactions in different regions of the human colon. *J Appl Bacteriol* 1992;72:57-64.
- 34 Govers MJ, Termont DS, et al. Characterization of the adsorption of conjugated and unconjugated bile acids to insoluble, amorphous calcium phosphate. *J Lipid Res* 1994;35:741-8.
- 35 Rakhshandehroo M, Knoch B, et al. Peroxisome proliferator-activated receptor alpha target genes. *PPAR Res* 2010;2010.
- 36 Muller M, Banning A, et al. *Nrf2* target genes are induced under marginal selenium-deficiency. *Genes Nutr* 2010;5:297-307.

# Chapter 7

## General discussion and future perspectives

## **General discussion and future perspectives**

The consumption of diets high in red meat is associated with an increased risk to develop colon cancer [1,2,3]. However, the consumption of white meat (poultry and fish) does not increase colon cancer risk [4,5]. Red meat contains the iron-porphyrin pigment heme and several epidemiological studies show an association between heme intake and the risk of colon cancer [6,7]. Heme is mainly present in the body as the prosthetic group of hemoglobin, myoglobin and cytochromes. In blood, many protective mechanisms exist to keep free heme levels low [8,9]. This is necessary as free heme is very reactive and cytotoxic. In the intestinal lumen, however, these protective mechanisms are not present and upon digestion dietary heme becomes freely available in the digestive tract. Heme is poorly absorbed in the small intestine and therefore the majority of the ingested heme enters the colon [10,11]. When rats were fed a heme diet their colonic surface epithelium was injured resulting in a compensatory hyperproliferation to replace the injured cells [12]. As proliferation occurs in the crypts, a surface to crypt signaling mechanism was suggested. In this thesis we investigated the underlying molecular mechanisms by which heme initiates hyperproliferation. As gene expression profiles of the mouse are well-studied and because many mouse knockout models are available, we studied the effects of heme on colonic gene expression and hyperproliferation in mice.

## **Surface to crypt signaling**

In chapter 2 we showed that dietary heme reached and injured the surface epithelial cells of mouse colon. However, heme did not directly affect the crypt cells. As surface injury initiates hyperproliferation in the crypt, this supported the hypothesis that a signaling mechanism from the injured surface cells to the proliferative crypt cells initiated the observed compensatory hyperproliferation. Possible signaling molecules must be molecules secreted from the surface epithelium having their receptors in the crypts. As proliferation is normally a tightly controlled and well-balanced process [13] it is very likely that several molecules, rather than just one, are involved in surface to crypt signaling initiating hyperproliferation. If the epithelial proliferation rate would depend on one signaling molecule only, the risk to lose homeostasis is high.

Chapter 2 showed that the signaling occurred via downregulation of feedback inhibitors of proliferation. Cap-dependent protein translation was inhibited in heme-fed mice, as shown by the surface-specific upregulation of 4E-BP1 mRNA and protein level. We speculate that a decrease of feedback inhibitors of proliferation, rather than an increase of growth factors, is responsible for the initiation of compensatory hyperproliferation. It becomes difficult, if not impossible, for injured cells to invest energy in the synthesis of a signaling molecule. By inhibiting protein synthesis and by downregulating feedback inhibitors of proliferation the injured cells prevent energy dissipation. In this view, a healthy cell is thus secreting feedback inhibitors to maintain homeostasis, but once the cell

gets injured these signals are lost and hyperproliferation starts to replace the injured cell. Despite the surface-specific inhibition of the cap-dependent translation there are many upregulated gene-transcripts present in the surface epithelium upon heme feeding. Examples are the epithelial growth factors Amphiregulin (Areg) and Epiregulin (Ereg) which were upregulated 9 and 6-fold respectively (chapter 2). However, these growth factors did not play a role in heme-induced hyperproliferation, as they were not translated into protein. Moreover, Areg and Ereg were upregulated under heme plus Abx conditions where no hyperproliferation was initiated (chapter 6). Repressed transcripts can be saved in stress granules [14,15] and translated once stress is over. Moreover, there is evidence that stress-related transcripts are not translated via cap-dependent translation which is inhibited, but via cap-independent translation using internal ribosome entry sites [15]. This implies that stress-related transcripts can be translated to protein when cap-dependent translation is blocked, which could explain the heme-induced upregulation of Hmox1 at gene and protein level. Taken together, our study showed an increase in mRNA transcripts of several genes that were not translated into protein. Thus, there was a discrepancy between transcription and translation, emphasizing the importance to verify transcriptome changes at protein level. Therefore, proteomics analysis on scrapings of heme-fed mice is an interesting direction for future research allowing us to investigate possible signaling molecules in more detail.

Next to the observed upregulation of 4E-BP1, microRNAs (miRs) might contribute to translation inhibition, causing a decrease in protein products which is greater than the observed decrease in mRNA. MiRs are small non-coding ribonucleic acids with mature transcripts of 18-25 nucleotides that interact with their target mRNA. Such interactions cause degradation of mRNA and/or can inhibit mRNA at the translational level [16]. Preliminary data showed the upregulation of several miRs, such as miR-21 and let-7c, in colon of heme-fed mice. The possible role for miRs in the heme-induced translational repression requires further study.

We identified Wif1, IL-15, Ihh and Bmp2 as possible signaling molecules to initiate hyperproliferation (chapter 2). In all experiments described in this thesis, IL-15 and Bmp2 showed a consistent downregulation by heme, which coincided with increased proliferation. IL-15 and Bmp2 were thus considered as robust and reliable biomarkers of cytotoxicity induced stress. Wif1 was borderline significantly downregulated by heme (q-value of 0.017) in the antibiotics (Abx) experiment (chapter 6). It should be noted that Wif1 signal intensities are low in scrapings, as Wif1 is solely expressed in the enteroendocrine cell fraction (chapter 2). We validated the heme-induced downregulation of Wif1 by immunohistochemistry (chapter 2, Figure 4) and qPCR. Ihh was not changed at gene expression level in the time course experiment (chapter 5). However, it possible that Ihh protein levels were decreased after day 4 of heme feeding as cap-dependent translation is blocked. Protein levels of Ihh should thus be determined before further conclusions can

be drawn. Due to the translation inhibition, all signaling molecules could have lower levels than expected based on their gene expression. If further validated in humans, Wif1, IL-15, Ihh and Bmp2 could possibly be used as early biomarkers of colon cancer risk. As basal levels of these signaling molecules might vary between persons, it is important to determine their levels in colon biopsies before and after a dietary intervention.

### **Oxidative versus cytotoxic stress**

Heme induced both oxidative and cytotoxic stress in the colon which could injure the epithelial surface cells. Chapter 3 showed that the heme diet in PPAR $\alpha$  KO mice, which were less protects against oxidative stress, did not induce additional hyperproliferation compared to wild-type mice. In chapter 4 it was described that cytotoxic stress rather than oxidative stress induced hyperproliferation. Oxidative stress was instantaneously generated, while there was a lag time for the formation of cytotoxicity and the induction of hyperproliferation. In chapter 6 we described that when heme and Abx are given simultaneously oxidative stress was increased and sensed by the colonocytes, while hyperproliferation was absent. All these independent studies show that there is no direct causal role for oxidative stress in the heme-induced hyperproliferation. Besides, in all these studies oxidative stress always precedes cytotoxic stress. A study of Pierre et al [17] shows that addition of antioxidants to the heme diet to lower oxidative stress, prevents all detrimental effects of heme in the colon. Besides lowering oxidative stress, antioxidants also prevented the heme-induced cytotoxicity. Heme-induced oxidative and cytotoxic stress were both also prevented by replacing polyunsaturated fat by monounsaturated fat [17] and by adding chlorophyll to the diet [18,19].

From previous studies it is known that not heme in its native form injures the enterocytes, but heme is converted in the gut to a toxic metabolite causing cell injury [12]. This toxic heme factor is a covalently modified porphyrin [12] with a molecular weight higher than that of heme [19]. It is hard to identify its exact structure as the cytotoxic molecule (or molecules) is refractory to ionization and therefore undetectable by mass spectrometry [19]. It was suggested that the formation of the toxic factor is radical catalyzed [12]. Diets supplemented with porphyrin or iron (which are the constituents of heme) or bilirubin (the major breakdown product of heme) did not induce cytotoxicity or hyperproliferation [12]. Based on the results of the dietary interventions described above we could speculate that heme-induced oxidative stress is causal for the formation of cytotoxicity, and that cytotoxicity is subsequently causing the surface injury leading to compensatory hyperproliferation. The toxic heme metabolite might be formed by the reaction of heme with lipid peroxides formed during ROS reactions (chapter 4). This could explain the lag time observed in the formation of the cytotoxicity, as a certain amount of lipid peroxidation products must be present before they can react with heme. The identification of the cytotoxic heme factor was not the purpose of this thesis.



However, it would be useful for future research if the exact structure could be elucidated, as the structure could shed light on the mechanism of formation of the cytotoxic heme factor. In chapter 3 we speculated that the microbiota play a role in the formation of the toxic heme metabolite. The microbial community needs several days to adapt to a change in diet, which could explain the lag time in the induction of cytotoxicity. The microbial composition indeed changed on the heme-diet (chapter 5), but there was no major role for bacteria in the formation of cytotoxicity (chapter 6). The lag time in cytotoxicity can therefore not be explained by the change in microbiota.

### **Apoptosis and hyperproliferation**

Besides increasing proliferation, heme induced inhibition of apoptosis (chapter 2) contributing to the increased amount of cells per crypt. Several apoptosis inhibitors were upregulated at the surface epithelium (Xiap, Bcl2l1 and Ier3) and in the crypt (Birc5). Remarkable, in chapter 4 we saw Birc5 differentially expressed at day 4, so before the increase in cytotoxicity and induction of hyperproliferation. This might suggest that inhibition of apoptosis occurred before induction of hyperproliferation, implying that ROS stress, rather than cytotoxic stress, is responsible for apoptosis inhibition. It is also possible that our cytotoxicity assay was not sensitive enough to detect a possible small increase in cytotoxicity at day 4, which could have induced apoptosis inhibition. The necrosis inducer Ripk3 was slightly induced at day 4, but differentially expressed after day 4, indicating that epithelial cells die predominantly by necrosis after day 4 [20].

### **Stem cells and enteroendocrine cells**

In the colon, new cells originate from stem cells in the crypts [21]. Several genetic markers identify these stem cells, such as Lgr5, Ascl2, Sox4, Sox9, Cd44 and Ephb3 [22]. Heme significantly downregulated the expression of these stem cell markers except for Cd44 (Figure 1) in the colon scrapings from the study described in chapter 2. Using LCM we confirmed that these markers were higher expressed in crypts than in surface epithelium. First we thought that the downregulation of stem cell markers could be a dilution effect due to the 2-fold increase in the total number of cells per crypt, which decreases the relative contribution of the stem cells. However, heme downregulated the expression of Lgr5 and Ascl2 specifically in the crypts (Figure 1), excluding a dilution effect. We speculate that due to the high proliferation rate the a-symmetrical proliferation in crypts becomes symmetrical and leads to the loss of stem cells. Another possibility is that Lgr5 and Ascl2 expression levels are lower due to the high proliferation rate. The study described in chapter 4 showed that the expression of stem-cell markers was not decreased when 0.2  $\mu\text{mol}$  heme/g heme was given. This dosage did induce hyperproliferation implying that the downregulated expression of stem cell markers is not causal for hyperproliferation and might be dose-dependent.

The expression of enteroendocrine cell markers (such as chromogranin A and B, tryptophan hydroxylase 1 (Tph1) and P-selectin) as well as the number of enteroendocrine cells (chapter 2) was lowered upon heme feeding (both in 0.2 and 0.5  $\mu\text{mol}$  heme/g). In the time course experiment (chapter 4) it was observed that the downregulation of enteroendocrine markers coincided with the induction of hyperproliferation. However, the enteroendocrine cell markers were also downregulated by heme plus Abx when no hyperproliferation was observed (chapter 6). This indicates that the lower number of enteroendocrine cells are not a consequence of the higher proliferation rate and the subsequent lower differentiation time for cells, as was suggested in the discussion of chapter 2. Tph1 is the rate-limiting enzyme in serotonin production. Tph1 expression was downregulated by heme in all experiments, which most probable lowered serotonin levels. Imbalances in serotonin levels are associated with various gastrointestinal disorders [23]. The role of serotonin in heme-induced hyperproliferation is subject for future research. Preliminary analysis showed a decrease in serotonin levels in the mucosa and in feces of heme treated mice, but that was not reproducible in a later analysis. This lack of analytical reproducibility requires further investigation.

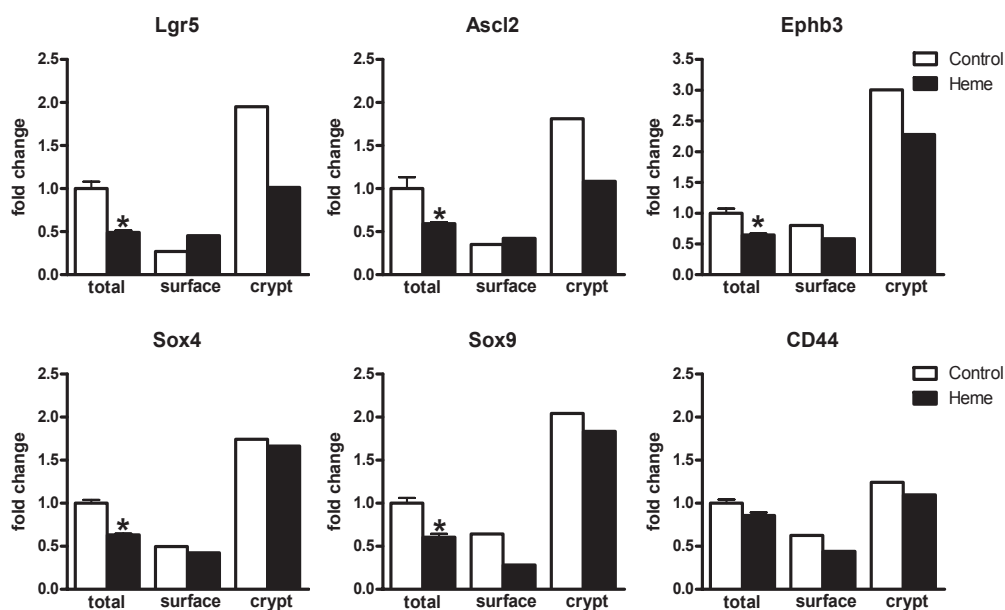


**Figure 1.** Expression levels of crypt cell markers in total scrapings, in surface and crypt cells. Expression levels of total scrapings are based on microarray analysis of individual mice ( $n=7$  control and  $n=9$  heme-fed mice) as described in chapter 2. \*  $q<0.01$ . Surface- and crypt-specific microarray gene expression profiles are obtained from pooled tissue samples obtained by laser capture microdissection ( $n=4$  controls,  $n=3$  heme-fed mice). Surface and crypt expression values are normalized for the expression of total scrapings in control mice.

## **The role of microbiota and the mucus barrier in heme-induced hyperproliferation**

In chapter 5 we showed that there is no direct role for the microbiota in the surface to crypt signaling, as the changed microbial composition did not elicit functional changes in host microbe cross-talk. That microbiota did somehow play a crucial role in the heme-induced hyperproliferation was shown in chapter 6. When Abx was given simultaneously with the heme diet, cytotoxicity was increased but hyperproliferation was not induced. There was a difference in the sensing of the cytotoxicity in the heme versus the heme with Abx group, which suggested a role for the microbiota in determining the mucus barrier function. This is very plausible as microbiota influence many properties of the protective mucus layer [24,25].

If the mucus barrier is indeed limiting heme-induced cytotoxicity, mice that have no mucus barrier should develop higher levels of compensatory hyperproliferation on the heme diet. Moreover, if bacteria facilitate the heme-induced hyperproliferation by degrading the mucus layer, this would imply that Abx treatment does no longer protect against heme induced hyperproliferation in the absence of the mucus barrier. Mucin (Muc) 2 knockout mice could be used to study the importance of the mucus barrier on a heme diet. Muc2 is an important secreted mucin which is the major constituent of the outer mucus layer. Muc2 KO mice spontaneously develop colitis and hyperproliferation, indicating the importance of Muc2 for colonic protection [26]. It should be kept in mind that in Muc2 KO mice the membrane bound mucus layer, consisting of e.g. Muc1, 3, 4 and 13, might still be present.

Another way to study the possible protective role of the mucus layer is to fix colon tissue in such a way that mucin stays intact (e.g. Carnoy's fixation). One can stain the mucus layer itself, or stain the bacteria by FISH (Fluorescent In Situ Hybridization) with bacterial probes. Subsequently the distance from the bacteria to the surface epithelial cells can be visualized and the permeability of the mucus layer for bacteria can be determined. Unfortunately, this method does not indicate whether the toxic heme factor which is much smaller than bacteria can reach the surface epithelium.

If bacteria indeed play a major role in determining the thickness and the permeability of the mucus layer, it is beneficial to think of strategies to modulate the colon microbiota in a way that the mucin degradation and rebuilding capacity is well balanced. One could think of 'feeding' bacteria with other components than mucins, such as slow fermentable fibers (e.g. wheat bran), so that microbiota use the fibers instead of mucins as substrate. Modulating the properties of the mucus layer is not only interesting in relation to colon cancer, but also for other diseases such as inflammatory bowel disease.

## Differences between small intestine and colon

Although the length of the small intestine is several times that of the colon, the chance to develop cancer in the small intestine is much lower than the chance to develop colon cancer [27]. Somehow there must be a difference between the small- and large intestinal physiology that influences this difference in cancer risk. There are differences in the contents of the small intestine versus the colon (differences in e.g. bile acid profiles; in the abundance of microbes; in microbial composition and in bacterial metabolites). Besides, there can be differences in the mucosa (difference in e.g. cell types; in gene expression; in cell cycle regulation and in the immune system). From our studies we know that heme has different effects in the colon compared to the small intestine. Addition of heme to the diet induces hyperproliferation in rat colon, but not in small intestine [11], which we could confirm in our mice studies. From the study described in chapter 2 we also collected ileal scrapings (n=9 per group) and these were analyzed by microarray in a similar way as described for colon scrapings in chapter 2. Genes significantly induced by heme in the small intestine (1,218), in the colon (2,366) or in both (1,338) are visualized in Figure 2. Heme induced oxidative stress in both the small intestine as well as in the colon. This is illustrated by the activation of the transcription factor Nrf2 (Nfe2l2) playing a role in the antioxidant response. Furthermore, targets of Nrf2, such as Catalase (Cat) and Glutamate-cysteine ligase (Gclc) were upregulated in small intestine and colon (Figure 3A). Oxidative stress induced the production of lipid peroxidation products which activated several PPARs in small intestine and colon. Specifically in the colon, heme activated several oncogenes (e.g. Myc, E2f1, Foxm1 and Tbx2) and inhibited tumor suppressors (e.g. Cdkn2a, Tp53, Smarcb1, Rb1). Colonocytes sensed cytotoxicity, as shown by the colon specific induction of Birc5 and Ripk3 (Figure 3B). Furthermore, colonic hyperproliferation was induced, shown by the colon specific induction of Ki67 and Ccna2. Cytotoxicity sensing and hyperproliferation were not observed in the small intestine. This suggests that the toxic heme factor is formed in the colon, which is in line with our previous study [11]. It is relevant to further study differences in mucosal response to heme in both the small intestine versus the colon to get more insight in the mechanisms of heme-induced hyperproliferation and the increased colon cancer risk.

Differences between the small intestine and colon in expression of the putative heme [28] and folate [29,30,31,32] transporter Slc46a1 were also present. Slc46a1 was higher expressed in colon than in small intestine, while most heme uptake occurs in the small intestine. We like to speculate that there might be an alternative heme uptake route via the vitamin B12 transporter cubilin. The structure of vitamin B12 is very similar to that of heme. In the digestive tract vitamin B12 is bound to intrinsic factor which is required for vitamin B12 uptake. The vitamin B12-intrinsic factor complex is taken up by cubilin in the distal small intestine [33]. We found cubilin also expressed in the

colon, although expression levels were higher in small intestine. Heme significantly downregulated cubilin expression in the small intestine (data not shown). In the colon, cubilin is one of the most downregulated genes by heme. The study of Waxman et al. [34] shows that when heme is consumed together with intrinsic factor, an increased heme uptake is observed. Therefore, we like to speculate that cubilin is besides a vitamin B12 receptor also a heme transporter contributing to heme uptake in the small intestine and potentially also in the proximal colon.

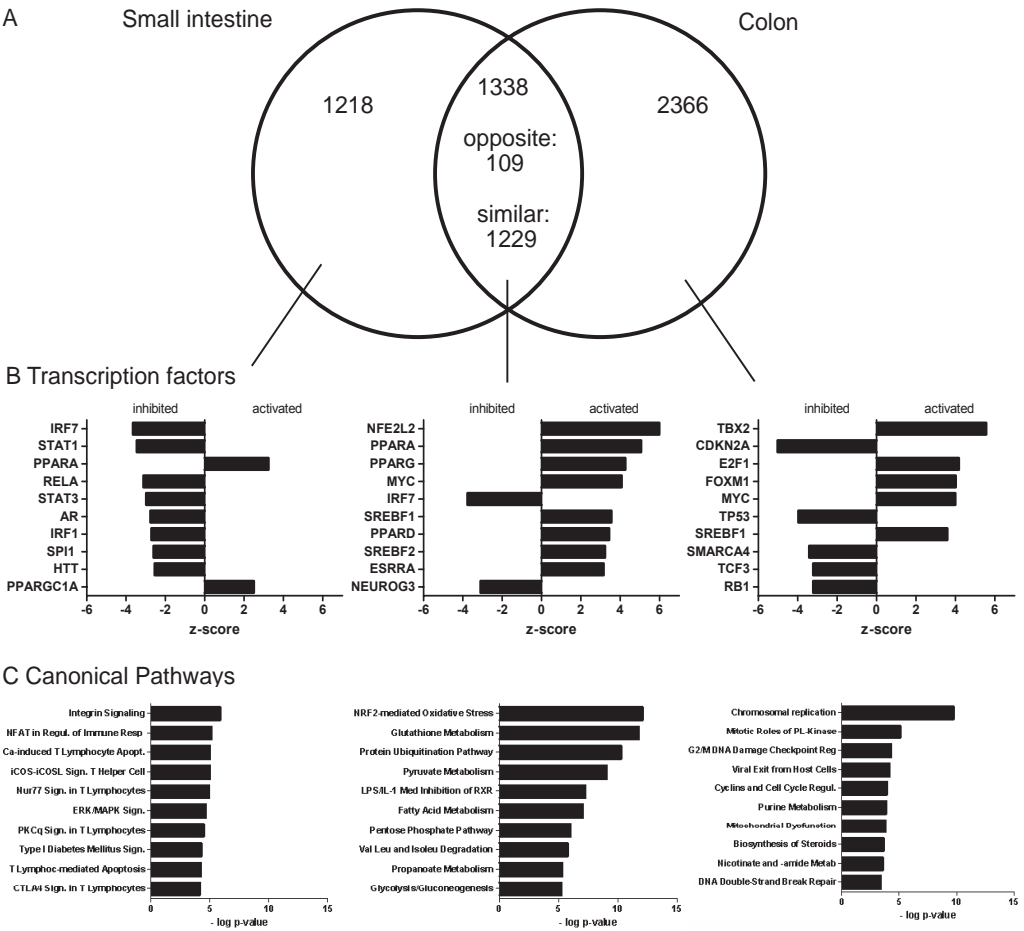


**Figure 2.** Overview of heme-induced genes in the small intestine, in the colon or in both. A. Venn-diagram showing the numbers of small intestine and colon specific regulated genes and the number of overlapping genes ( $q < 0.01$ ). B. Ingenuity analysis showing the activated or inhibited transcription factors (which have a z-score higher than 2 and a p-value  $< 0.05$ ) in both gut segments separately and in the overlap. Note that transcription factors activated in different segments include different target genes. C. Ingenuity analysis of most significant changed canonical pathways.

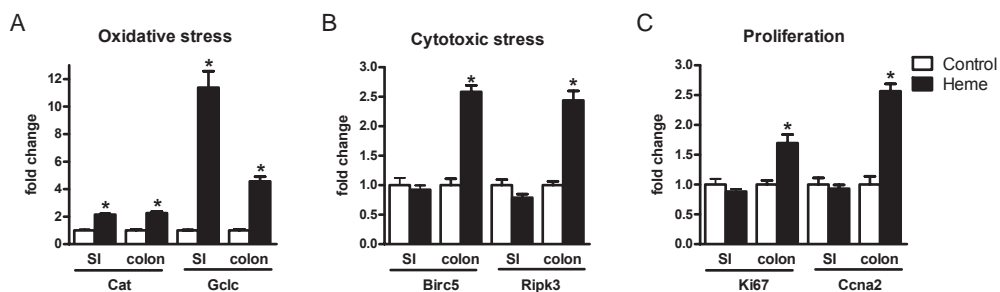


**Figure 3.** Expression levels of oxidative stress markers Cat and Gclc (A) cytotoxicity sensing genes Birc5 and Ripk3 (B) and proliferation markers Ki67 and Ccna2 (C). Expression levels of control groups are set at one. Expression of the heme groups is relative to the controls. Data are represented as mean  $\pm$  SEM,  $n=9$  for heme and control small intestine,  $n=7$  for heme colon,  $n=7$  for control colon). \*  $p < 0.01$ .

## Relevance to human studies

The heme-induced aberrant turnover of crypt cells observed in the studies described in this thesis were observed and identical for 2 mouse strains; C57BL6/J mice (chapters 2, 4, 5 and 6) and SV129 mice (chapter 3). This aberrant turnover is identical to that induced by heme in rats [35], suggesting that this heme effect is species independent. This is further supported by the finding that the protective effect of chlorophyll against heme in rats is also observed in epidemiological studies in humans [6]. Besides, microbiota changes upon heme consumption for human and mice (chapter 5) show similarities, such as the increase in several *Bacteroides* species [36,37]. This suggests that the mechanisms described in this thesis can be extrapolated to humans.

We tried to mimic the human situation as much as possible in our experiments. A physiological relevant dose of heme was taken. The dose of 0.2  $\mu\text{mol/g}$  heme used in chapter 4 for mice equals a daily intake of approximately 160 g of red meat for humans. Besides, the heme diet was a 'Western' purified high fat diet which mimics the diet of the Western human population. Moreover, the bile acid composition of mice is different from that of humans, with a higher amount of taurine conjugated bile acids in mice [38] compared to men [39]. Therefore, cysteine levels were kept low in the diets of mice to lower the taurine conjugation and increase the glycine conjugation of bile acids. To make sure that these lower cysteine levels did not influence the heme-induced hyperproliferation, a pilot study was performed in which cysteine was added to the diet with 0.5  $\mu\text{mol heme/g}$  and there was no difference in heme-induced hyperproliferation. The post-prandial pH of the stomach of rodents is between 4.5 and 5 [40] while this is between 2 and 2.5 in humans [41]. The pH in the stomach of rodents is thus more alkaline than the pH optimum for pepsin, implying that gastric protein denaturation and digestion is less efficient in rodents compared to humans. To control for that hemin instead of meat protein or haemoglobin was added to the diet. Furthermore, diets were

low in fibers, as the Western diet does not contain much fiber. This is of relevance for the microbiota, which uses the mucus layer as a substrate when no fermentable fibers are present in the diet.

Our results may have implications for future epidemiological studies investigating the association between red meat and colorectal cancer risk. Previously, several confounders that can modify this association were identified. Calcium and chlorophyll intake should be taken into account as these components protect against the deleterious effects of heme [11,19] and might therefore modify the association. Besides, antioxidant intake can have an effect [17]. We speculate based on the results described in chapter 6 that also microbiota composition and fiber intake can influence the association between red meat consumption and colorectal cancer risk. A recently published study suggests that in humans 3 main microbial profiles, so-called 'enterotypes' exist [42]. Two of those enterotypes are dominated by mucin degrading bacteria. As we found that the mucin barrier is an important player in the heme-induced hyperproliferation, it would be of interest to see if there are differences in colon cancer risk between these 3 enterotypes.

There is evidence that processed meat increases the risk of colon cancer to a larger extent than red meat [1] and it is thus advised to limit the intake of red meat and to avoid processed meats. It is hard to investigate the association between processed meat and colorectal cancer as there is no clear definition of processed meats [1]. Processed meat is commonly used to refer to meat, usually red meat, which is salted, cured, smoked or to which preservatives are added [1]. However, these different processing methods can have different effects on colorectal cancer risk. The unclear definition can bias the outcome of epidemiological studies. Both red and processed meats contain heme, which could explain their association with an increased cancer risk. There is not much known about white processed meat and the risk of colon cancer [1]. It is interesting to study the possible differential association of red and white processed meat with colon cancer risk, as this could shed light on whether the processing itself, or heme can be responsible for the observed association. When studying this, it is important to consider the total meal composition. If one consumes heme together with calcium or chlorophyll, heme will no longer exert its detrimental effects on the mucosa [11,19]. We suggest that red meat might be consumed more often as part of a complete meal, so in the presence of vegetables which contain chlorophyll and fibers, while processed meats might be eaten as a snack between meals or on a sandwich. These differences in meal composition could influence associations between red or processed meat and colorectal cancer. It is important to get more insight in the differences between red and processed meat intake and their association with colorectal cancer risk to eventually provide solid dietary recommendations for red and processed meat consumption.



## REFERENCES

- 1 World Cancer Research Fund. Food, Nutrition, Physical Activity and the Prevention of Cancer: a Global Perspective. Washington, DC: American Institute for Cancer Research, 2007.
- 2 Larsson SC, Wolk A. Meat consumption and risk of colorectal cancer: a meta-analysis of prospective studies. *Int J Cancer* 2006;119:2657-64.
- 3 Norat T, Bingham S, et al. Meat, fish, and colorectal cancer risk: the European Prospective Investigation into cancer and nutrition. *J Natl Cancer Inst* 2005;97:906-16.
- 4 Giovannucci E, Rimm EB, et al. Intake of fat, meat, and fiber in relation to risk of colon cancer in men. *Cancer Res* 1994;54:2390-7.
- 5 Larsson SC, Rafter J, et al. Red meat consumption and risk of cancers of the proximal colon, distal colon and rectum: the Swedish Mammography Cohort. *Int J Cancer* 2005;113:829-34.
- 6 Balder HF, Vogel J, et al. Heme and chlorophyll intake and risk of colorectal cancer in the Netherlands cohort study. *Cancer Epidemiol Biomarkers Prev* 2006;15:717-25.
- 7 Lee DH, Anderson KE, et al. Heme iron, zinc, alcohol consumption, and colon cancer: Iowa Women's Health Study. *J Natl Cancer Inst* 2004;96:403-7.
- 8 Latunde-Dada GO, Simpson RJ, et al. Recent advances in mammalian haem transport. *Trends Biochem Sci* 2006;31:182-8.
- 9 Kumar S, Bandyopadhyay U. Free heme toxicity and its detoxification systems in human. *Toxicol Lett* 2005;157:175-88.
- 10 Young G, Rose I, et al. Haem in the gut. I. Fate of haemoproteins and the absorption of haem. *J Gastroenterol Hepatol* 1989;4:537-45.
- 11 Sesink AL, Termont DS, et al. Red meat and colon cancer: dietary haem-induced colonic cytotoxicity and epithelial hyperproliferation are inhibited by calcium. *Carcinogenesis* 2001;22:1653-9.
- 12 Sesink AL, Termont DS, et al. Red meat and colon cancer: the cytotoxic and hyperproliferative effects of dietary heme. *Cancer Res* 1999;59:5704-9.
- 13 Hall PA, Coates PJ, et al. Regulation of cell number in the mammalian gastrointestinal tract: the importance of apoptosis. *J Cell Sci* 1994;107 (Pt 12):3569-77.
- 14 Anderson P, Kedersha N. Stress granules: the Tao of RNA triage. *Trends Biochem Sci* 2008;33:141-50.
- 15 Sonenberg N, Hinnebusch AG. Regulation of translation initiation in eukaryotes: mechanisms and biological targets. *Cell* 2009;136:731-45.
- 16 Gu S, Kay MA. How do miRNAs mediate translational repression? *Silence* 2010;1:11.
- 17 Pierre F, Tache S, et al. Meat and cancer: haemoglobin and haemin in a low-calcium diet promote colorectal carcinogenesis at the aberrant crypt stage in rats. *Carcinogenesis* 2003;24:1683-90.
- 18 de Vogel J, Jonker-Termont DS, et al. Natural chlorophyll but not chlorophyllin prevents heme-induced cytotoxic and hyperproliferative effects in rat colon. *J Nutr* 2005;135:1995-2000.
- 19 de Vogel J, Jonker-Termont DS, et al. Green vegetables, red meat and colon cancer: chlorophyll prevents the cytotoxic and hyperproliferative effects of haem in rat colon. *Carcinogenesis* 2005;26:387-93.
- 20 Vandenabeele P, Declercq W, et al. The role of the kinases RIP1 and RIP3 in TNF-induced necrosis. *Science signaling* 2010;3:re4.
- 21 Cheng H, Leblond CP. Origin, differentiation and renewal of the four main epithelial cell types in the mouse small intestine. V. Unitarian Theory of the origin of the four epithelial cell types. *Am J Anat* 1974;141:537-61.
- 22 Itzkovitz S, Lyubimova A, et al. Single-molecule transcript counting of stem-cell markers in the mouse intestine. *Nat Cell Biol* 2012;14:106-U93.
- 23 Keszthelyi D, Troost FJ, et al. Understanding the role of tryptophan and serotonin metabolism in gastrointestinal function. *Neurogastroenterol Motil* 2009;21:1239-49.
- 24 Szentkuti L, Riedesel H, et al. Pre-epithelial mucus layer in the colon of conventional and germ-free rats. *The Histochemical journal* 1990;22:491-7.



- 25 Wlodarska M, Willing B, et al. Antibiotic treatment alters the colonic mucus layer and predisposes the host to exacerbated *Citrobacter rodentium*-induced colitis. *Infection and immunity* 2011;79:1536-45.
- 26 Van der Sluis M, De Koning BA, et al. Muc2-deficient mice spontaneously develop colitis, indicating that MUC2 is critical for colonic protection. *Gastroenterology* 2006;131:117-29.
- 27 Jemal A, Siegel R, et al. Cancer statistics, 2010. *CA: a cancer journal for clinicians* 2010;60:277-300.
- 28 Shayeghi M, Latunde-Dada GO, et al. Identification of an intestinal heme transporter. *Cell* 2005;122:789-801.
- 29 Zhao R, Diop-Bove N, et al. Mechanisms of membrane transport of folates into cells and across epithelia. *Annu Rev Nutr* 2011;31:177-201.
- 30 West AR, Oates PS. Mechanisms of heme iron absorption: current questions and controversies. *World J Gastroenterol* 2008;14:4101-10.
- 31 Andrews NC. When is a heme transporter not a heme transporter? When it's a folate transporter. *Cell Metab* 2007;5:5-6.
- 32 Laftah AH, Latunde-Dada GO, et al. Haem and folate transport by proton-coupled folate transporter/haem carrier protein 1 (SLC46A1). *Br J Nutr* 2009;101:1150-6.
- 33 Kozyraki R. Cubilin, a multifunctional epithelial receptor: an overview. *J Mol Med (Berl)* 2001;79:161-7.
- 34 Waxman S, Pratt P, et al. Malabsorption of hemoglobin iron in pernicious anemia: correction with intrinsic factor--containing substances. *J Clin Invest* 1968;47:1819-25.
- 35 de Vogel J, van-Eck WB, et al. Dietary heme injures surface epithelium resulting in hyperproliferation, inhibition of apoptosis and crypt hyperplasia in rat colon. *Carcinogenesis* 2008;29:398-403.
- 36 Maier BR, Flynn MA, et al. Effects of a high-beef diet on bowel flora: a preliminary report. *Am J Clin Nutr* 1974;27:1470-4.
- 37 Zimmer J, Lange B, et al. A vegan or vegetarian diet substantially alters the human colonic faecal microbiota. *European journal of clinical nutrition* 2011.
- 38 Alnouti Y, Csanaky IL, et al. Quantitative-profiling of bile acids and their conjugates in mouse liver, bile, plasma, and urine using LC-MS/MS. *J Chromatogr B Analyt Technol Biomed Life Sci* 2008;873:209-17.
- 39 Sjovall J. Bile Acids in Man under Normal and Pathological Conditions Bile Acids and Steroids-73. *Clinica Chimica Acta* 1960;5:33-41.
- 40 Sprong RC, Hulstein MF, et al. High intake of milk fat inhibits intestinal colonization of *Listeria* but not of *Salmonella* in rats. *J Nutr* 1999;129:1382-9.
- 41 Fordtran JS, Locklear TW. Ionic constituents and osmolality of gastric and small-intestinal fluids after eating. *Am J Dig Dis* 1966;11:503-21.
- 42 Arumugam M, Raes J, et al. Enterotypes of the human gut microbiome. *Nature* 2011;473:174-80.



# Summary

Colorectal cancer is a leading cause of cancer deaths in Western countries. The risk to develop colorectal cancer is associated with the intake of red meat. Red meat contains the porphyrin pigment heme. Heme is an irritant for the colonic wall and it is previously shown that the addition of heme to the diet of rats induces hyperproliferation. Hyperproliferation increases the risk of endogenous mutations, which subsequently increases the risk to develop colon cancer. The aim of this thesis was to elucidate the diet-modulated signaling from an injured surface epithelium to the proliferative stem cells in the crypt to initiate compensatory hyperproliferation.

In chapter 2 we showed that when heme is added to the diet of mice, there is an increased cytotoxicity of the colonic contents. Heme-fed mice showed decreased apoptosis and increased compensatory epithelial hyperproliferation resulting in hyperplasia. Gene expression levels of mouse colon after heme feeding were analyzed by microarrays and showed 3,710 differentially expressed genes ( $q < 0.01$ ) of which many were involved in proliferation and stress response. Stainings for the enzyme Heme oxygenase-1 and expression levels of heme- and stress-related genes showed that heme affected the epithelial surface cells, but that heme did not reach the crypt cells. Heme caused injury of the surface epithelial cells, and as proliferation originates from the stem cells in the crypts this implied that there must be a signaling mechanism from the injured surface to the stem cells in the crypts to start the hyperproliferation. In chapter 2 several surface to crypt signaling molecules were identified. Heme downregulated inhibitors of proliferation, such as Wnt inhibitory factor 1, Indian hedgehog and Bone morphogenetic protein 2. Furthermore, heme downregulated the cytokine Interleukin-15. Heme upregulated the expression of the growth factors Amphiregulin, Epiregulin and of Cyclooxygenase-2 mRNA in the surface. However, their protein/metabolite levels were not increased as heme induced surface-specific inhibition of translation by increasing the levels of the translation inhibitor 4E-BP1. We concluded that heme induced colonic hyperproliferation and hyperplasia by downregulating the surface to crypt signaling of feedback inhibitors of proliferation.

Besides many proliferation and stress-related genes, many PPAR $\alpha$  target genes were upregulated upon heme feeding. As PPAR $\alpha$  is proposed to protect against oxidative stress and lipid peroxidation, we hypothesized in chapter 3 that absence of PPAR $\alpha$  leads to more colonic surface injury, which subsequently leads to increased compensatory hyperproliferation in colonic crypts upon heme-feeding. This hypothesis was tested using wild-type and PPAR $\alpha$  knockout mice receiving a heme diet. Proliferation levels and gene expression profiles were determined. Heme induced luminal cytotoxicity and lipid peroxidation to the same extent in wild-type and PPAR $\alpha$  knockout mice. We showed that PPAR $\alpha$  does not play a role in the heme-induced hyperproliferation, as heme induced hyperproliferation both in wild-type as well as in PPAR $\alpha$  knockout mice. Stainings for alkaline phosphatase activity and expression levels of Vanin-1 and Nrf2-targets

indicated a compromised antioxidant defense in the heme-fed PPAR $\alpha$  knockout mice. We concluded that PPAR $\alpha$  plays a protective role in colon against oxidative stress, but PPAR $\alpha$  does not mediate heme-induced hyperproliferation. This implied that oxidative stress of surface cells is not the main determinant of heme-induced hyperproliferation and hyperplasia.

Heme was shown to increase both reactive oxygen species as well as cytotoxicity of the colonic contents of mice. So far, the time dependency of the heme-induced oxidative stress and cytotoxic stress on the initiation of hyperproliferation was not studied. Therefore, in chapter 4 the effects of dietary heme on the colonic mucosa after 2, 4, 7 and 14 days of heme feeding were determined. This study showed that the effects of dietary heme on the colonic mucosa can be separated in acute and delayed effects. Acutely, heme increased oxidative stress which caused an increase in lipid peroxidation products. Besides, there was an acute activation of PPAR $\alpha$  target genes, most probable induced by the generated oxidized lipids. Nrf2 target genes were activated acutely which played a role in the protection against oxidative stress. Delayed effects which occurred after day 4 of heme feeding, were increased luminal cytotoxicity and the induction of hyperproliferation. This suggested that the cytotoxicity, rather than oxidative stress, induced hyperproliferation. Remarkably, the surface epithelial cells sensed heme after day 4, although heme was present in the colon several hours after ingestion of the heme diet. This suggested that the mucus barrier played a role in the protection of the surface epithelium the first days of heme feeding.

As the colon is densely populated by bacteria, the microbiota might play a role in modulating the surface to crypt signaling inducing hyperproliferation. To explore the role of the colonic microbiota we simultaneously investigated the effects of dietary heme on colonic microbiota and on the host mucosa of mice (chapter 5). Using 16S rRNA phylogenetic microarrays, it was determined that heme increased Bacteroidetes and decreased Firmicutes in colonic contents. This shift in the microbiota was most likely caused by a selective susceptibility of Gram-positive bacteria to heme cytotoxic fecal water. This susceptibility was not observed for Gram-negative bacteria and allowed the expansion of the Gram-negative community. The increased amount of Gram-negative bacteria, which likely caused an increased mucosal exposure to lipopolysaccharide (LPS), did not elicit a detectable immune reaction in the host mucosa. The absence of an immune reaction might be influenced by the strong upregulation of Secretory leukocyte peptidase inhibitor (Slpi) at gene and protein level, which is known to suppress excessive immune reactions. We showed that there was no functional change in the sensing of the bacteria by the mucosa, as changes in inflammation pathways and Toll- like receptor signaling were not detected. In conclusion, the change in microbiota did not cause the observed hyperproliferation and hyperplasia via inflammation pathways.

In the study described in chapter 6 we investigated whether microbiota play a causal role in the heme-induced hyperproliferation. In this study mice received a control or a heme diet with or without broad spectrum antibiotics (Abx). Similar to previous experiments, heme induced epithelial hyperproliferation. Interestingly, when heme was administered together with Abx there was no induction of hyperproliferation. Heme induced oxidative stress in the heme group as well as in the heme plus Abx group. Cytotoxicity was also induced in both heme groups. As bacteria were decreased by 100 to 1000 fold in abundance upon Abx treatment it is unlikely that bacteria play a major role in the formation of the cytotoxic factor. Whole genome transcriptomics showed that Abx blocked the heme-induced differential expression of oncogenes, tumor suppressors and cell turnover genes. Moreover, Abx blocked the mucosal sensing of luminal cytotoxicity indicating that Abx increased the mucus barrier. Abx eliminated mucin-degrading bacteria, such as *Akkermansia*, and sulfate-reducing bacteria (SRBs) that produce sulfide. In-vitro studies showed that sulfide is more potent than N-acetylcysteine and cysteine in splitting disulfide bonds, indicating that SRB generated sulfide can denature mucins and thus open the mucus barrier. This study showed that the microbiota plays an important facilitating role in the heme-induced hyperproliferation and hyperplasia by breaking the mucus barrier and thereby decreasing the protection against luminal irritants such as the toxic heme metabolite.

# Samenvatting

Dikke darmkanker is een van de belangrijkste oorzaken van kankersterfte in de Westerse wereld. In Nederland wordt jaarlijks bij ongeveer 11.000 mensen dikke darmkanker vastgesteld en daarvan overlijden er jaarlijks 5.000. Het ontstaan van darmkanker hangt voor een klein deel af van erfelijke factoren en voor een veel groter deel van omgevingsfactoren, zoals voeding. Het eten van rood vlees verhoogt de kans op het ontstaan van darmkanker. Eten van wit vlees (zoals kip en vis) verhoogt dit risico echter niet. Rood vlees bevat het rode pigment heem. Het heem molecuul bevat ijzer en is van belang voor zuurstoftransport. Heem is een stof die slecht wordt opgenomen in de dunne darm met als gevolg dat een groot deel van het heem terechtkomt in de dikke darm.

Dewandvandedikkedarmisgeplooid. Aan het darmoppervlak zitten de oppervlaktecellen die in contact komen met de niet-geabsorbeerde voedingscomponenten. Onderin de plooien (crypten) bevinden zich de cryptcellen waarin de celdeling plaatsvindt. Normaal gesproken is de celdeling een goed gecontroleerd proces en is het aantal delende cellen in de crypt in balans met het aantal afstervende cellen aan het oppervlak. Echter, uit eerdere studies in ratten blijkt dat deze balans wordt verstoord als er heem in de darm komt. Heem irriteert en beschadigt de oppervlaktecellen in de dikke darm. Deze cellen gaan dood en moeten vervangen worden om er voor te zorgen dat er geen gaten in het darmepitheel vallen en daartoe wordt de celdeling in de crypt verhoogd. Bij een verhoogde celdeling neemt de kans op het ontstaan van mutaties (fouten) in het DNA toe. Daarnaast is er ook minder tijd om de ontstane mutaties te repareren. Een opeenstapeling van mutaties kan dan leiden tot een ongeremde groei van cellen waardoor een tumor kan ontstaan.

Het doel van mijn onderzoek was om uit te zoeken hoe beschadigde oppervlaktecellen die in contact komen met niet geabsorbeerde voedingscomponenten, zoals heem, kunnen signaleren naar de cryptcellen waar de celdeling plaatsvindt om vervolgens die celdeling te verhogen (zie voor een schematische weergave Figuur 2 van de introductie). Omdat je dit onderzoek niet zomaar bij mensen kunt uitvoeren is er een diermodel gebruikt. Muizen krijgen heem toegevoegd aan hun voeding gedurende 14 dagen. In hoofdstuk 2 van dit proefschrift hebben we laten zien dat wanneer je heem toevoegt aan het dieet van muizen dit, net als bij ratten, een meer toxische en irriterende darminhoud veroorzaakt wat leidde tot beschadiging en dood van oppervlaktecellen. Vervolgens ontstond er een verhoogde celdeling om de beschadigde cellen te vervangen. De balans tussen het aantal dode cellen en de nieuwgevormde cellen was verstoord en dit veroorzaakte een overproductie van nieuwe cellen. Vervolgens ontstonden er diepere crypten met meer cellen.

Alle cellen bevatten DNA waarin de genetische informatie ligt opgeslagen in ongeveer 30.000 genen. Genen bevatten de informatie die nodig is om eiwitten te maken die bij allerlei processen in de cel een rol spelen. Om van een gen tot een eiwit te komen



wordt er eerst een kopie gemaakt van het DNA van het gen. Deze kopie noemen we messenger(boodschapper)-RNA (mRNA) en dit mRNA kan vervolgens worden vertaald naar eiwit. Het aantal mRNA kopieën van een gen is een maat voor de activiteit (expressie) van dat gen en voorspelt de hoeveelheid van bepaalde eiwitten in de cel. Door gebruik te maken van een soort chips, de zogenaamde microarrays, kunnen we het aantal mRNA kopieën van een gen en daarmee de genexpressie bepalen. Een bepaalde behandeling (zoals in dit proefschrift een voeding waaraan heem is toegevoegd) kan de expressie van genen en daarmee de aanmaak van eiwitten in een cel beïnvloeden. In de studie beschreven in hoofdstuk 2 hebben we de expressie van genen in darmcellen van muizen, die de heemvoeding hebben gekregen, bekeken. Dat expressieprofiel hebben we vergeleken met dat van muizen op een controlevoeding. Er waren 3.710 genen die verschillend (differentieel) tot expressie kwamen in de dikke darm van muizen die heem toegevoegd hadden gekregen aan hun voeding, ten opzichte van muizen die de controlevoeding zonder heem hebben gekregen. Veel van deze veranderde genen coderen voor eiwitten die een rol spelen in de celdeling of in de stress-respons. Het heem had alleen de oppervlaktecellen direct beschadigd en geen direct beschadigende invloed op cellen in de crypten. Er moet dus een signaal van de beschadigde oppervlaktecellen naar de cryptcellen gaan om de celdeling te verhogen. Om deze signalering te kunnen bestuderen hebben we in deze studie met behulp van een laser techniek oppervlaktecellen en cryptcellen geïsoleerd en apart onderzocht. We hebben signalen geïdentificeerd die van de beschadigde oppervlaktecellen naar de cryptcellen signaleren om de celdeling te verhogen (zie Figuur 5B in hoofdstuk 2). Deze eiwitsignalen zijn Indian hedgehog, Bone morphogenetic protein 2, Wnt inhibitory factor 1 en Interleukin-15. Deze signalen zijn in staat om de celdeling te remmen als er genoeg gezonde cellen zijn. Echter, als deze signalen wegvallen, omdat heem de oppervlaktecellen beschadigt, dan wordt de celdeling niet langer door deze moleculen geremd. De celdeling gaat dan ongeremd door en dit verhoogt de kans op het ontstaan van darmkanker. Met dit onderzoek is inzicht verkregen in het mechanisme waardoor de voedingscomponent heem de signalering en de celdeling in de dikke darm kan veranderen en daarmee het risico op het ontwikkelen van darmkanker kan verhogen. Een volgende stap is om te onderzoeken of in de mens deze signaalmoleculen ook een zelfde rol spelen in de regulatie van de celdeling in de dikke darm.

Zoals gezegd waren de door heem veranderde genen vooral betrokken bij de celdeling en de reactie op stress. Opmerkelijk was echter dat we ook een groot aantal PPAR $\alpha$  target genen verhoogd tot expressie zagen komen. PPAR $\alpha$  is een transcriptiefactor die de expressie van genen die een rol spelen in vetmetabolisme reguleert. In hoofdstuk 3 hebben we onderzocht of de transcriptiefactor PPAR $\alpha$  een rol speelt in de heem-geïnduceerde verhoogde celdeling. Heem veroorzaakte oxidatieve stress in de dikke darm. Het wordt gesuggereerd in de literatuur dat PPAR $\alpha$  beschermend werkt tegen

reactieve moleculen, de zogenaamde zuurstofradicalen, die worden gemaakt tijdens oxidatieve stress. Muizen die geen PPAR $\alpha$  hebben, ook wel PPAR $\alpha$ -knockout muizen genoemd, zouden dan dus minder goed beschermd zijn tegen oxidatieve stress. Onze hypothese was dat wanneer PPAR $\alpha$  een belangrijke rol speelt in de hyperproliferatie het zo moet zijn dat de PPAR $\alpha$ -knockout muizen op een heemvoeding die minder beschermd zijn, meer schade hebben aan de oppervlaktecellen en dus een hogere compensatoire celdeling moeten ontwikkelen, dan gewone (zogenaamde wild-type) muizen met PPAR $\alpha$  op een heemvoeding. We zagen echter geen verschil in celdeling in de PPAR $\alpha$ -knockout muizen ten opzichten van de wild-type muizen hetgeen betekent dat PPAR $\alpha$  geen rol speelt in de verhoogde celdeling. Wel zagen we door de expressie van bepaalde genen dat PPAR $\alpha$  in de darm een beschermende rol speelt tegen oxidatieve stress, en dat muizen met PPAR $\alpha$  dus beter kunnen omgaan met oxidatieve stress. Dit betekent ook dat de door heem geïnduceerde oxidatieve stress niet de celdeling aanzet, omdat we zagen dat in zowel de knockout als de wild-type dieren de verhoogde celdeling door heem even groot was.

Heem veroorzaakt dus zowel oxidatieve als cytotoxische stress in de dikke darm. Er is echter nooit gekeken naar de tijdsafhankelijkheid van deze processen tijdens het ontstaan van een verhoogde celdeling. Daarom hebben we in hoofdstuk 4 de effecten van de heemvoeding op de darmwand na 2, 4, 7 en 14 dagen bestudeerd. We konden concluderen dat heem een direct en een verlaat effect veroorzaakt. Heem induceerde direct (al op dag 2) een verhoging van de oxidatieve stress en activeerde PPAR $\alpha$ -targetgenen. Op dat moment was er echter nog geen verhoogde celdeling. Pas na 4 dagen consumptie van heemvoeding nam de cytotoxiciteit van de darminhoud toe en werd de verhoogde celdeling gezien. Het lijkt er dus op dat niet de oxidatieve stress maar de cytotoxische stress de verhoogde celdeling aanzet. Opmerkelijk was dat heem een aantal uren na consumptie al in de dikke darm aanwezig was, maar dat het genexpressieprofiel van de oppervlaktecellen liet zien dat deze oppervlaktecellen pas na 4 dagen in contact kwamen met het heem. Dit zou kunnen wijzen op een belangrijke rol voor de slijmlaag (de mucuslaag) in de darm. Deze mucuslaag beschermt de oppervlaktecellen voor niet-geabsorbeerde voedingscomponenten die aanwezig zijn in de darminhoud. Daarnaast beschermt deze laag tegen bacteriën die aanwezig zijn in de darm.

In de dikke darm komen erg veel bacteriën voor. Deze bacteriën (de microbiota genoemd) zouden de signalering van het oppervlak naar de crypt kunnen moduleren. In de studie beschreven in hoofdstuk 5 hebben we de effecten van heem op de samenstelling van de microbiota en op de darmwand gelijktijdig onderzocht. Met speciale chips (arrays) die specifiek bacterieel DNA detecteren hebben we kunnen vaststellen dat heem de Bacteroidetes verhoogde en de Firmicutes verlaagde in de inhoud van de dikke darm. Bacteroidetes zijn zogenaamde Gram-negatieve bacteriën en Firmicutes zijn Gram-positief. Gram-negatieve bacteriën hebben een dubbele celmembraan die lipopolysaccharide (LPS)

bevat. Gram-positieve bacteriën hebben een enkele celmembraan zonder LPS. De door heem veroorzaakte toename van Gram-negatieven en afname van Gram-positieven wordt waarschijnlijk veroorzaakt door een selectieve gevoeligheid van de Gram-positieven voor de cytotoxiciteit. De Gram-negatieven, met hun dubbele celmembraan, bleken niet zo gevoelig voor deze cytotoxiciteit en daardoor kon deze populatie uitgroeien. Het LPS op de celmembraan van Gram-negatieve bacteriën kan een immuun respons aanzetten. Ondanks de sterke toename van Gram-negatieven op de heemvoeding trad er geen immuun respons op in deze muizen. Deze immuun respons kon zijn onderdrukt door de sterke inductie van Secretory leukocyte peptidase inhibitor (Slpi) zowel op gen als eiwit niveau. Verder hebben we gezien dat er geen functionele veranderingen waren in de 'sensing' van de door heem veranderde microbiota. Er waren geen veranderingen in ontstekings-gerelateerde genen of in de activiteit van de zogenaamde Toll-like receptoren die bacteriën kunnen detecteren. Dus we konden concluderen dat de verandering in de microbiota, geïnduceerd door heem, geen verhoogde celdeling veroorzaakte via ontstekingsmechanismen.

Toch sluit het onderzoek beschreven in hoofdstuk 5 niet uit dat de microbiota een causale rol speelt in de heem-geïnduceerde verhoogde celdeling via andere mechanismen. Daarom bestudeerden we in hoofdstuk 6 wat er in de darmwand gebeurde wanneer muizen de heemvoeding kregen maar ze geen tot weinig bacteriën in hun darmen hadden. In deze studie kregen muizen een controledieet of het heemdieet. De helft van de controle en de helft van de heem muizen kregen ook antibiotica in hun drinkwater om de bacteriën in hun darm te doden. Net als in alle voorgaande proeven veroorzaakte heem een verhoogde celdeling. Opmerkelijk was dat wanneer muizen de heemvoeding kregen met antibiotica er geen verhoogde celdeling optrad. Heem veroorzaakte oxidatieve stress in alle heem gevoerde muizen, dus zowel met als zonder antibiotica. Ook de cytotoxiciteit was verhoogd in alle heem gevoerde muizen. Doordat de aantallen bacteriën in de darm met een factor 100 tot 1000 afnamen, maar er nog steeds cytotox was, is het niet aannemelijk dat de bacteriën een grote rol spelen in de vorming van deze toxische factor. Heem veroorzaakte een verandering in tumor-suppressorgenen, oncogenen en in celdelings-gerelateerde genen. Wanneer er echter ook antibiotica werd toegevoegd aan de heemvoeding bleek de verandering in deze genen geblokkeerd te zijn.

Daarnaast blokkeerde antibiotica ook de sensing van de cytotoxiciteit door de darmwand, wat wijst op een verandering in de beschermende slijmlaag van de darm. Antibiotica verlaagde de hoeveelheid van slijm-afbrekende bacteriën zoals *Akkermansia* en van sulfaat-reducerende bacteriën die sulfide produceren. Sulfide kan de disulfide-bindingen, die de slijmlaag stevig houden, afbreken en dus kunnen sulfaat-reducerende bacteriën de slijmlaag openen (zie Figuur 6 in hoofdstuk 6). Deze studie laat zien dat microbiota een rol spelen in de heem-geïnduceerde verhoogde celdeling doordat ze slijmlaag kunnen openbreken en daarmee de beschermende werking van de slijmlaag tegen irriterende stoffen, aanwezig in de darminhoud (zoals het toxische heem) kunnen verlagen.



# Dankwoord

Dit was het dan. Mijn promotieonderzoek zit erop. Nu ben ik 'onthemd'. Op deze plek wil ik graag alle mensen bedanken die hebben bijgedragen aan de totstandkoming van dit proefschrift.

Allereerst wil ik mijn co-promotor Roelof bedanken. Roelof, jij begon ooit met het heem-onderzoek en zoals het gaat met onderzoek; het is nooit af. Helaas zijn met mij als je laatste aio nog lang niet alle vragen beantwoord, maar we hebben toch meer inzicht gekregen in verschillende processen. Jouw kennis is enorm en je kwam vaak enthousiast met nieuwe ideeën en theorieën aanzetten! Meestal moest ik die nieuwe ideeën even laten bezinken en nalezen (liefst in Stryer natuurlijk), maar daarna was ik even enthousiast. Bedankt voor al je suggesties en discussies, maar ook voor je persoonlijke interesse tijdens mijn promotie. Ik hoop dat je samen met Marieke kunt gaan genieten van je pensioen.

Mijn promotor Michael, ik wil je bedanken dat je me de mogelijkheid hebt gegeven om binnen jouw groep te promoveren. Ik heb er erg veel geleerd de afgelopen jaren. Daarnaast bedankt voor alle discussies die we hebben gevoerd en voor je vertrouwen en de vrijheid die je mij en Roelof gaf bij het doen van het onderzoek.

Anneke, wij zijn samen begonnen aan dit project en ik heb zo'n drie jaar met je samen mogen werken. Ik heb erg veel geleerd van onze discussies en van onze experimenten op het lab. Bovendien was het altijd erg gezellig! Fijn dat ik altijd bij je kon binnenlopen met mijn vragen. Bedankt ook nog voor de mooie heem-tegel die zeker met me meegaat naar mijn nieuwe werkplek! Ik hoop dat onze paden elkaar nog eens kruisen.

Nicole, via jou ben ik bij NMG terecht gekomen toen ik mijn bachelorscriptie kwam schrijven. Dat beviel zo goed dat ik twee jaar daarna terug ben gekomen om een afstudeervak te doen. Jij hebt me enthousiast gemaakt voor het moleculaire darmonderzoek. Ik vond het dan ook erg leuk dat we tijdens mijn aio-project veel samen konden werken en samen een studie hebben kunnen uitvoeren wat heeft geresulteerd in een mooi paper! Ook jouw deur stond altijd voor me open. Ik ben je erg dankbaar voor alles wat je al die jaren voor me hebt gedaan.

Jan, jouw kennis over mucines en microbiota is erg waardevol geweest voor het project. Mijn dank daarvoor. Verder is het erg fijn dat wanneer ik een manuscript bij je inlever ik er altijd van op aan kan dat dat snel en tot in detail is nagekeken. Verder wil ik je ook bedanken voor je hulp bij de meer praktische zaken die kwamen kijken bij ons project. Toen ik begon met dit project was de microbiologie voor mij een onbekend veld. Michiel, bedankt voor alles wat je me hebt geleerd en voor je bijdrage aan onze proeven en papers. Denise, jij was altijd vol enthousiasme bezig met het onderzoek. Bedankt voor alle proeven die je hebt gedaan voor dit boekje en voor je betrokkenheid. Jammer dat we het laatste jaar niet meer samen hebben kunnen werken, maar ik wens je alle succes met je nieuwe uitdaging. Arjan, jou wil ik bedanken voor alle werkzaamheden die je van Denise hebt overgenomen. Aloys en Johan wil ik bedanken voor het heem-onderzoek wat zij al hadden gedaan en waar ik op kon voortborduren.

Ik wil de promotiecommissie hartelijk danken voor het beoordelen van dit proefschrift en voor hun aanwezigheid tijdens mijn promotie.

En dan mijn kamergenoten, met jullie was het nooit saai op kamer 0051. Diederik, leuk dat je zo'n 4 jaar geleden mijn kamergenoot werd! Bedankt voor je betrokkenheid, onze discussies en je humor. Ik vind het erg leuk dat je mijn paranimf wilt zijn. En wees gerust, ik zal 'ons' koffiezetapparaat bij NMG achterlaten, want je kunt vast nog wel wat kopjes koffie gebruiken bij het afmaken van jouw boekje. Rinke, bedankt voor je humor en voor je behulpzaamheid als ik weer eens met een vraag aan kwam zetten. Daniëlle en Milène, ook jullie wil ik bedanken voor de fijne tijd op 't werk en daarbuiten. Ik wens jullie beiden veel succes met jullie projecten. Suzan, bedankt voor het schoonhouden van onze kamer en voor onze leuke gesprekken. Ook alle oud-kamergenoten Mark, Bart, Laetitia en Maryam wil ik graag bedanken.

Jessica, mijn andere paranimf. Fijn dat ook jij naast me wil staan bij mijn promotie! Jij hebt me enorm geholpen bij teveel om op te noemen. Ik denk met veel plezier terug aan onze darmdiscussies, maar ook aan alle gezellige dingen die we samen hebben gedaan de afgelopen tijd. Samen eten of borrelen gaat ons toch beter af dan samen sporten, want ondanks alle goede voornemens hebben we denk ik maar twee keer samen gezwommen ;).

Natuurlijk wil ik ook graag alle andere NMG-ers bedanken voor hun bijdrage en voor de goede sfeer op de afdeling. Guido, of ik nou hulp nodig had met data-analyses, het maken van figuren of met de LCM, ik kon altijd bij je terecht. Bedankt voor al je hulp en ondersteuning. Sander, bedankt voor je betrokkenheid bij met name het PPAR hoofdstuk en natuurlijk voor de onvergetelijke NWO-afterparty die je hebt georganiseerd! Wilma, jouw vrolijke begroeting 's morgens vroeg deed me altijd goed. Bedankt voor je interesse in mij en in mijn onderzoek. Frits bedankt voor je hulp op 't lab en voor je grappen. Lydia ik wil jou ook 'even' bedanken voor je heldere blik op dingen en je goede adviezen. Natasha, I wish you all the best in Sweden. Susan, jij veel succes met je onderzoek in Australië. Philip en Mark, bedankt voor jullie hulp bij de vele arrays die er gedaan zijn. Ohid, you finished just before me, congratulations! Thanks for your help with statistics and for the nice discussions we had. Jan, bedankt voor je hulp als mijn PC het liet afweten. Sheril and Fenni, you are both very friendly persons and it is nice to have you around. Katja en Inge, bedankt voor de fijne tijd en veel succes gewenst met jullie aio-projecten. Mona, je bent nog maar net bij NMG, maar je stelde gelijk veel vertrouwen in me. Ik wens je veel succes met je carrière.

En dan zijn er natuurlijk de analisten die me erg veel hebben geholpen met labwerk. Mechteld, allereerst bedankt voor de qPCRs en alle arrays, die jij en Jenny voor me hebben gedaan. Verder wil ik je bedanken voor het organiseren van allerlei activiteiten tijdens en na het werk. Vele uitjes, Sinterklaasfeestjes en borrels hebben we aan jou te danken. Jenny, Shohreh, Mieke, Karin en Carolien, allen heel erg bedankt voor al jullie hulp.

Els, zonder jou is het toch anders bij NMG. Ik mis je niet alleen op het lab, maar sinds je weg bent zijn we ook niet meer op de hoogte van alle nieuwtjes.

Verder wil ik alle ex-NMGers bedanken die vooral in het begin van mijn aio-tijd een rol hebben gespeeld.

Ook bedank ik de studenten Emmy en Gerdien voor jullie bijdrage aan mijn onderzoek en jullie inzet.

Cornelia, jij hebt echt antwoord op alle vragen! Daar heb ik dankbaar gebruik van mogen maken. Bedankt voor je hulp en je gezelligheid.

Dan wil ik de 'Witkamp-groep' bedanken. Renger, bedankt voor je ideeën en suggesties voor ons prostaglandine experiment. Michiel, ontzettend bedankt voor de metingen die je voor ons hebt gedaan en voor je hulp bij het afronden van mijn proefschrift. Nikkie en Jvalini, veel succes met jullie aio-projecten. Mieke, Jocelijn, Klaske, Pierluigi, Ya and Zheng, it was a pleasure to work with you.

Verder wil ik graag de medewerkers van het CKP bedanken. In het bijzonder bedank ik Bert, Rene, Wilma en Judith voor de hulp bij het opzetten en uitvoeren van onze studies.

Muriel, Clara en Erwin, bedankt voor de fijne samenwerking en voor jullie microbiologische input. Milkha en Tom, bedankt voor jullie hulp met onze experimenten en ik wens jullie beide veel succes met het afronden van jullie proefschrift!

Linda en Bruno, jullie wil ik ook bedanken voor al jullie hulp en de gezellige samenwerking. Beiden erg veel succes met jullie projecten, maar dat gaat zeker helemaal goed komen! Verder wil ik ook de mensen van het A1001 team van TI Food and Nutrition bedanken voor alle interessante en leuke projectmeetings.

Nizo-ers Marleen en Marloes, bedankt voor de fijne samenwerking en ook voor de leuke tijden op congres.

Nico Abeling en Jos Sewalt wil ik bedanken voor hun analytische ondersteuning.

Antoine, leuk dat je het aandurfde om ook te 'lasergamen' in Wageningen. Het was altijd gezellig als je er was en ik hoop dat alle uren schieten mooie resultaten zullen opleveren.

Naast het werk is ontspanning natuurlijk ook belangrijk. Daarom dank ik Diederik, Els, Bas, Mike, Merel, Vera, Katja en Milene voor de vele uurtjes squash, de bezoeken aan het terras op vrijdagmiddag en voor alle andere gezellige dingen.

Verder wil ik Sonja, Sovianne, Bianca, Puck, Hadassa, Mieke, Antje, Kim en Saskia bedanken voor hun vriendschap en alle steun de afgelopen tijd. Sonja, ik verheug me al op onze vakantie na mijn promotie! Sovianne en Bianca, het is erg fijn om jullie dicht in de buurt te hebben en samen af te spreken. Mieke, ik vond het erg fijn om mijn aio-ervaringen te kunnen delen met iemand die in hetzelfde schuitje zat. Bedankt voor al je steun! Saskia, jij ook bedankt voor je support bij het afronden van mijn boekje. Wie weet wonen we binnenkort weer iets dicht bij elkaar...



Mijn schoonfamilie; Bram en Leonie, Annelieke en Benjamin, Sander en Rosalinde en natuurlijk oma Cor. Ik heb me vanaf het begin af aan welkom gevoeld bij jullie. Bedankt voor jullie steun en voor de gezellige en ontspannen weekenden op de Welberg.

Mijn familie wil ik bedanken voor alle betrokkenheid en steun de afgelopen jaren. Lieve Ellen, jij was altijd geïnteresseerd in wat ik deed en hoe het met me ging. Ik weet zeker dat je ook graag bij mijn promotie was geweest, maar helaas heeft dat niet zo mogen zijn. Lieve Joke en Ab, jullie huis staat altijd open voor onze bezoeken in de weekenden. Bedankt voor jullie gastvrijheid, jullie interesse en steun. Ab, ik heb veel geleerd van je nuchtere kijk op 't leven. Het doet me veel verdriet dat je mijn promotie niet meer mee mag maken.

Mijn lieve kleine (en grotere) zus Nelleke, bedankt voor alle gezellige momenten en voor je steun. Het is altijd fijn om met jou en Rik af te spreken. Ik wens je veel succes met jouw promotie. Ik weet zeker dat jij over een paar jaar ook Doctor bent! Rik, bedankt voor je tijd en creativiteit die je hebt gestoken in het maken van de cover. Ik ben erg blij met het resultaat!

Lieve papa en mama, jullie hebben me altijd de vrijheid en de mogelijkheid gegeven om datgene te doen wat ik wilde. Bedank voor jullie vertrouwen in mij, jullie steun, betrokkenheid en voor alle goede zorgen. Het is altijd fijn om een weekend 'thuis' te zijn en lekker te kunnen uitrusten in Hengelo.

Lieve Matthijs, deze laatste plaats in het dankwoord en de eerste stoel bij de promotie zijn voor jou. We hebben al veel moeten lachen om alle clichés die ik hier voor je op zou kunnen schrijven. Dat ga ik dus ook maar niet doen. Het belangrijkste is dat ik jou het meest van iedereen wil bedanken voor alles wat je afgelopen tijd voor me hebt gedaan en betekend. Je had gelijk; het is allemaal gelukt! En mijn artikelen zijn niet eens bij de Duckstad Courant terecht gekomen ;-).

Bedankt,  
Noortje



## About the author

## **CURRICULUM VITAE**

Noortje IJssennagger was born on the 8th of March, 1984, in Hengelo, the Netherlands. After completing secondary school in Hengelo at S.G. Twickel in 2002, she started both her Bachelor and later her Master in Nutrition and Health at the Wageningen University. During her studies she performed her minor Master thesis about the efficiency of metabolic pathways and their consequences for weight management at the Human and Animal Physiology Group of Wageningen University. Her major Master thesis was performed at the Nutrition, Metabolism and Genomics Group in Wageningen, in which she investigated the role of the protein Oit1 as a potential secreted biomarker of early phase metabolic syndrome. Her internship was performed at the Locus for Homocysteine and related vitamins, University of Bergen, Norway. Her project was entitled: 'European variation in B-vitamins, metabolites and the MTHFR polymorphisms of the one carbon metabolism'. She obtained her MSc-degree cum laude in 2007. Then she started her PhD in September 2007 at Top Institute Food and Nutrition and the Nutrition Metabolism and Genomics group of Wageningen University under the supervision of Dr. R. van der Meer and Prof. Dr. M. Müller. This PhD project was part of a larger project within TI Food and Nutrition entitled: 'Nutritional and microbial modulation of intestinal epithelial integrity'. The results of the PhD project are described in this thesis.

## LIST OF PUBLICATIONS (FULL PAPERS)

### This thesis

IJssennagger N, Rijnierse A, de Wit NJ, Jonker-Termont D, Dekker J, Müller M, van der Meer R. Dietary haem stimulates epithelial cell turnover by downregulating feedback inhibitors of proliferation in murine colon. *Gut* 2012; 61:1041

IJssennagger N, de Wit NJ, Müller M, van der Meer R. Dietary heme-mediated PPAR $\alpha$  activation does not affect the heme-induced epithelial hyperproliferation and hyperplasia in mouse colon. *PLoS One*. 2012;7(8):e43260.

IJssennagger N, Rijnierse A, de Wit NJ, Boekschoten MV, Dekker J, Schonewille AJ, Müller M, van der Meer R. Dietary heme induces acute oxidative stress but delayed cytotoxicity and compensatory hyperproliferation in mouse colon. *Submitted*

IJssennagger N, Derrien M, van Doorn GM, Rijnierse AR, van den Bogert B, Müller M, Dekker J, Kleerebezem M, van der Meer R. Dietary heme alters microbiota and mucosa of mouse colon without functional changes in host-microbe cross-talk. *Under review*

IJssennagger N, Belzer C, Hooiveld GJ, Dekker J, Müller M, Kleerebezem M, van der Meer R. Microbiota facilitates dietary heme-induced epithelial hyperproliferation and hyperplasia by breaking the mucus barrier. *In preparation*.

### Other

Eussen SJPM, Nilsen RM, Midttun Ø, Hustad S, IJssennagger N, Meyer K et al. North-south gradients in plasma concentrations of B-vitamins and other components of one-carbon metabolism in Europe: Results from the EPIC study. *Submitted*

Steegenga WT, de Wit NJ, Boekschoten MV, IJssennagger N, Lute C, Keshtkar S, Grootte Bromhaar MM, Kampman E, de Groot LC, Müller M. Structural, functional and molecular analysis of the effects of aging in the small intestine and colon of C57BL/6J mice. *BMC Med Genomics*. 2012; 5:38

de Wit NJ, IJssennagger N, Oosterink E, Keshtkar S, Hooiveld GJ, Mensink RP, Hammer S, Smit JW, Müller M, van der Meer R. Oit1/Fam3D, a gut-secreted protein displaying nutritional status-dependent regulation. *The Journal of Nutritional Biochemistry*, 2012 jan 4 [Epub ahead of print]

Schreurs VVAM, Aarts MJ, IJssennagger N, Hermans J, Hendriks WH. Energetic and metabolic consequences of aerobic and an-aerobic ATP production. *Agro Food Industry Hi-Tech* 2007; 18:25

## **OVERVIEW OF COMPLETED TRAINING ACTIVITIES**

### **Discipline specific activities**

Masterclass Nutrigenomics, Wageningen (2007)  
4th Hands-on course: Advanced microarray data analysis, Maastricht (2008)  
NWO Voedingsdagen, Deurne (2008)  
Wageningen Nutritional Sciences Forum: Too much- Too little, Arnhem (2009)  
Digestive Disease Week, Chicago (2009)  
Faseb Summer Research conference, Gastrointestinal tract XIII, Snowmass (2009)  
NWO Voedingsdagen, Deurne (2009)  
NWO Voedingsdagen, Deurne (2010)  
12th Gut Day Symposium, Gent (2010)  
1st International Symposium, Microbes for health, Paris (2010)  
Nugo Week, Wageningen (2011)  
NWO Voedingsdagen, Deurne (2011)  
13th Gut Day Symposium, Wageningen (2011)  
22nd Biennial Congress of the European Association for cancer research, Barcelona (2012)

### **General courses**

Course on Laboratory Animal Science, Wageningen (2007)  
Vlag PhD week, Bilthoven (2007)  
Scientific Writing (2009)  
Career perspectives (2011)

### **Optionals**

Preparation of research proposal (2007)  
PhD tour, Scandinavia (2009)  
Excursion to the Technical University of Munich (2011)  
Journal club from Human Nutrition and NMG group (2007-2009)  
NMG group weekly science meetings (2007-2012)  
Project meetings Tifn A1001 (2007-2012)



The research described in this thesis was financially supported by TI Food and Nutrition

Financial support from Wageningen University and TI Food and Nutrition for printing this thesis is gratefully acknowledged

Cover: Colonic crypts, with red crypt affected by heme.

Cover design: Rik van der Pluym

Printed by: GVO drukkers en vormgevers B.V. | Ponsen & Looijen

© Noortje IJssennagger, 2012